INVESTIGATING THE MOLECULAR MECHANISM OF PHOSPHOLAMBAN REGULATION OF THE Ca^{2+}-PUMP OF CARDIAC SARCOPLASMIC RETICULUM

Brandy Lee Akin

Submitted to the faculty of the University Graduate School
in partial fulfillment of the requirements
for the degree
Doctor of Philosophy
in the Department of Biochemistry and Molecular Biology,
Indiana University

December 2010

Accepted by the Faculty of Indiana University, in partial
fulfillment of the requirements for the degree of Doctor of Philosophy.

Larry R. Jones, M.D., Ph.D., Chair

Loren J. Field, Ph.D.

Doctoral Committee

Andy Hudmon, Ph.D.

Thomas D. Hurley, Ph.D.

November 4, 2010

Peter J. Roach, Ph.D.

To

My Family

ACKNOWLEDGEMENTS

I am sincerely grateful to the chair of my research committee, Dr. Larry Jones, for his guidance, encouragement, and patience during my dissertation studies. I could not have had a better mentor. I am also grateful to the other members of my research committee: Dr. Peter Roach, Dr. Tom Hurley, Dr. Andy Hudmon, and Dr. Loren Field, for their guidance and expertise. Finally, I would like to thank my husband Jon and our children Adelaide and Jonathan for always being there for me. You inspire and motivate me every day of my life. Thank you.

ABSTRACT

Brandy Lee Akin

INVESTIGATING THE MOLECULAR MECHANISM OF PHOSPHOLAMBAN REGULATION OF THE Ca^{2+}-PUMP OF CARDIAC SARCOPLASMIC RETICULUM

The Ca^{2+} pump or Ca^{2+}-ATPase of cardiac sarcoplasmic reticulum, SERCA2a, is regulated by phospholamban (PLB), a small inhibitory phosphoprotein that decreases the apparent Ca^{2+} affinity of the enzyme. We propose that PLB decreases Ca^{2+} affinity by stabilizing the Ca^{2+}-free, *E*2·ATP state of the enzyme, thus blocking the transition to *E*1, the high Ca^{2+} affinity state required for Ca^{2+} binding and ATP hydrolysis. The purpose of this dissertation research is to critically evaluate this idea using series of cross-linkable PLB mutants of increasing inhibitory strength (N30C-PLB < PLB3 < PLB4). Three hypotheses were tested; each specifically designed to address a fundamental point in the mechanism of PLB action.

Hypothesis 1: SERCA2a with PLB bound is catalytically inactive. The catalytic activity of SERCA2a irreversibly cross-linked to PLB (PLB/SER) was assessed. Ca^{2+}-ATPase activity, and formation of the phosphorylated intermediates were all completely inhibited. Thus, PLB/SER is entirely catalytically inactive.

Hypothesis 2: PLB decreases the Ca^{2+} affinity of SERCA2a by competing with Ca^{2+} for binding to SERCA2a. The functional effects of N30C-PLB, PLB3, and PLB4 on Ca^{2+}-ATPase activity and phosphoenzyme formation were measured, and correlated with their binding interactions with SERCA2a measured by chemical cross-linking. Successively higher Ca^{2+} concentrations were required to both activate

the enzyme co-expressed with N30C-PLB, PLB3, and PLB4 and to dissociate N30C-PLB, PLB3, and PLB4 from SERCA2a, suggesting competition between PLB and Ca^{2+} for binding to SERCA2a. This was confirmed with the Ca^{2+} pump mutant, D351A, which is catalytically inactive but retains strong Ca^{2+} binding. Increasingly higher Ca^{2+} concentrations were also required to dissociate N30C-PLB, PLB3, and PLB4 from D351A, demonstrating directly that PLB competes with Ca^{2+} for binding to the Ca^{2+} pump.

Hypothesis 3: PLB binds exclusively to the Ca^{2+}-free E2 state with bound nucleotide (E2·ATP). Thapsigargin, vanadate, and nucleotide effects on PLB cross-linking to SERCA2a were determined. All three PLB mutants bound preferentially to *E*2 state with bound nucleotide (*E*2·ATP), and not at all to the thapsigargin or vanadate bound states.

We conclude that PLB inhibits SERCA2a activity by stabilizing a unique *E*2·ATP conformation that cannot bind Ca^{2+}.

Larry R. Jones, M.D., Ph.D., Chair

TABLE OF CONTENTS

LIST OF TABLES x

LIST OF FIGURES xi

ABBREVIATIONS xiii

CHAPTER 1—INTRODUCTION 1

A. Excitation-contraction coupling in cardiac myocytes 1

B. Regulation of PLB by the β-adrenergic signaling pathway 3

C. The β-adrenergic pathway and heart failure 5

D. The mechanism of Ca^{2+} transport by SERCA2a 6

E. PLB structure and function 9

F. Developing a model of PLB regulation of SERCA2a using chemical cross-linking 11

G. Purpose 19

1. Hypothesis 1: SERCA2a with PLB bound is catalytically inactive 20

a. Testing the catalytic activity of SERCA2a with PLB bound 20

2. Hypothesis 2: PLB decreases the Ca^{2+} affinity of SERCA2a by competing with Ca^{2+} for binding to the enzyme 21

a. Using cross-linkable PLB supershifters to test for competitive binding of PLB and Ca^{2+} to SERCA2a 22

b. Using PLB supershifters in conjunction with D351A-SERCA2a to test for competitive binding of PLB and Ca^{2+} to SERCA2a 23

c. Determining the effect of PLB on maximal Ca^{2+}-ATPase activity 24

3. Hypothesis 3: PLB binds exclusively to the *E*2·ATP conformation of the Ca^{2+} pump 25

a. Investigating the conformational specificity of the PLB to SERCA2a binding interaction using the effectors TG, vanadate, and nucleotides (ATP, ADP, and AMP) 25

CHAPTER 2—EXPERIMENTAL PROCEDURES 26

A. Materials 26

B. Mutagenesis and baculovirus production 26
C. Protein expression and characterization 26
D. Ca^{2+}-ATPase assay 27
E. Cross-linking PLB to SERCAC2a 28
1. Standard Cross-linking (small scale) 28
2. Large scale cross-linking 28
3. Cross-linking under Ca^{2+}-ATPase conditions 29
F. Monitoring formation of the phosphorylated intermediates, *E*1~P and *E*2-P 30
1. Phosphorylation of $E1 \cdot Ca_2$ by [γ-^{32}P]ATP 30
2. Phosphorylation of *E*2 by $^{32}P_i$ (back door phosphorylation) 30
CHAPTER 3—RESULTS 31
A. Hypothesis 1: SERCA2a with PLB bound is catalytically inactive 31
1. Large scale pre-cross-linking of N30C-PLB to SERCA2a 31
2. Phosphorylation of pre-cross-linked membranes with [γ^{32}P]ATP and $^{32}P_i$ to form *E*1~P and *E*2-P 32
3. Resolution of PLB-free SERCA2a (catalytically active SERCA2a) from PLB/SER (catalytically inactive SERCA2a) 34
B. Hypothesis 2: PLB decreases the Ca^{2+} affinity of SERCA2a by competing with Ca^{2+} for binding to the enzyme 36
1. Co-expression of SERCA2a with N30C-PLB, PLB3 and PLB4 36
2. Ca^{2+} activation of Ca^{2+}-ATPase activity and Ca^{2+} inhibition of PLB cross-linking to SERCA2a 37
3. Ca^{2+} stimulation of *E*1~P formation correlated with Ca^{2+} inhibition of PLB cross-linking to SERCA2a 41
4. The effect of 2D12 on Ca^{2+}-ATPase activity and PLB cross-linking 41
5. The effect of Ca^{2+} on PLB cross-linking to D351A 43
C. Hypothesis 3: PLB binds exclusively to the $E2 \cdot$ATP conformation of the Ca^{2+} pump 46
1. The effect of TG and nucleotides on PLB cross-linking to WT-SERCA2a pump 46

2. The effects of TG and nucleotides on PLB cross-linking to D351A-SERCA2a 49
3. The effects of vanadate on PLB cross-linking to SERCA2a 50
CHAPTER 4—DISCUSSION 52
A. Hypothesis 1: SERCA2a with PLB bound is catalytically inactive 52
B. Hypothesis 2: PLB decreases the Ca^{2+} affinity of SERCA2a by competing with Ca^{2+} for binding to the enzyme 53
1. PLB supershifters reveal competitive binding of PLB and Ca^{2+} to SERCA2a 53
2. Confirming competitive binding of PLB and Ca^{2+} to SERCA2a using catalytically inactive D351A 54
3. The effects of PLB on the V_{max} of SERCA2a 55
4. The physiological effects of PLB 56
5. Structural considerations: long distance communication between the Ca^{2+} binding sites and the catalytic site 57
C. Hypothesis 3: PLB binds exclusively to the E2·ATP conformation of the Ca^{2+} pump 58
1. PLB binds to deprotonated *E*2·ATP 59
2. The affinity of PLB for SERCA2a 60
D. Conclusions and future directions 61
REFERENCES 63
CURRICULUM VITAE

LIST OF TABLES

Table 1. K_{Ca} values (μM) for Ca^{2+}-ATPase activation and $E1{\sim}P$ formation, and K_i values (μM) for Ca^{2+} inhibition of PLB cross-linking.....37

Table 2. K_{TG} values (μM) for TG inhibition of PLB cross-linking to the Ca^{2+}-ATPase 46

Table 3. K_{ATP} values (μM) for ATP stimulation of PLB4 cross-linking to the Ca^{2+}-ATPase, determined at different TG concentrations.....49

LIST OF FIGURES

Figure 1. Excitation-Contraction Coupling and Ca^{2+} Cycling in Cardiac Myocytes....2

Figure 2. Effect of the Catalytic Subunit of PKA (CSU) and the Anti-PLB monoclonal Antibody (2D12) on Ca^{2+}-Uptake by Guinea Pig Ventricular SR Vesicles....4

Figure 3. Crystal Structures of the *E*2 and *E*1 Conformations of SERCA....7

Figure 4. Reaction Cycle of SERCA2a....8

Figure 5. Amino Acid Sequence of PLB....9

Figure 6. Structural Model for the Interaction Between PLB and SERCA2a....11

Figure 7. Sites of PLB Cross-linking to SERCA2a with Homo- and Hetero-bifunctional Cross-linkers....12

Figure 8. Ca^{2+} Inhibition of Cross-linking of Residues 45-52 of PLB to V89C-SERCA2a....13

Figure 9. Effect of Ca^{2+}on Cross-linking of N30C-PLB to SERCA2a with BMH....14

Figure 10. Ca^{2+} Effect on Cross-linking of Phosphorylated and Dephosphorylated PLB to SERCA2a....14

Figure 11. ATP Dependence of PLB Cross-Linking....15

Figure 12. ATP Concentration-Dependence on Cross-linking and *E*2-P Formation....16

Figure 13. TG Inhibition of Cross-Linking of Residues 45-52 of PLB to V89C-SERCA2a....17

Figure 14. Our Model of PLB Regulation of SERCA2a Activity....18

Figure 15. Complete Amino Acid Sequences of the Cross-linkable PLB Mutants,N30C-PLB, PLB3, and PLB4....23

Figure 16. Effect of PLB Cross-linking to SERCA2a on Maximal Ca^{2+}-ATPase Activity....32

Figure 17. Effect of PLB Cross-Linking to SERCA2a on Maximal *E*1~P and *E*2-P Formation....33

Figure 18. Phosphorylation of Pre-Cross-Linked Membranes and LDS-PAGE Resolution of PLB-free SERCA2a from PLB/SER 35
Figure 19. Amido Black Staining and Immunoblot of SERCA2a Co-Expressed with N30C-PLB, PLB3, and PLB4 36
Figure 20. Ca^{2+} activation of Ca^{2+}-ATPase Activity and Ca^{2+} Inhibition of Cross-linking.....39
Figure 21. PLB Effect on Formation of the Phosphorylated Enzyme Intermediate 40
Figure 22. Effect of 2D12 on Ca^{2+}-ATPase activity and PLB cross-linking to SERCA2 42
Figure 23. Ca^{2+} effect on PLB cross-linking to D351A 44
Figure 24. TG effect on PLB cross-linking.....47
Figure 25. Nucleotide Effect on PLB4 Cross-Linking to Wild-Type SERCA2a and D351A 48
Figure 26. Vanadate Effect on PLB Cross-Linking to SERCA2a 50

LIST OF ABBREVIATIONS

SR	sarcoplasmic reticulum
PLB	phospholamban
SERCA	sarco(endo)plasmic reticulum Ca^{2+}-ATPase
SERCA1a	isoform of Ca^{2+}-ATPase in fast twitch skeletal muscle
SERCA2a	isoform of Ca^{2+}-ATPase in cardiac SR
2D12	anti-PLB monoclonal antibody
MOPS	3-(N-morpholino)propanesulfonic acid
M	transmembrane domain
E1	high Ca^{2+}-affinity conformation of Ca^{2+}-ATPase
*E*2	low Ca^{2+} affinity conformation of Ca^{2+}-ATPase
K_{Ca}	Ca^{2+} concentration required for half-maximal effect
K_i	concentration giving half-maximal inhibition
KMUS	N-[-maleimidoundecanoyloxy]sulfosuccinimide ester.
PKA	cAMP-dependent protein kinase
CaMKII	calmodulin kinase II
TG	thapsigargin
P_i	inorganic phosphate
V_{max}	maximal velocity

CHAPTER 1—INTRODUCTION

A. EXCITATION-CONTRACTION COUPLING IN CARDIAC MYOCYTES

Ca^{2+} cycling through the SR of cardiac myocytes mediates contraction and relaxation of the heart (1). A contraction event is initiated when an electrical stimulus (action potential) originating from pacemaker cells in the sinoatrial node, arrives at the T-tubule of the cardiomyocyte, depolarizing the plasma membrane (sarcolemma). Membrane depolarization activates the voltage-dependent L-type Ca^{2+} channel also known as the dihydropyridine receptor (**Fig. 1**). Upon activation, the L-type Ca^{2+} channel permits small amount of extracellular "activator" Ca^{2+} to enter the cell. Then, through the process known as Ca^{2+} induced Ca^{2+} release, the "activator" Ca^{2+} triggers the opening of the Ca^{2+} release channels/ryanodine receptors in the membrane of the SR, and much of the intralumenal SR Ca^{2+} store is released into the cytoplasm (1). As cytosolic Ca^{2+} concentration increases to micromolar levels, Ca^{2+} ions bind to the troponin C subunit of the regulatory troponin complex, initiating a conformational change that relieves inhibition of the actin/myosin cross-bridge cycle, allowing myofilament contraction to occur (1). The mechanism by which the electrical signal (action potential) is converted into a mechanical response (myofilament contraction) is known as excitation-contraction coupling, a process fundamental to both cardiac and skeletal muscle.

Myofilament relaxation occurs when intracellular Ca^{2+} concentration is decreased to diastolic levels (nanomolar levels); Ca^{2+} is either removed from the cell by the plasma membrane Ca^{2+}-ATPase and the Na^{+}/Ca^{2+} exchanger, or pumped back into the lumen of the SR by the sarco(endo)plasmic reticulum Ca^{2+}-ATPase, SERCA2a. The majority of the intracellular Ca^{2+} (approximately 70%) is re-sequestered back into the lumen of the SR by the Ca^{2+} pump, SERCA2a, making Ca^{2+} available for the next contraction (1). Therefore, the rate of Ca^{2+} transport by SERCA2a determines both the rate of myofilament relaxation, and the size of the contractile-dependent SR Ca^{2+} store. Ca^{2+} pump activity is regulated by phospholamban (PLB), a small inhibitory phosphoprotein that acts as a molecular brake on enzyme activity (2, 3). Due to its essential role in maintaining Ca^{2+}

homeostasis in cardiac muscle cells, SERCA2a, and the mechanism by which SERCA2a activity is regulated by PLB is of great scientific and clinical interest. The overall purpose of this dissertation research was to investigate the molecular mechanism of PLB regulation of SERCA2a.

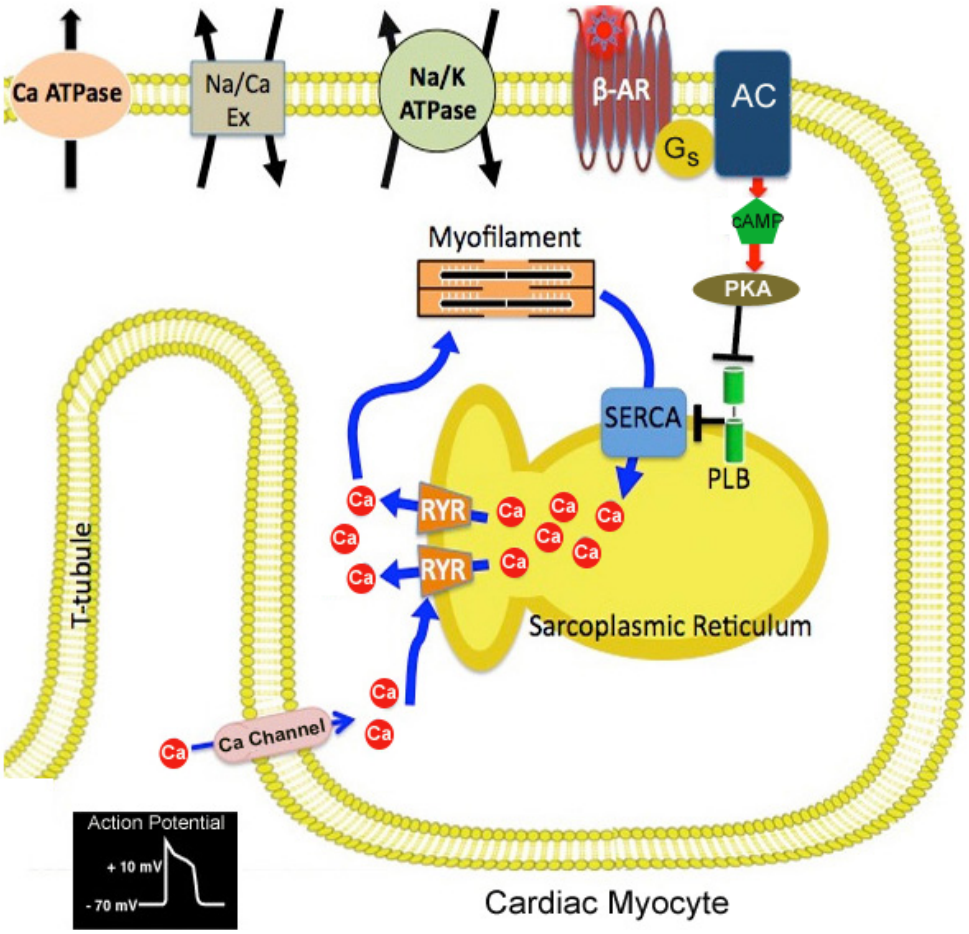

Figure 1. Excitation-Contraction Coupling and Ca^{2+} Cycling in Cardiac Myocytes Simplified scheme depicting E-C coupling and SR Ca^{2+} cycling in cardiac ventricular myocytes. Membrane depolarization causes Ca^{2+} to enter the cell through the voltage-dependent sarcolemmal Ca^{2+} channel. This small influx in Ca^{2+} causes Ca^{2+} to be released from the SR by the ryanodine receptor (RYR), triggering myofilament contraction. Ca^{2+} is subsequently removed from the cytosol by the sarcolemmal Ca^{2+}-ATPase, the Na^{+}/Ca^{2+} exchanger, and by SERCA2a, the Ca^{2+}-ATPase in the SR membrane. Most of the cytosolic Ca^{2+} is re-sequestered into the lumen of the SR by SERCA2a, allowing myofilament relaxation to occur and making Ca^{2+} available for the next contraction. SERCA2a activity is modulated by the inhibitory phosphoprotein PLB. De-phosphorylated PLB inhibits Ca^{2+}-ATPase activity, and PKA phosphorylation of PLB reverses this inhibition. PKA activity is regulated via the β_1-adrenergic receptor signaling pathway. Catecholamine activation of the β-receptor results in G_S-mediated activation of adenylate cyclase (AC). AC converts ATP to cAMP, and activates PKA.

B. REGULATION OF PLB BY THE β-ADRENERGIC SIGNALING PATHWAY

In response to physical or psychological stress, cardiac output (the volume of blood pumped per unit time) by human hearts is increased within seconds, and the percentage increase in cardiac output above that required under resting conditions is defined as the cardiac reserve (1-3). The rate and strength of myocardial contraction and relaxation is regulated through the β-adrenergic signaling pathway (1-3). When an individual becomes stressed, epinephrine is released into the blood stream by the sympathetic nervous system, activating β-adrenergic receptors in the plasma membrane of cardiac myocytes (**Fig. 1**). The β-receptor is a G-protein coupled-receptor, which when stimulated activates a hetero-trimeric G-protein complex. The stimulatory $G_{s\alpha}$ subunit dissociates from the G-protein complex and activates adenylate cyclase. Adenylate cyclase converts ATP to cAMP, increasing the concentration of cAMP in the cell, and activating cAMP-dependent protein kinase (PKA) (**Fig. 1**). In response to β-adrenergic stimulation, PKA phosphorylates several downstream targets including the L-type Ca^{2+} channel, troponin I, and PLB (3). PKA phosphorylation of the sarcolemmal Ca^{2+} channel permits a greater influx of extracellular Ca^{2+} across the plasma membrane (2). PKA phosphorylation of troponin I, a subunit of the regulatory troponin complex, decreasing the affinity of troponin C for Ca^{2+}, allowing for weaker myofilament contraction to occur at lower ionized Ca^{2+} concentrations (2). Phosphorylation of PLB by PKA (or calmodulin kinase II (CaMKII), see below) reverses PLB inhibition of SERCA2a, increasing the apparent Ca^{2+} affinity of the enzyme and increasing the rate of Ca^{2+} uptake into the SR (2, 3).

However, although all three of these Ca^{2+} handling pathways contribute to the positive inotropic and lusitropic effects of β-adrenergic stimulation, studies have shown that the PLB/SERCA2a pathway is the dominant pathway responsible for PKA-mediated enhanced cardiac contractility (4, 5). For example, PLB knock out mice (completely devoid of PLB expression) exhibited dramatically enhanced rates of contraction and relaxation, even under basal conditions, and were nearly completely unresponsive to β-adrenergic stimulation of the heart (4). Thus contractility in the

hearts of mice lacking PLB is always near the maximal level, indicating that PKA phosphorylation of PLB is the central pathway responsible for β-adrenergic stimulation of the heart (4).

The effect of PKA phosphorylation of PLB on $^{45}Ca^{2+}$-uptake by guinea pig ventricular SR vesicles is shown in **Fig. 2** (5). At 50 nM Ca^{2+} concentration, phosphorylation of PLB by PKA resulted in a two- to four-fold increase in SR Ca^{2+} up-take relative to control membranes. **Fig. 2** also shows the similar stimulatory effect of the anti-PLB monoclonal antibody, 2D12, on SR Ca^{2+}up-take. 2D12 binds to residues 7-13 of PLB, near the site of PKA phosphorylation (Ser^{16}), and reverses Ca^{2+} pump inhibition even more potently than PKA phosphorylation of PLB (5, 6). It is important to note that the stimulatory effect of 2D12 on SR Ca^{2+}-uptake was completely inhibited by addition of a PLB peptide (residues 2-25), which binds up the 2D12 antibody. In the same study, the stimulatory effect of 2D12 (and blocking of the stimulatory effect of 2D12 by the PLB peptide 2-25) was also demonstrated in intact cardiomyocytes, confirming that PKA phosphorylation of PLB is the main pathway responsible for β-adrenergic stimulated enhanced contractility (5). It has been suggested by our group that PKA phosphorylation of

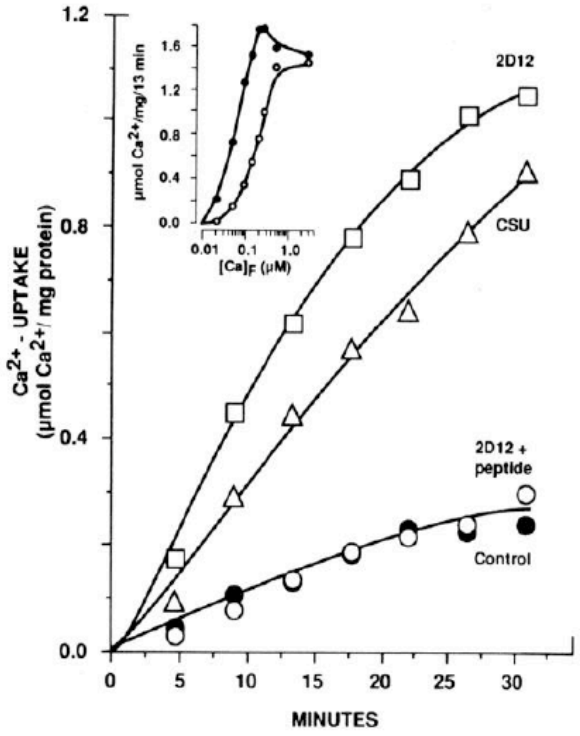

Figure 2. Effect of the Catalytic Subunit of PKA (CSU) and the Anti-PLB Monoclonal Antibody (2D12) on Ca^{2+}-Uptake by Guinea Pig Ventricular SR Vesicles Time courses of Ca^{2+}-uptake are plotted for control vesicles (open circles), vesicles pre-phosphorylated with CSU (triangles), and vesicles pre-incubated with 2D12, with (filled circles) or without the PLB peptide 2-25 (squares). Taken directly from Sham, J.S., Jones, L.R., and Morad, M. (1991) *Am. J. Physiol.* **261**, H1344-H1349.

PLB and binding of the 2D12 antibody to PLB both reverse Ca^{2+}-pump inhibition by weakening protein-protein interactions between PLB and the Ca^{2+}-ATPase (6).

In response to β-agonist stimulation, PLB is also phosphorylated by CaMKII at Thr^{17}. Like PKA phosphorylation, phosphorylation of PLB by CaMKII reverses PLB inhibition of SERCA2a, and it has been suggested that the effects of dual phosphorylation of PLB (at both Ser^{16} and Thr^{17}) may be additive (2, 3). However, the physiological role of CaMKII phosphorylation of PLB remains unclear (2, 6). Nevertheless, low basal contractility and heart rate are maintained in large part through PLB inhibition of Ca^{2+}-ATPase activity, and cardiac output is increased through β-adrenergic stimulated phosphorylation of PLB by PKA and CaMKII (**Fig. 2** and 1-5).

C. THE β-ADRENERGIC PATHWAY AND HEART FAILURE

Although not the direct focus of this dissertation research, it seems important to briefly address the role of PLB in cardiac dysfunction and heart failure. Heart failure is the condition in which the body's oxygen requirements are not met due to insufficient pumping of blood by the heart. It is a complex and progressive disorder with many causes that develops slowly over time. Heart failure typically results from underlying conditions such as atherosclerosis or hypertension, which either damage the heart muscle directly, or make it harder for the heart to pump blood efficiently (7). In any case, an inefficient cardiovascular system means that the heart must work harder to circulate blood to the body, which leads to pathological growth and remodeling of the heart (7). When left unchecked, this compensatory mechanism often leads to end-stage heart failure and sudden death. On the molecular level, aberrant SR Ca^{2+}-cyling is a characteristic of both cardiac dysfunction and end-stage heart failure (8). Therefore, as a key regulatory complex controlling intracellular Ca^{2+} concentrations and contractility, the role of SERCA2a and PLB in pathological cardiac remodeling and heart failure is currently an active area of investigation (8).

Genetic analysis of individuals with family histories of heart failure led to the discovery of several mutated proteins that cause heritable cardiomyopathies (7). The

preponderance has been found in contractile proteins, including mutations in actin, myosin, and tropomyosin (7). More recently, however, mutated forms of PLB have been identified, which appear be directly responsible for causing the disease (9-11). In addition, in several recent studies of failing myocardium, reduced SERCA2a expression, altered PLB to SERCA2a ratio, or reduced phosphorylation of PLB was reported (12-14), suggesting that SERCA2a and PLB may be directly involved in the pathogenesis of heart failure. On the contrary, Movsesian *et al*. reported that SERCA2a and PLB protein levels are unaltered in failing myocardium (15). Regardless, the pivotal role of the PLB/SERCA2a interaction in regulating intracellular Ca^{2+} concentrations and contractility has made them a potential target for therapeutic treatment of heart failure, underscoring the necessity of elucidating the molecular mechanism of PLB action.

D. THE MECHANISM OF Ca^{2+} TRANSPORT BY SERCA2a

SERCA is a large protein of nearly 1000 amino acids that actively transports Ca^{2+} into the lumen of the SR (and counter-transports luminal H^+ to the cytoplasm) at the expense of ATP hydrolysis. As a member of the P-type ATPase super-family, SERCA forms a high-energy phosphorylated intermediate as an integral part of its reaction cycle (16). Formation of this high-energy intermediate drives Ca^{2+} transport across the SR membrane, during which the Ca^{2+}-ATPase converts from a high Ca^{2+} affinity state (*E*1) to a low Ca^{2+} affinity state (*E*2) (17, 18). Crystal structures of SERCA1a in both the *E*1 and *E*2 states have been determined and are shown in cartoon form in **Fig. 3B** and **Fig. 3A**, respectively (17, 18). SERCA2a is the cardiac specific isoform of the Ca^{2+} pump, whereas SERCA1a is the isoform found in skeletal muscle (2, 3). The two proteins have high sequence homology with greater than 90% identical amino acid residues (2, 3).

SERCA2a has a large transmembrane domain composed of 10 α-helices (M1-M10), as well as a cytoplasmic head group with three functional domains: nucleotide binding (N) domain, phosphorylation (P) domain, and actuator (A) domain (**Fig. 3**). ATP binds within the N-domain, and the P-domain contains the conserved Asp^{351} that

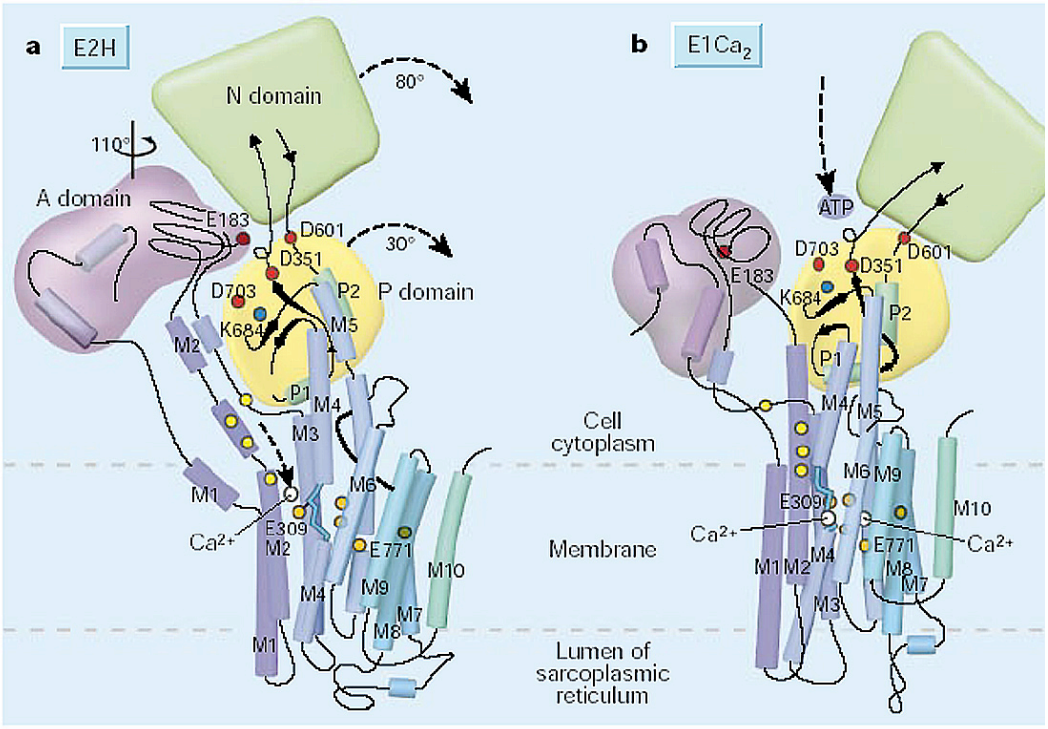

Figure 3. Crystal Structures of the *E*2 and *E*1 Conformations of SERCA 3-D structures of SERCA1a in the *E*2 (a) and *E*1 (b) conformations with bound Thapsigargan and Ca^{2+} respectively. Image taken directly from Green, N.M and MacLennan (2002) *Nature.* **418**, 598-599 (19).

is phosphorylated by ATP to form the high-energy acylphosphoprotein intermediate that drives Ca^{2+} transport across the membrane (17, 18). Specific residues within the A-domain form a TGES loop, which is directly involved in hydrolysis of the phosphorylated intermediate (17, 18). Two Ca^{2+} binding sites (I and II) are located side by side within the transmembrane domain between transmembrane helices M4, M5, and M6 (17, 18).

A simplified catalytic cycle of SERCA2a, beginning with the high Ca^{2+} affinity *E*1·ATP conformation is shown in **Fig. 4**. Ca^{2+} binding at Site 1 (*E*1·ATP·Ca_1) is followed by a slow isomeric transition (*E*1·ATP·Ca_1 to *E*1'·ATP·Ca_1), which facilitates cooperative binding of the second Ca^{2+} ion at Site II (*E*1·ATP·Ca_2). Ca^{2+} occupancy at both sites triggers transfer of the gamma phosphate of the bound ATP to Asp^{351} within the P-domain, forming the high-energy

acylphosphoprotein intermediate, $E1{\sim}P{\cdot}ADP{\cdot}Ca_2$. Next, as the Ca^{2+} pump converts from $E1{\sim}P{\cdot}ADP{\cdot}Ca_2$ to $E2\text{-}P{\cdot}ADP{\cdot}Ca_2$, Ca^{2+} is transported across the membrane and released into the SR lumen. ADP dissociates (forming *E*2-P), followed by hydrolytic cleavage of the phosphorylated Asp^{351}, producing inorganic phosphate bound, $E2{\cdot}P_i$. Dissociation of P_i, and subsequent binding of ATP yields $E2{\cdot}ATP$. It should be noted that when the enzyme is in the Ca^{2+}-free *E*2 state, the carboxyl groups involved in formation of the Ca^{2+} binding sites are all thought to be protonated, whereas when the enzyme is in the *E*1 state, the carboxyl groups are not protonated and have a high affinity for Ca^{2+} (18). The high affinity Ca^{2+} pump inhibitor thapsigargin (TG)

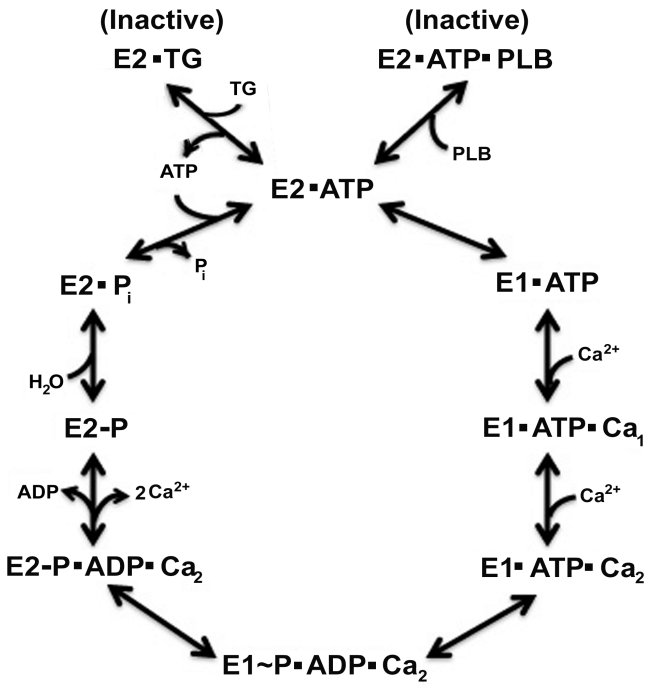

Figure 4. Reaction Cycle of SERCA2a *E*1 and *E*2 represent the high and low Ca^{2+}-affinity conformations of SERCA2a, respectively. After sequential binding of two Ca^{2+} ions to *E*1, the enzyme is phosphorylated with the γ-phosphate of ATP at Asp^{351}, forming the high energy intermediate, $E1{\sim}P$. Ca^{2+} translocation across the SR membrane occurs during the *E*1 to *E*2 transition. TG inhibits Ca^{2+}-ATPase activity by forming a dead-end complex with the enzyme in *E*2 (*E*2·TG) (34). *E*2·TG has a greatly reduced affinity for ATP relative to TG-free *E*2 (61, 62). PLB cross-linking studies indicate that PLB binds preferentially to *E*2 with bound ATP (*E*2·ATP·PLB). PLB does not bind to *E*2·TG or *E*2·cyclopiazonic acid (21), *E*2-P (22) or to the Ca^{2+} pump with Ca^{2+} binding site 1 (23) or both sites (22, 27) occupied. It is notable that under conditions favoring formation of *E*2 (the absence of Ca^{2+} and presence of DMSO) the Ca^{2+} pump can be phosphorylated in the reverse direction by P_i forming *E*2-P. From **Akin, B.L.**, Chen, Z., and Jones, L.R. (2010) *J. Biol. Chem.* **285**, 28540-28552.

inhibits Ca^{2+}-ATPase activity by forming a dead-end complex with the enzyme in *E*2 (*E*2·TG), and it was recently suggested that the *E*2 state stabilized by TG is the fully protonated H_n*E*2 state (20 and **Fig. 4**). Cross-linking studies by our group have suggested that PLB inhibits Ca^{2+} pump turnover by stabilizing the Ca^{2+}-free, *E*2 state with bound nucleotide, *E*2·ATP (6, 21-23 and **Fig. 4**, and as further characterized by this dissertation research).

In addition to its role in catalysis, ATP also interacts with the enzyme in a non-catalytic, modulatory fashion, accelerating multiple steps in the Ca^{2+} pump reaction cycle, including the *E*2-P to *E*1·ATP·Ca_2 transition (20). In a recent study by Jensen *et al*. it was suggested that TG binds to the fully protonated H_n*E*2 state of SERCA2a, and that ATP binding at the modulatory site (ATP binding site in *E*2) accelerates the *E*2-P to *E*1·ATP·Ca_2 transition by stimulating deprotonation of *E*2, initiating the *E*2 to *E*1 transition (20). According to the authors, there is a single ATP binding site that converts from modulatory mode (*E*2·ATP) to catalytic mode (*E*1·ATP·Ca_2). In recently published work presented as part of this dissertation research, our group proposed that the conformation of SERCA2a that binds PLB is the deprotonated *E*2·ATP state with nucleotide bound at the modulatory site (24).

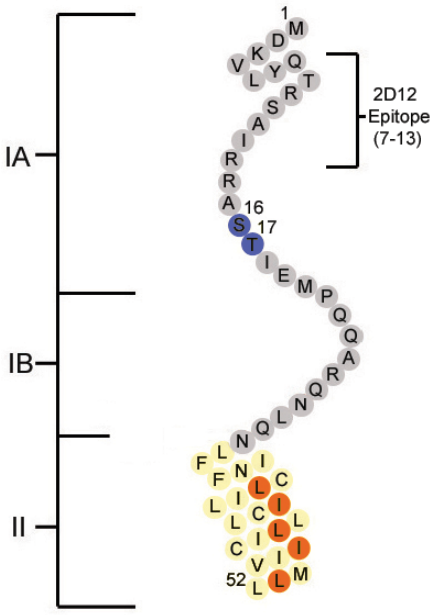

Figure 5. Amino Acid Sequence of PLB Amino acid sequence of canine PLB. Domains I (A and B) and II are shown. Transmembrane residues are shown in yellow. Ser^{16} and Thr^{17} (blue) are the sites of phosphorylation. The residues involved in formation of the Leu/Iso zipper are shown in orange. Residues 7-13 comprise the epitope for the anti-PLB antibody, 2D12, which reverses PLB inhibtion of the Ca^{2+}-APTase.

E. PLB STRUCTURE AND FUNCTION

PLB is a 52 amino acid single-span membrane protein localized to the SR of cardiac and smooth muscle cells (2, 3). Monomeric PLB has two structural domains: a cytosolic N-terminal domain I (residues 1-32), and a C-terminal transmembrane

domain II (residues 33-52) (**Fig. 5**). Early analysis of PLB by SDS-PAGE showed that PLB monomers oligomerize to form stable homo-pentamers (2, 3). Subsequent mutational analysis showed that the PLB pentamer is stabilized by an intra-molecular Leu/Ile zipper, formed by residues leu^{37}, leu^{44}, leu^{51}, Ile^{40}, and Ile^{47} within transmembrane domain II (25), and mutation of any of the residues to Ala destabilizes PLB pentamer formation and enhances Ca^{2+} pump inhibition by PLB (26, 27). Based upon these results it was concluded the PLB monomer is the active species that binds to and inhibits Ca^{2+} pump activity, and that PLB inhibitory function is increased by mutations that increase PLB monomer content in the membrane (26, 27). Due to their ability to decrease the Ca^{2+} affinity of SERCA2a (increase the K_{Ca} of enzyme activation) more than wild-type PLB, these superinhibitory monomeric PLB mutants were termed "supershifters" (26). Subsequent mutagenesis studies showed that Ca^{2+} pump inhibition by PLB was also enhanced by mutations that did not affect the PLB monomer to pentamer ratio observed by SDS-PAGE (22, 28). It was proposed that theses superinhibitory PLB mutants retaining the ability to form pentamers must have an increased binding affinity for the Ca^{2+} pump relative to wild-type PLB (22, 28). Collectively, all of these results suggested that there is dynamic equilibrium between PLB pentamers, PLB monomers, and PLB/SERCA2a heterodimers in the membrane, and PLB inhibition of Ca^{2+}-ATPase activity is enhanced by point mutations that either increase PLB monomer formation by destabilizing the PLB pentamer (e.g. L37A (26, 27)), or otherwise enhance PLB monomer binding interactions with the Ca^{2+} pump (e.g. N27A (28) and V49G (22)).

Consistent with these *in vitro* studies, depressed cardiac function and super-inhibition of the Ca^{2+}-ATPase was observed transgenic mice overexpressing monomeric PLB supershifters (L37A (29)) and PLB supershifters retaining the ability to form pentamers (N27A (30) and V49G (31)), relative to mice overexpressing wild-type PLB. Mice overexpressing the pentameric PLB supershifters developed cardiac hypertrophy, dilated cardiomyopathy and premature death compared to mice overexpressing wild-type PLB (30, 31). Moreover, whereas isoproterenol stimulation (activating the β_1-adernergic pathway) completely reversed Ca^{2+}-ATPase inhibition by the monomeric PLB supershifters, isoproterenol stimulation was not sufficient to

completely reverse the inhibitory effects of the more potent pentameric PLB supershifters (30-31). These findings are consistent with the theory that PLB supershifters retaining the ability to form pentamers have a higher binding affinity for the Ca^{2+} pump relative to wild-type PLB.

F. DEVELOPING A MODEL OF PLB REGULATION OF SERCA2a USING CHEMICAL CROSS-LINKING

The work discussed thus far clearly demonstrates that PLB is a key regulator of myocardial contractile kinetics, and that proper regulation of Ca^{2+}-ATPase activity by PLB is required for normal cardiac function and survival. Yet despite its prominent role in regulating cardiac function, the physical basis of enzyme inhibition by PLB has remained unclear, and presently several fundamentally different models exist.

A major impediment to solving the molecular mechanism of PLB regulation of SERCA2a has been an inability to measure PLB binding interactions with the Ca^{2+} pump. Our group has overcome this hurdle using chemical cross-linking. PLB can be irreversibly covalently coupled to SERCA2a in native membranes, facilitating direct measurement of PLB binding to SERCA2a. This technique has enabled us to study protein-protein interactions

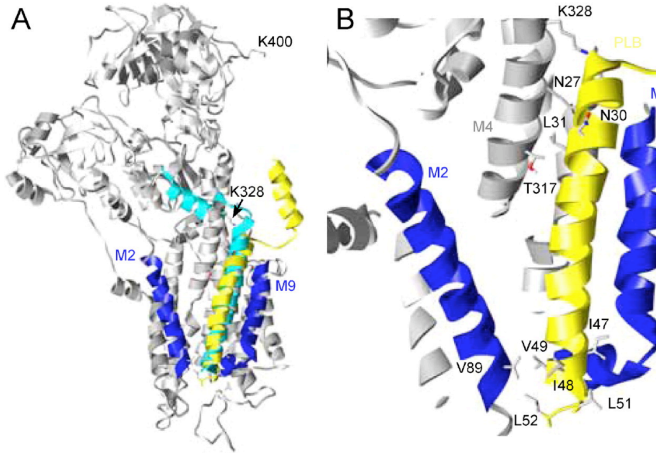

Figure 6. Structural Model for the Interaction Between PLB and SERCA2a A, Two independent structures for PLB were docked next to the structure of the *E*2 state of SERCA bound to TG. The cyan PLB was derived from a monomeric mutant, whereas the yellow PLB was extracted from the pentameric structure of a construct corresponding to the WT human sequence. B, Close-up of the C-terminus of PLB. It is wedged between the lumenal end of M2 and a loop between M9 and M10 of SERCA (colored blue), suggesting that M2 must move to accommodate PLB binding and that Val^{49} controls access to this binding site. Taken directly from Chen, Z., **Akin, B.L.**, Stokes, D.L., and Jones, L.R. (2006) *J.Biol.Chem*. **281**, 14163-14172.

between PLB and SERCA2a, and the allosteric factors that controlling the interaction (6, 21-24). Using chemical cross-linking we have identified several key points of interaction between PLB and the Ca^{2+} pump, which in conjunction with the crystal structures of the enzyme (17, 18) enabled us to model the three-dimensional interactions between the two proteins (**Fig. 6**).

In initial cross-linking studies, fully functional, Cys-less PLB (with Cys residues 36, 41, and 46 mutated to Ala) was used as a background for making Cys scanning point mutants of PLB. Lone Cys residues inserted at discrete locations within PLB were then probed for cross-linking to Cys or Lys residues of SERCA2a using homo (thiol specific), or heterobifunctional (thiol to amine specific) cross-linking reagents, respectively. Cys residues within both domain I (cytoplasmic) and domain II (transmembrane) of PLB have been cross-linked to Cys and Lys residues of SERCA2a at the cytoplasmic extension of M4 and at the C-terminus of M2 (**Fig. 7**).

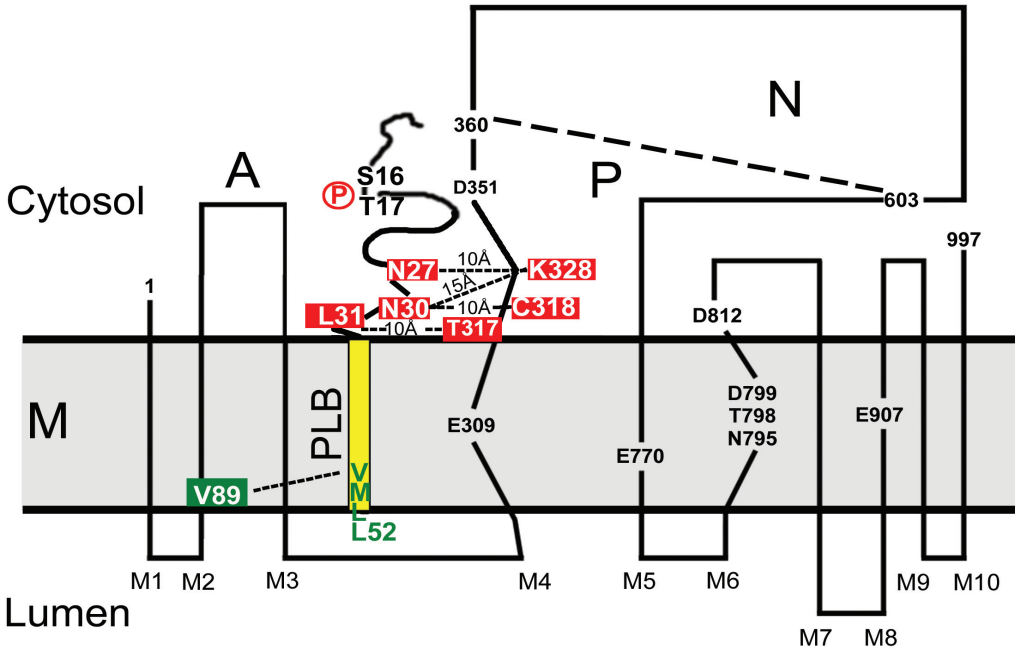

Figure 7. Sites of PLB Cross-linking to SERCA2a with Homo- and Hetero-bifunctional Cross-linkers PLB mutants have been cross-linked to SERCA2a cytoplasmic extension of M4 (red) and at the C-terminus of M2 (green). Modified from Jones, L.R., Cornea, R.L., and Chen, Z. (2002) *J. Biol. Chem.* **277**, 28319-28329.

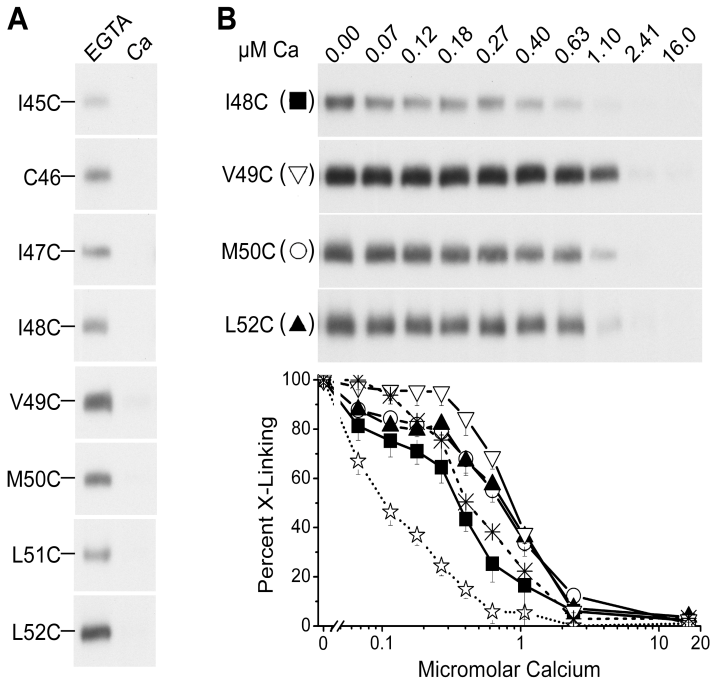

Figure 8. **Ca^{2+} Inhibition of Cross-linking of Residues 45-52 of PLB to V89C-SERCA2a** I45C- through V49C-PLB and L51C- and L52C-PLB were cross-linked to V89C-SERCA2a with bBBr. M50C-PLB was cross-linked to V89C-SERCA2a with BMH. Cross-linking was conducted in buffer containing 1 mM EGTA with no added Ca^{2+} (*EGTA*), or in *E*2 buffer containing 10 μM added Ca^{2+}, with no EGTA. Taken directly from Chen, Z., **Akin, B.L.**, Stokes, D.L., and Jones, L.R. (2006) *J.Biol.Chem*. **281**, 14163-1417.

PLB cross-linking to SERCA2a at each of these sites was completely inhibited by micromolar Ca^{2+} concentration (**Fig. 8**). This suggests that binding of PLB and Ca^{2+} to SERCA2a is mutually exclusive. Importantly, when Ca^{2+} inhibition of PLB cross-linking was correlated with Ca^{2+} stimulation of Ca^{2+}-ATPase activity, cross-linking was inhibited over the same range of Ca^{2+} concentration as Ca^{2+}-ATPase activity was stimulated. This is exemplified in **Fig. 9**, which shows the cross-linking curve of N30C-PLB to Cys^{318} of WT-SERCA2a, correlated with the ATPase activity measured from the same microsomal prep. Note that as micromolar Ca^{2+} increases, PLB cross-linking to SERCA2a is inhibited (panel A), whereas the Ca^{2+}-ATPase is activated (panel B). An inverse relationship between PLB cross-linking to SERCA2a and Ca^{2+} pump inhibition has proven consistent with all cross-

linking pairs discovered to date, strongly suggesting that PLB competes with Ca^{2+} for binding to the enzyme. Consistent with this interpretation, assays measuring Ca^{2+} inhibition of PLB cross-linking indicate that when PLB is phosphorylated by PKA, a lower concentration of Ca^{2+} is required to dissociate PLB from Ca^{2+} pump (**Fig. 10**). This suggests that phosphorylation of PLB at Ser^{16} by PKA decreases its binding affinity for the Ca^{2+} pump.

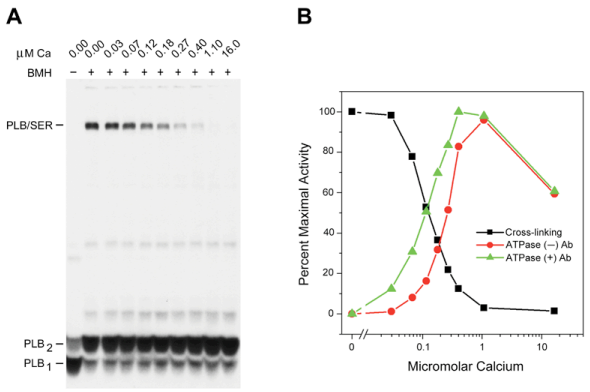

Figure 9. Effect of Ca^{2+}on Cross-linking of N30C-PLB to SERCA2a with BMH A, Ca^{2+} inhibition of PLB N30C-PLB cross-linking with BMH. B, Ca^{2+}-ATPase activity of the same microsomal preparation measured in the presence and absence of the anti-PLB antibody, 2D12, which reverses PLB inhibition like phosphorylation by protein kinase A. Taken from Jones, L.R., Cornea, R.L., and Chen, Z. (2002) *J. Biol. Chem.* **277**, 28319-28329.

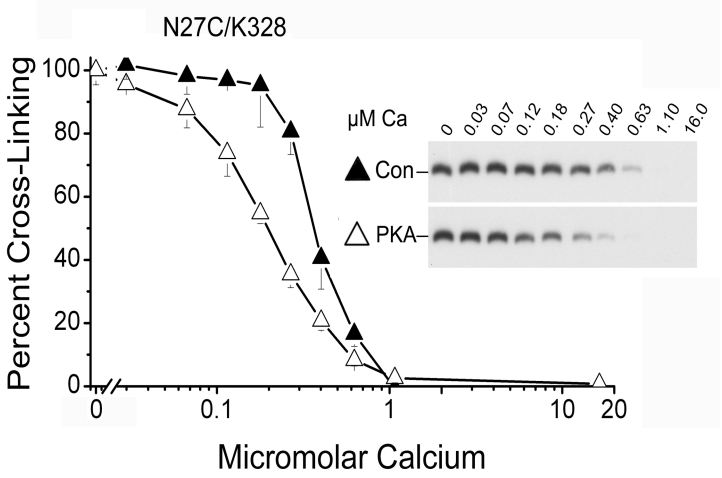

Figure 10. Ca^{2+} Effect on Cross-linking of Phosphorylated and Dephosphorylated PLB to SERCA2a PLB pre-phosphorylated in the presence (PKA) or absence (Con) of PKA was cross-linked to SERCA2a at varying Ca^{2+} concentrations. The inset shows the immunoblot with anti-PLB antibody obtained after cross-linking. Plot depicts cross-linking inhibition as a function of ionized Ca^{2+} concentration. Taken directly Chen, Z., **Akin, B.L.**, and Jones, L.R. (2007) *J. Biol. Chem.* **282**, 20968-20976.

In addition to being completely inhibited by micromolar Ca^{2+} concentration (**Figs. 8-10**), another hallmark of the PLB to SERCA2a cross-linking reaction is its nucleotide dependence. ATP stimulated PLB cross-linking to SERCA2a by 2-3-fold at nearly all cross-linking sites tested when measured in the absence of Ca^{2+} **(Fig. 11).** This suggests that PLB binds preferentially to nucleotide-bound *E*2 state (*E*2·ATP). PLB cross-linking to SERCA2a was also stimulated by ADP, but was unaffected by AMP, measured in the absence of Ca^{2+} (21). This indicates that the β-phosphate of the nucleotide is involved in formation of the *E*2 state that binds PLB.

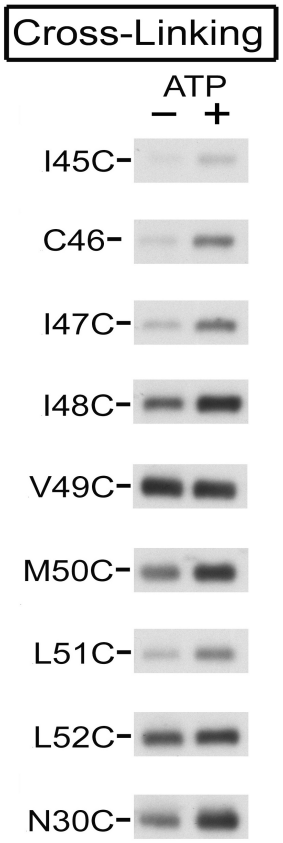

Figure 11. ATP Dependence of PLB Cross-Linking I45C- through L52C-PLC were co-expressed with V89C-SERCA2a in Sf21 insect cells. PLB was then cross-linked to V89C-SERCA2a in the presence and absence of 3 mM ATP. Taken directly from Chen, Z., **Akin, B.L.**, Stokes, D.L., and Jones, L.R. (2006) *J.Biol.Chem*. **281**, 14163-14172.

Early kinetic studies showed that the *E*2 state of SERCA2a could be phosphorylated in the reverse direction by P_i to form *E*2-P (*E*2 + P_i → *E*2-P, or "back-door phosphorylation") (32, 33). It was also shown that there are two distinct *E*2 conformations of SERCA2a: one with bound ATP (*E*2·ATP) which cannot be phosphorylated by P_i, and a second stabilized by low pH or Me_2SO that is readily phosphorylated by P_i to form *E*2·P_i (32, 33). When PLB cross-linking to SERCA2a was measured simultaneously with *E*2-P formation by P_i, ATP stimulated PLB cross-linking to SERCA2a over the same concentration range as ATP inhibited formation of *E*2-P (**Fig. 12)**. Based upon these results it was concluded that PLB binds to *E*2·ATP, but not to *E*2-P or *E*2·P_i (22).

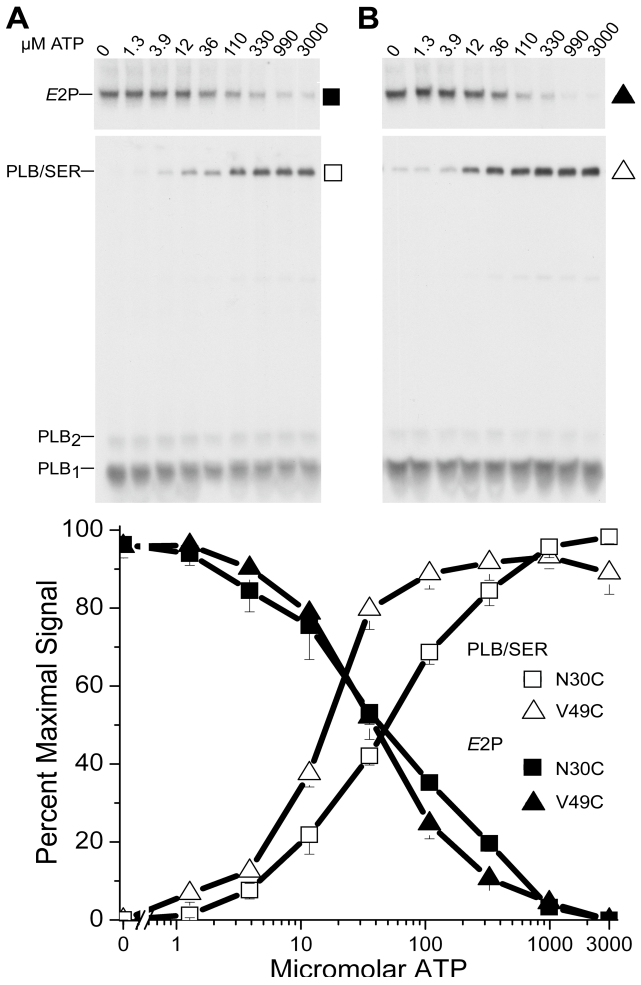

Figure 12. ATP Concentration-Dependence on Cross-linking and *E*2-P Formation N30C-PLB co-expressed with WT-SERCA2a (A) and V49C-PLB co-expressed with V89C-SERCA2a (B) was cross-linked in *E*2-P buffer. Upper autoradiograms show *E*2-P formation, and middle autoradiograms show PLB cross-linked to SERCA2a. The bottom graph shows the ATP concentration-dependence for stimulation of PLB-cross-linking to SERCA2a (open symbols) and for inhibition of *E*2-P formation (filled symbols). In the plot, baseline values obtained in the absence of ATP were set at 0% and 100% for protein cross-linking and *E*2-P formation, respectively (n = 5). Taken directly from Chen, Z., **Akin, B.L.**, Stokes, D.L., and Jones, L.R. (2006) *J.Biol.Chem*. **281**, 14163-14172.

A final signature characteristic of the PLB to SERCA2a cross-linking reaction is its sensitivity to the Ca^{2+} pump inhibitor TG. TG binds with nanomolar affinity to the Ca^{2+}-ATPase in *E*2, forming a dead-end complex, *E*2·TG, and irreversibly inhibiting the enzyme (34, 35 and **Fig. 2)**. Measured in the absence of Ca^{2+}, TG

completely inhibits PLB cross-linking to SERCA2a (**Fig. 13A** and **B)**. This indicates that PLB does not bind to the *E*2 state of SERCA2a stabilized by TG. When ATP was included in assays measuring TG effects on PLB cross-linking, the K_i for TG inhibition of PLB cross-linking was increased by approximately 4-fold (**Fig. 13C**), strongly supporting the idea that PLB binds preferentially with the nucleotide bound Ca^{2+}-ATPase in *E*2.

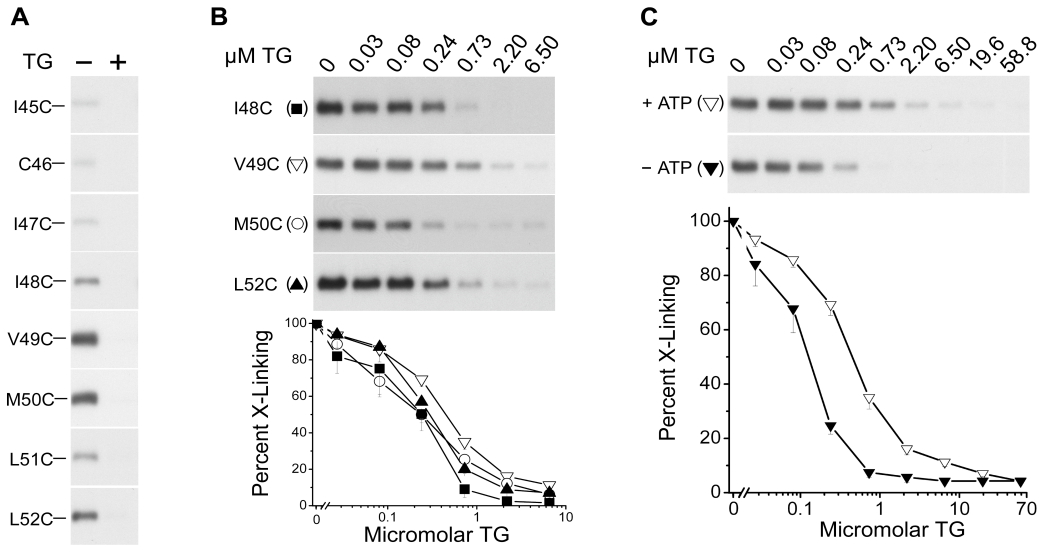

Figure 13. TG Inhibition of Cross-Linking of Residues 45-52 of PLB to V89C-SERCA2a A, Cross-linking of PLB mutants to V89C-SERCA2a in the presence and absence of 40 μM TG. B, TG inhibition of PLB cross-linking. Upper panel shows immunoblots and Lower panel show the plot of TG inhibition of PLB cross-linking. C, Effect of 3 mM ATP on TG inhibition of cross-linking. Upper panels show immunoblots and Lower panel shows the graph of TG inhibition of cross-linking. From Chen, Z., **Akin, B.L.**, Stokes, D.L., and Jones, L.R. (2006) *J.Biol.Chem*. **281**, 14163-14172.

Collectively, these cross-linking results point to a simple mechanism of PLB regulation of SERCA2a shown in **Fig. 14**. PLB stabilizes a single unique conformation of the Ca^{2+} pump, the low Ca^{2+} affinity *E*2·ATP state and blocks the transition to *E*1, the conformation required for high-affinity Ca^{2+} binding and ATP hydrolysis. SERCA2a with PLB bound cannot bind Ca^{2+} and is catalytically inactive, and PLB must completely dissociate before the enzyme can transition to *E*1 and initiate Ca^{2+} transport. By antagonizing formation of *E*1, PLB significantly decreases the fraction of Ca^{2+} pumps available to transport Ca^{2+} at sub-saturating Ca^{2+}

concentration. This is manifested as a decrease in the apparent Ca^{2+} affinity of the Ca^{2+}-ATPase, the hallmark of PLB inhibition (2, 3). At saturating Ca^{2+} concentration PLB is not bound to the enzyme, therefore, PLB has no effect on maximal Ca^{2+}-ATPase activity. Phosphorylation of PLB by PKA and binding of the 2D12 antibody to PLB decrease the affinity of SERCA2a for PLB, allowing PLB inhibition of Ca^{2+}-ATPase activity to be reversed at a lower Ca^{2+} concentration.

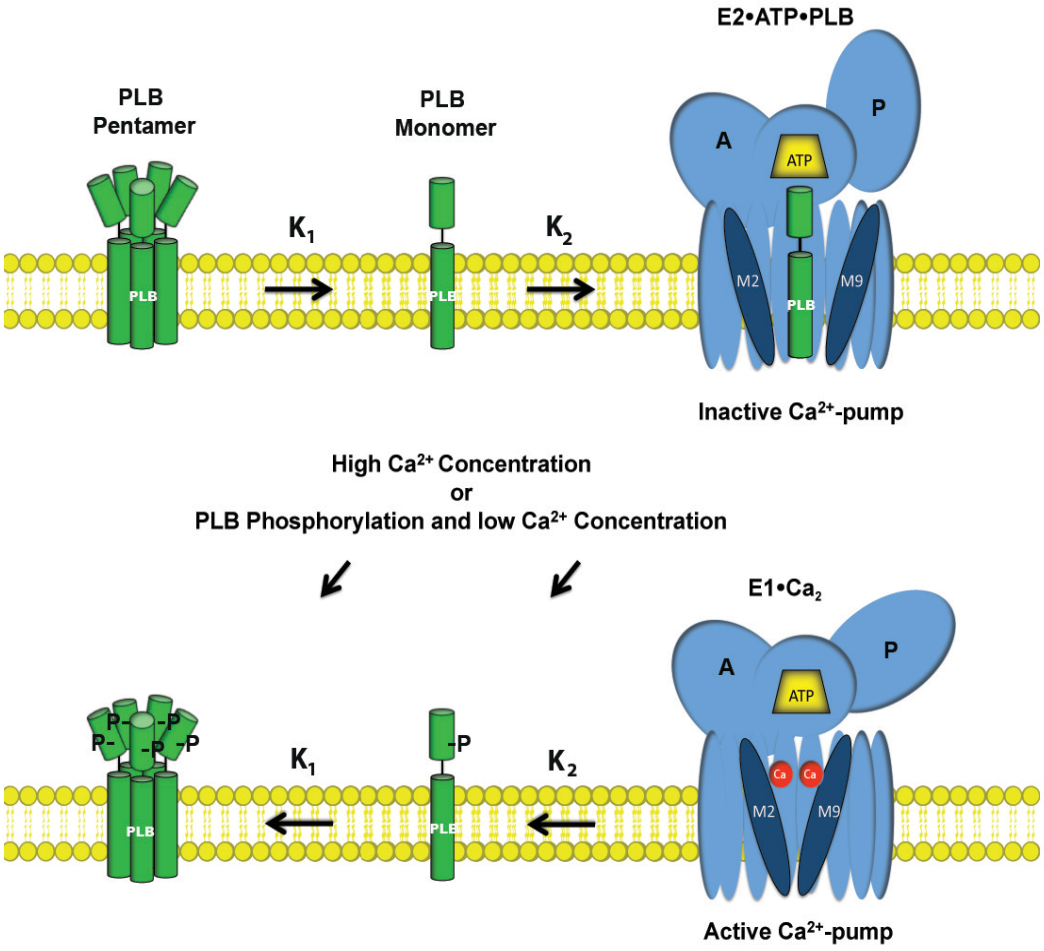

Figure 14. Our Model of PLB Regulation of SERCA2a Activity There is a dynamic equilibrium between PLB pentamers, PLB monomers, and PLB/SERCA2a heterodimers. PLB binds exclusively to the *E*2·ATP conformation of the Ca^{2+} pump and immobilizes it in this state. Ca^{2+}-ATPase inhibition by PLB is reversed by complete dissociation of PLB from SERCA2a, induced by micromolar Ca^{2+} concentration or by PLB phosphorylation and low micromolar Ca^{2+} concentration.

This model of mutually exclusive binding of PLB and Ca^{2+} is consistent with the crystal structures of SERCA2a determined in both the *E*1 and *E*2 states (17, 18). Cross-linking studies predict that PLB binds to *E*2 of SERCA2a within a groove formed between transmembrane helices M2, M4, and M9 (**Fig. 6**). When SERCA2a is in *E*1 with bound Ca^{2+}, this groove is closed at the C-terminus (17, 18), blocking PLB access to the binding pocket.

However, despite strong biochemical and structural evidence supporting this model of PLB regulation of SERCA2a, several alternate models of PLB inhibition have recently emerged. These models differ from the model just described in three main respects:

1) We maintain that PLB binding interactions with SERCA2a are dynamic, and PLB associates and dissociates from the enzyme in a Ca^{2+}-dependent fashion. On the other hand, other groups maintain that PLB is essentially a subunit of SERCA2a that remains tightly bound to the enzyme throughout the catalytic cycle (36, 37).

2) According to our model, PLB binds exclusively to the *E*2·ATP conformation of the Ca^{2+} pump and blocks the *E*2 to *E*1 transition. However, others have suggested that PLB acts elsewhere, or at multiple points in the catalytic cycle to slow or inhibit enzyme turnover (36-41).

3) Our model states that high Ca^{2+} concentration completely dissociates PLB from the Ca^{2+} pump. Therefore, at saturating Ca^{2+} concentration, PLB is not bound, and has no effect on maximal Ca^{2+}-ATPase activity. On the contrary, several recent studies have reported that PLB either decreased or increased the V_{max} of the Ca^{2+}-ATPase at saturating Ca^{2+} concentration (42-45).

G. PURPOSE

The purpose of this dissertation research was to critically evaluate our model of PLB regulation of SERCA2a, and to clarify the major points of discrepancy

between our model and the other current models. To do this I proposed three hypotheses to be tested, each one specifically designed to address a fundamental point in the mechanism of PLB action.

1. HYPOTHESIS 1: SERCA2a WITH PLB BOUND IS CATALYTICALLY INACTIVE

There are two schools of thought with respect to PLB binding interactions with SERCA2a. In the first, PLB is essentially a subunit of SERCA2a that remains tightly bound to the enzyme throughout its entire reaction cycle. Using fluorescent probes to monitor interactions between PLB and SERCA in both reconstituted and native membranes, Li *et al*. (36) and Chen *et al.* (37) concluded that PLB binds so tightly to SERCA2a that it essentially never dissociates, remaining bound to the enzyme throughout the full catalytic cycle. On the other hand, several groups, including ours, have shown that there is a dynamic equilibrium between PLB pentamers, PLB monomers, and PLB-SERCA heterodimers (21, 46-50). Moreover, based upon our recent work with chemical cross-linking we have proposed that PLB stabilizes the Ca^{2+} free, *E*2·ATP conformation of SERCA2a and blocks the *E*2 to *E*1 transition. In order for enzyme to transition to *E*1 and initiate Ca^{2+} transport, PLB must first completely dissociate from the enzyme (6, 21-23). Thus, at any given time within a cardiomyocyte, there are two distinct populations of SERCA2a: one inactive population of SERCA2a with bound PLB (SERCA2a·PLB), and a second active, PLB-free population, pumping Ca^{2+} at the normal rate.

a. TESTING THE CATATLYTIC ACITIVITY OF SERCA2a WITH PLB BOUND

To address this point of uncertainty, I developed a method to test the catalytic activity of SERCA2a with PLB irreversibly bound to it. First, chemical cross-linkers were used to covalently couple PLB to SERCA2a to form PLB/SER (PLB/SER refers to PLB covalently cross-linked to SERCA2a), and Ca^{2+}-ATPase activity was

measured. Then, [γ-^{32}P]ATP and $^{32}P_i$ were used to phosphorylate PLB/SER, in order to determine if SERCA2a can undergo the catalytic half-reactions to form *E*1~P and *E*2-P, respectively, when PLB is bound. Finally, PLB-free SERCA2a was resolved from PLB/SER via a cross-linking induced mobility-shift on LDS-PAGE, while maintaining the labile acyl-phosphate of *E*1~P and *E*2-P. These experiments revealed that PLB/SER was entirely catalytically inactive and unphosphorylatable by either [γ-^{32}P]ATP or $^{32}P_i$, and thus forcibly kinetically stalled by the binding of PLB.

2. HYPOTHESIS 2: PLB DECREASES THE Ca^{2+} AFFINITY OF SERCA2a BY COMPETING WITH Ca^{2+} FOR BINDING TO SERCA2a

It is generally accepted that PLB decreases the apparent Ca^{2+} affinity of the SERCA2a, while having little or no effect on the V_{max} of the enzyme measured at saturating Ca^{2+} concentration (2, 3). However, whether PLB increases the K_{Ca} of Ca^{2+}-ATPase activation by decreasing the actual Ca^{2+} binding affinity of the enzyme (21, 23, 44, 51) or by affecting one or more catalytic steps in the reaction cycle (36-41) has remained unclear. Cantilina *et al.* (38) originally proposed that that PLB decreases the apparent Ca^{2+} affinity of SERCA2a by slowing the isomeric transition that follows binding of the first Ca^{2+} ion, enabling cooperative binding of the second Ca^{2+} ion. According to this model, PLB does not affect the actual Ca^{2+} binding affinity of SERCA2a (the actual amount of Ca^{2+} bound to the enzyme at a given low Ca^{2+} concentration), but rather the kinetics of enzyme activation by bound Ca^{2+}. On the other hand, our cross-linking results suggest that mutually exclusive binding of PLB and Ca^{2+} is the underlying mechanism of Ca^{2+}-ATPase inhibition by PLB. If PLB competes for Ca^{2+} binding to SERCA2a by stabilizing the Ca^{2+}-free enzyme in *E*2, and antagonizing formation of *E*1, then by mass action, PLB should decrease the fraction of Ca^{2+} pumps available to bind and transport Ca^{2+} at sub-saturating Ca^{2+} concentration. This would be manifested as a decrease in the apparent Ca^{2+} affinity of the Ca^{2+}-ATPase (2, 3).

a. USING CROSS-LINKABLE PLB SUPERSHIFTERS TO TEST FOR COMPETITIVE BINDING OF PLB AND Ca^{2+} TO SERCA2a

Ideally, to test the theory that PLB competes with Ca^{2+} for binding to SERCA2a, Ca^{2+} binding assays would be used to directly determine if a population of Ca^{2+} pumps expressed alone and free from PLB bind Ca^{2+} with higher affinity than a population of Ca^{2+} pumps co-expressed with PLB. Unfortunately, accurate measurement of Ca^{2+} binding affinity with $^{45}Ca^{2+}$ requires relatively high expression levels of the Ca^{2+} ATPase (52), which is difficult to achieve in recombinant systems (53). As an alternative, we have shown that the Ca^{2+} affinity of the enzyme is accurately estimated by assaying Ca^{2+} inhibition of PLB cross-linking to SERCA2a. For example, **Fig. 9** shows that PLB cross-linking was inhibited by micromolar Ca^{2+}concentration over the same concentration range as enzyme activation occurs. However, since cross-linking assays cannot be used to assess the Ca^{2+} affinity of SERCA2a expressed alone, the direct effect of PLB on Ca^{2+} affinity has yet to be determined. I overcame this limitation by instead comparing the effects of series of cross-linkable PLB mutants of increasing inhibitory strength on Ca^{2+} binding to the Ca^{2+} pump. If PLB competes for Ca^{2+} binding to the Ca^{2+}-ATPase, then as PLB becomes a stronger inhibitor of enzyme activity, higher concentrations of Ca^{2+} should be required to dissociate it from the Ca^{2+} pump.

Two cross-linkable supershifters, PLB3 (N27A, N30C, L37A-PLB) and PLB4 (N27A, N30C, L37A, V49G-PLB), were made by combining the N30C cross-linking mutation with other gain-of-function mutations (**Fig. 15**). PLB3 and PLB4 are strongly inhibitory compared to N30C-PLB (which has a normal inhibitory strength (21)), while remaining cross-linkable to the Ca^{2+}-pump, thus allowing their physical interactions with SERCA2a to be measured simultaneously with their functional effects on enzyme activity. The results, described in detail below, showed that higher concentrations of Ca^{2+} were required to both activate the enzyme co-expressed with the increasingly inhibitory PLB mutants and to dissociate the PLB mutants from the Ca^{2+} pump, consistent with PLB competing with Ca^{2+} for binding to the enzyme.

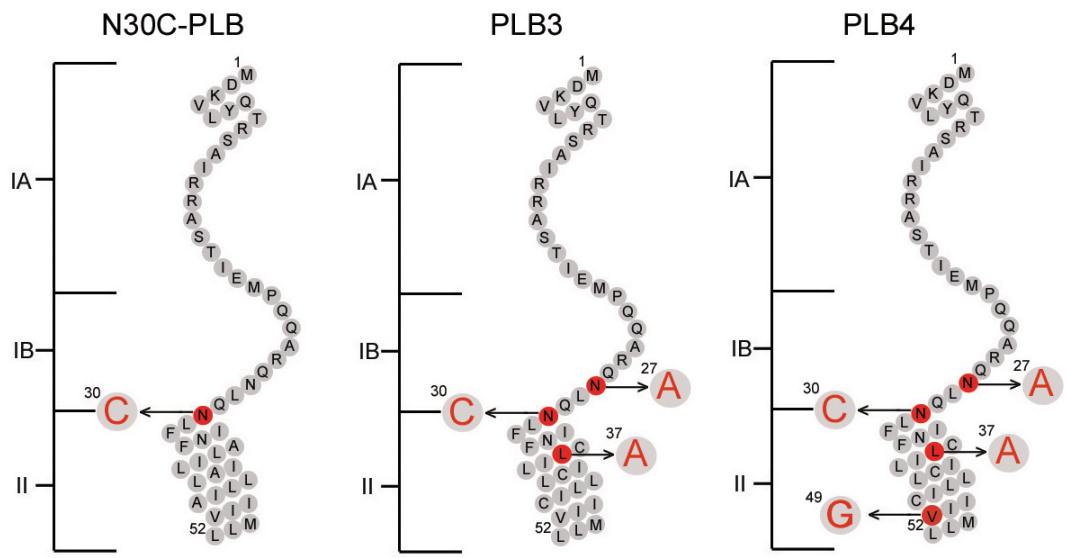

Figure 15. Complete Amino Acid Sequences of the Cross-linkable PLB Mutants, N30C-PLB, PLB3, and PLB4 I and II designate cytoplasmic and transmembrane domains of PLB, respectively. Domain IA contains Ser^{16} and Thr^{17}, the residues phosphorylated in response to β-adrenergic stimulation. The point mutations N27A in domain IB (28) and L37A (26, 27) and V49G (22, 31) in domain II are all supershifting mutations. The N30C mutation in domain IB allows PLB to be cross-linked to Lys^{328} of SERCA2a with KMUS (21). For consistency with previous publications, N30C-PLB was made on the Cys-less PLB background in which Cys residues 36, 41, and 46 were mutated to Ala (6, 21-23). From **Akin, B.L.**, Chen, Z., and Jones, L.R (2010) *J.Biol.Chem*. **285**, 28540-28552.

b. USING CROSS-LINKABLE PLB SUPERSHIFTERS IN CONJUNCTION WITH D351A-SERCA2a TO TEST FOR COMPETITIVE BINDING OF PLB AND Ca^{2+}

To test directly for competition between PLB and Ca^{2+} for binding to SERCA2a, I also took advantage of the Ca^{2+}-pump mutant, D351A. During catalysis, Asp^{351} is phosphorylated by ATP to form the high-energy acylphosphoprotein intermediate, $E1{\sim}P{\cdot}Ca_2$ (**Fig. 4**). Replacement of aspartic acid at this position renders the enzyme catalytically inactive (53, 54). Although inactive at the site of ATP hydrolysis, D351A retains the ability to bind Ca^{2+} and maintains the thermodynamic

equilibrium between *E*1 and *E*2 (53, 55, 56). Therefore, if PLB acts by stabilizing *E*2 and shifting the $E1 \cdot Ca_2 \leftrightarrow E2 \cdot$PLB equilibrium away from *E*1, then like the wild-type enzyme, higher concentrations of Ca^{2+} should be required to dissociate the increasingly inhibitory PLB mutants from D351A. The advantage of using D351A for these experiments is that enzyme turnover is prevented, therefore the system is at equilibrium with respect to Ca^{2+} binding (**Fig. 4**). The results showed that like wild-type SERCA2a, higher concentrations of Ca^{2+} were required to inhibit cross-linking of the increasingly inhibitory PLB mutants to D351A.

c. DETERMINING THE EFFECT OF PLB ON MAXIMAL Ca^{2+}-ATPASE ACTIVITY

If PLB binding and Ca^{2+} binding to SERCA2a are mutually exclusive, and micromolar Ca^{2+} concentration completely dissociates PLB from the Ca^{2+} pump, then at saturating Ca^{2+}concentration PLB should have no effect on maximal enzyme activity, relative to SERCA2a expressed alone. On the other hand, in several recent studies PLB was reported to either decrease (44) or increase (42, 43, 45) the V_{max} of the Ca^{2+}-ATPase. To address this discrepancy directly, maximal Ca^{2+}-ATPase activity of SERCA2a expressed alone was compared to that of SERCA2a co-expressed with PLB mutants of normal (N30C-PLB) and superinhibitory strength (PLB3 and PLB4). Importantly, prior to functional analysis, quantitative Western blotting was used to carefully determine protein expression levels in the membranes, and Ca^{2+}-ATPase activities were corrected for variability in SERCA2a expression between preparations. The results showed that PLB molecules of normal inhibitory strength (N30C-PLB) did not significantly affect the V_{max} of the Ca^{2+}-ATPase, whereas the superinhibitory PLB mutants, PLB3 and PLB4, reduced the V_{max} of the enzyme substantially.

3. HYPOTHESIS 3: PLB BINDS EXCLUSIVELY TO THE *E*2·ATP CONFORMATION OF THE Ca^{2+} PUMP

a. INVESTIGATING THE CONFORMATIONAL SPECIFICTY OF THE PLB TO SERCA2a BINDING INTERACTION USING THE EFFECTORS TG, VANADATE, AND NUCLEOTIDES (ATP, ADP AND AMP)

In previous studies we have shown that PLB cross-linking to SERCA2a is completely inhibited by Ca^{2+} (*E*1·Ca_2), thapsigargin (*E*2·TG), and P_i (*E*2·P_i and *E*2-P), but augmented substantially by ATP (6, 21-23). Based upon these results we proposed that PLB binds exclusively to the Ca^{2+}-free *E*2 state of SERCA2a, preferentially with bound nucleotide, *E*2·ATP. According to this model, the superinhibitory PLB mutants, PLB3 and PLB4, should also bind preferentially to the *E*2·ATP state, only more tightly than N30C-PLB. Therefore, to gain further insights on the specific conformation of the Ca^{2+} pump that binds PLB, and to estimate the relative binding affinities of the PLB mutants for SERCA2a, the effects of thapsigargin, vanadate, and nucleotides on PLB cross-linking to SERCA2a were determined. The results indicate that the PLB supershifters also act by stabilizing the *E*2·ATP conformation of the Ca^{2+} pump. Moreover, we were able to estimate the binding affinity of the different PLB mutants for SERCA2a. In the presence of ATP, N30C-PLB had an affinity for *E*2·ATP approaching that of vanadate (micromolar), whereas PLB3 and PLB4 had much higher affinities, several fold greater than even TG, the highest affinity SERCA2a inhibitor yet reported (nanomolar or higher).

CHAPTER 2—EXPERIMENTAL PROCEDURES

A. MATERIALS

The cross-linking agent KMUS was purchased from Pierce. [γ-^{32}P]ATP was obtained from PerkinElmer Life Sciences, and thapsigargin and sodium orthovanadate were purchased from Sigma.

B. MUTAGENISIS AND BACULOVIRUS PRODUCTION

The baculovirus expression system was used to co-express the canine isoforms of both WT and mutant SERCA2a and PLB in insect cell membranes. Mutation of canine SERCA2a and PLB cDNAs was conducted as described previously (27). For consistency with previous cross-linking studies, N30C-PLB was made on the Cys-less PLB background, in which Cys residues 36, 41, and 46 were mutated to Ala (21). N30C-PLB has been previously well characterized, and is fully functional with an inhibitory potency similar to wild-type PLB (21). In control experiments, identical results were obtained when N30C-PLB was made on the wild-type PLB background with Cys residues 36, 41, and 46 unaltered (data not shown). cDNAs encoding PLB3 and PLB4 were generated on the wild-type PLB cDNA background inserted in the transfection vector pVL1393, using the QuickChange™ XL-Gold system (Stratagene). D351A was made similarly using canine cardiac SERCA2a cDNA as the template (21). All mutated cDNAs were confirmed by DNA sequencing of the plasmid vectors. Baculoviruses encoding mutated proteins were generated as described previously with BaculoGold™ (Pharmengen) linearized baculovirus DNA (21).

C. PROTEIN EXPRESSION AND CHARACTERIZATION

Sf21 insect cells were co-infected with baculoviruses encoding PLB and SERCA2a as described previously (27). Viral titers were adjusted to give an expression level of PLB to SERCA2a of approximately 4:1, as used in previous publications (6, 21-23). Cells were harvested 60 h after co-infection, washed with

phosphate-buffered saline, and homogenized with a Polytron for 90 s at 15,000 rpm. Crude microsomal pellets were then collected by centrifuging at 48,000 x g for 20 min. Microsomes were re-suspended at a protein concentration of 6-10 mg/ml in 0.25 M sucrose, 10 mM MOPS (pH 7.0) and stored frozen in small aliquots at -40 °C. Protein concentrations were determined by the Lowry method. PLB and SERCA2a contents in the membrane samples were determined by quantitative Western blotting with the monoclonal antibodies, 2D12 and 2A7-A1, respectively (21). Only membranes expressing PLB and SERCA2a at a molar ratio of approximately 4:1 were used for further analyses.

D. Ca^{2+}-ATPASE ASSAY

Ca^{2+}-ATPase activities were measured at 37 °C in buffer containing 50 mM MOPS (pH 7.0), 100 mM KCl, 3 mM $MgCl_2$, 3.0 mM ATP, 5 mM NaN_3, 3 μg/ml of the Ca^{2+} ionophore, A23187, and 1 mM EGTA. Ionized Ca^{2+} concentrations were set by varying the $CaCl_2$ concentration from 0-1.2 mM. In certain assays, only maximal Ca^{2+}-ATPase activity was measured in the absence of EGTA and with 50 μM added $CaCl_2$ (**Figs. 16** and **17**). Some assays were conducted in the presence and absence of the anti-PLB monoclonal antibody, 2D12, which reverses PLB inhibition of SERCA2a (5, 6, 57). Ca^{2+}-dependent ATPase activities were determined in a reaction volume of 1 ml containing 50 -100 μg of membrane protein during a 30 - 60 min incubation. P_i release from ATP was measured colorimetrically (21). Maximal Ca^{2+}-ATPase activities ranged between 15 and 25 μmol of P_i/mg of protein/h for all samples, which is approximately 25-40% of the maximal Ca^{2+}-ATPase activity typically reported for dog cardiac SR vesicles (57). In some Ca^{2+}-ATPase assays, small aliquots were taken from the assay tubes during the incubations, in order to simultaneously measure PLB cross-linking to SERCA2a (see below). K_{Ca} values are the Ca^{2+} concentrations at which the Ca^{2+}-ATPase is half maximally active as determined directly from the data plots.

E. CROSS-LINKING PLB TO SERCA2a

1. STANDARD CROSS-LINKING (SMALL SCALE)

In most experiments, cross-linking of N30C of PLB to Lys^{328} of SERCA2a with KMUS was conducted identically as previously described (22). Cross-linking reactions were conducted with 11 μg of membrane protein in 12 μl of buffer. The final concentrations of PLB and SERCA2a in the cross-linking tubes were 1.2 μM and 0.3 μM, respectively. Standard cross-linking buffer contained 50 mM MOPS (pH 7.0), 3.0 mM $MgCl_2$, 100 mM KCl, 3 mM ATP, and 1 mM EGTA with zero to 1.2 mM added $CaCl_2$. In some experiments, ATP concentrations were varied, or different nucleotides were used, as indicated in the figure legends. In the experiments with the SERCA2a inhibitors TG and vanadate, TG was added from a 1 mM stock solution in ethanol, and sodium orthovanadate was added from a 15 mM stock solution in H_2O. Cross-linking reactions were started by adding 0.75 μl of 1.6 mM KMUS dissolved in Me_2SO (final KMUS concentrations 0.1 mM), and incubated for 2 min at room temperature. Reactions were stopped by adding 7.5 μl of gel loading buffer containing 15% SDS and 100 mM dithiothreitol. Samples were subjected to SDS-PAGE, and Western blotting with the anti-PLB antibody, 2D12, using ^{125}I-protein A or alkaline phosphatase for PLB visualization. In the experiments measuring the effects of 2D12, blots were probed directly with ^{125}I-2D12, and protein A was omitted (6). Radioactive signals (representing SERCA2a with bound PLB) were quantified using a Bio-Rad Personal Fx Phosphoimager. The K_i values for inhibition of PLB cross-linking were determined directly form the data plots, and is the Ca^{2+}, TG, or vanadate concentration at which cross-linking was 50% inhibited.

2. LARGE SCALE CROSS-LINKING

In order test the catalytic activity of PLB-bound SERCA2a, PLB was cross-linked to SERCA2a on large-scale (PLB/SER), and then the catalytic activity of PLB/SER was determined by measuring its ability to hydrolyze ATP and to be phosphorylated with [γ-^{32}P]ATP or $^{32}P_i$, to form *E*1~P and *E*2-P, respectively. "Pre-cross-linking" the membranes on large scale in advance allowed for multiple

phosphorylation experiments (by both [γ-^{32}P]ATP and $^{32}P_i$) to be performed on identical membranes, eliminating a potential source of variability. Also, pelleting and re-suspending the cross-linked membranes prior to storage eliminated the excess cross-linker, ATP, and Ca^{2+} present during the initial cross-linking reaction.

Large scale cross-linking was done similar to the standard cross-linking described above, only 2.75 mg instead of 11 μg of membranes were used per reaction tube, and 300 μl Ca^{2+}-EGTA buffer was added to achieve free Ca^{2+} concentrations between 0 and 16.7 μM. Reactions were started with the addition of 187 μl of 1.6 mM KMUS in Me_2SO and incubated for 3 min; the final reaction volume was 3 ml. The reactions were stopped with the addition of 125 μl of 500 mM glycine and 500 mM DTT. The cross-linked membranes were centrifuged for 10 min at 100 K at 4 °C in a Beckman TL-100 centrifuge. The membranes were re-suspended in 10 mM MOPS and 0.25 M sucrose (pH 7.2) and stored in small aliquots at -80 °C.

3. CROSS-LINKING UNDER Ca^{2+}-ATPASE CONDITIONS

To assess Ca^{2+} effects on PLB cross-linking to SERCA2a, experiments were conducted at 37 °C in the same buffer used for measurement of Ca^{2+}-ATPase activity, as described above. 15 min after initiation of Ca^{2+}-ATPase reactions with ATP, 80 μl aliquots containing 8 μg of membrane protein were taken from Ca^{2+}-ATPase assay tubes and cross-linked with 1 mM KMUS for 15 s, giving the maximal cross-linking obtainable at each Ca^{2+} concentration tested. Reactions were stopped with gel loading buffer, and samples were then processed as described above. Cross-linking of PLB to D351A to assess Ca^{2+} affinity was determined under identical conditions.

It should be pointed out that the heterobifunctional cross-linker KMUS reacts irreversibly with Lys^{328} of SERCA2a and N30C of PLB whether the two proteins are bound or not. If the two proteins are bound when the cross-linker is added, then PLB is irreversibly cross-linked to SERCA2a by a single KMUS molecule. If the proteins are not bound when the cross-linker is added, then N30C of PLB can react with one KMUS molecule, and Lys^{328} of SERCA2a can react with a second KMUS molecule, thus blocking additional cross-linking of the two proteins as new PLB-SERCA2a

complexes are formed. Therefore, the amount of PLB-SERCA2a complex detected by cross-linking is essentially a "snapshot" of the amount of PLB-SERCA2a complex present at the time at which the cross-linker is added.

F. MONITORING FORMATION OF THE PHOSPHORYLATED INTERMEDIATES, *E*1~P AND *E*2-P

1. PHOSPHORYLATION OF *E*1·Ca_2 BY [γ-^{32}P]ATP

Phosphorylation of SERCA2a using [γ-^{32}P]ATP was conducted by incubating 11 μg of membrane protein (virgin membranes or pre-cross-linked membranes) in 12 μl buffer containing 50 mM MOPS (pH 7.0), 3.0 mM $MgCl_2$, 100 mM KCl, 1 mM EGTA, and 0 to 1.2 mM $CaCl_2$. Maximal *E*1~P formation was measured in the absence of EGTA and with 1 mM added $CaCl_2$. Phosphorylation was initiated by adding a final concentration of 200 μM [γ-^{32}P]ATP and conducted for 5 s at room temperature. Reactions were terminated with 7.5 μl of acidic gel loading buffer (pH 2.4) containing 3% LDS, and LDS-PAGE was conducted under acidic conditions as recently described (22). After electrophoresis, proteins were transferred to nitrocellulose and the radioactive acylphosphoprotein bands were visualized by autoradiography and quantified with the Fx Phosphoimager.

2. PHOSPHORYLATION OF *E*2 BY $^{32}P_i$ (BACK DOOR PHOSPHORYLATION)

Phosphorylation of SERCA2a by $^{32}P_i$ to form *E*2~P was done in buffer favoring formation of *E*2 (i.e. at pH 7.0, in the presence Me_2SO and in the absence of KCl, ATP, and Ca^{2+}). 11 μg of membranes were added to 12 μl buffer containing 40 mM MOPS, (pH 7.0), 20 mM $MgCl_2$, 20% Me_2SO, and 1.0 mM EGTA. Reactions are started by adding 1.0 μl of 3 mM P_i containing trace amounts of $^{32}P_i$. After a 10 min incubation at room temperature, the reactions were stopped with 7.5 μl LDS-PAGE sample loading buffer containing 3% LDS and the samples were processed as described above for the [γ-^{32}P]ATP-labeled samples.

CHAPTER 3—RESULTS

A. HYPOTHESIS 1: SERCA2a WITH BOUND PLB IS CATALYTICALLY INACTIVE

1. LARGE SCALE PRE-CROSS-LINKING OF N30C-PLB TO SERCA2a

SERCA2a was co-expressed with N30C-PLB in Sf21 insect cells, and the membranes were pre-cross-linked (N30C of PLB to Lys^{328} of SERCA2a) on large scale over a Ca^{2+} concentration range of 0–16.4 μM using the heterobifunctional cross-linker KMUS. After the cross-linking reactions were terminated, the membranes were pelleted, re-suspended, and stored in small aliquots at -80 °C until needed. The pre-cross-linked membranes were characterized by Western blotting with the anit-SERCA2a (2A7-A1) and anti-PLB (2D12) monoclonal antibodies. Total SERCA2a content in the membrane samples is shown in the upper panel of **Fig. 16A**, and the fraction of Ca^{2+} pumps pre-cross-linked to PLB (PLB/SER) is shown in the lower panel. As predicted based upon previous results, as Ca^{2+} concentration during the pre-cross-linking reaction was increased, N30C-PLB cross-linking to SERCA2a was inhibited. The plot of PLB/SER content in the membranes is shown in **Fig. 16B**. Maximal Ca^{2+}-ATPase activity of the pre-cross-linked membranes was then measured at saturating Ca^{2+} concentration (50 μM Ca^{2+}). Percent maximal Ca^{2+}-ATPase activity was then plotted against PLB/SER for each pre-cross-linked sample (**Fig. 16B**). Importantly, maximal Ca^{2+}-ATPase activities were inversely proportional to PLB/SER levels detected in the membranes by Western blotting. This indicates that there is a tight correlation between PLB cross-linking to SERCA2a, and inhibition of Ca^{2+}-dependent hydrolysis of ATP by the Ca^{2+} pump. This result demonstrates directly that when PLB is irreversibly bound to SERCA2a, the enzyme is catalytically inactive, and suggests that PLB immobilizes the enzyme in a Ca^{2+}-free state. Although this result shows that the overall catalytic cycle of SERCA2a is blocked by PLB binding, I went on to test whether the phosphorylation half-reactions

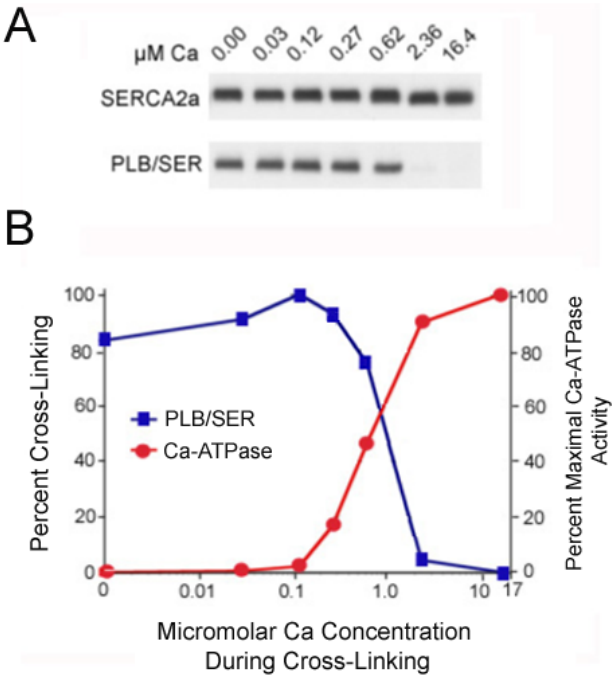

Figure 16. Effect of PLB Cross-linking to SERCA2a on Maximal Ca^{2+}-ATPase Activity N30C-PLB and SERCA2a were co-expressed in Sf21 insect cells. The membranes were then pre-cross-linked on large scale with the heterobifunctional cross-linker KMUS over a range of Ca^{2+} concentration 0-16.4 μM, as described in the METHODS. The pre-cross-linked membranes were then pelleted and re-suspended prior to Western blot characterization and functional analysis. A, Pre-cross-linked membrane samples were subjected to SDS-PAGE and immunoblotting with the anti-SERCA2a (upper blot, SERCA2a) and anti-PLB (lower blot, PLB/SER) antibodies. PLB/SER shows SERCA2a cross-linked to PLB. B, The plot shows the PLB/SER content in the samples pre-cross-linked at the Ca^{2+} concentration shown on the axis (blue). Percent maximal Ca^{2+}-ATPase activity of the same samples measured at 50 μM Ca^{2+} (red).

(forming *E*1~P and *E*2-P from [γ-^{32}P]ATP and $^{32}P_i$, respectively) were also blocked by PLB binding

2. PHOSPHORYLATION OF PRE-CROSS-LINKED MEMBRANES WITH [γ-^{32}P]ATP AND $^{32}P_i$ to from *E*1~P and *E*2-P

The membrane samples containing N30C-PLB pre-cross-linked to SERCA2a over a range of Ca^{2+} concentrations (0–16.4 μM) were phosphorylated under conditions favoring maximal phosphorylation by either [γ-^{32}P]ATP (at pH 7.0, in

buffer containing $MgCl_2$, KCl, and high Ca^{2+} concentration) or $^{32}P_i$, (at pH 7.0, in the presence Me_2SO and in the absence of KCl, ATP, and Ca^{2+}) to from *E*1~P and *E*2-P, respectively. Autoradiographs showing formation of *E*1~P and *E*2-P are shown in **Fig. 17A**. N30C-PLB cross-linking to SERCA2a was inhibited as the Ca^{2+} concentration during the pre-cross-linking reaction was increased, and formation of both *E*1~P and *E*2-P increased as cross-linking was inhibited (**Fig. 17A**). The plots of the signals of formation of *E*1~P and *E*2-P were virtually super-imposable with each other and with the plot of maximal Ca^{2+}-ATPase activity. Therefore, formation of the phosphorylated intermediates, *E*1~P and *E*2-P, and maximal Ca^{2+}-ATPase activity was inversely proportional to PLB/SER content in the membranes (**Fig. 17B**). This inverse correlation between PLB cross-linked to SERCA2a and *E*1~P and *E*2-P formation corroborates the results of the Ca^{2+}-ATPase assay, further supporting idea that SERCA2a with PLB bound is catalytically inactive.

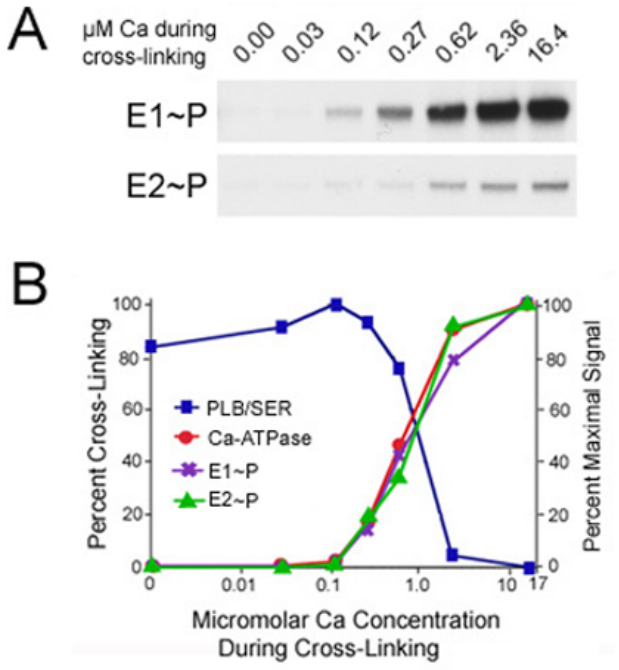

Figure 17. Effect of PLB Cross-Linking to SERCA2a on Maximal *E*1~P and *E*2-P Formation
A, Autoradiogram shows maximal *E*1~P and *E*2-P formation from [γ-^{32}P]ATP and $^{32}P_i$, respectively, in membranes containing N30C-PLB and SERCA2a pre-cross-linked to SERCA2a at the Ca^{2+} concentration shown. B, Plot shows percent maximal *E*1~P formation (purple x's), *E*2-P formation (green triangles), and Ca^{2+}-ATPase activity (red circles) measured in the pre-cross-linked membranes, plotted against the percent maximal cross-linking signal PLB/SER (blue squares).

3. RESOLUTION OF PLB-FREE SERCA2a (CATALYTICALLY ACTIVE SERCA2a) FROM PLB/SER (CATALYTICALLY INACTIVE SERCA2a)

When cross-linked to PLB, SERCA2a undergoes a small mobility shift that causes it to run at a slightly higher molecular weight on acrylamide gels than PLB-free SERCA2a (6). I took advantage of this cross-linking induced mobility shift in order to resolve SERCA2a from PLB/SER, to definitively determine if PLB/SER is phosphorylatable by either [γ-^{32}P]ATP or $^{32}P_i$. Three specific pre-cross-linked samples containing ~100%, 50%, and 0% PLB/SER (0%, 50%, and 100% maximal Ca^{2+}-ATPase activity, respectively) were phosphorylated with either [γ-^{32}P]ATP or $^{32}P_i$, subjected to LDS-PAGE, and transferred to nitrocellulose. Autoradiographs of the radioactive signals of *E*1~P and *E*2-P formation were obtained. The [γ-^{32}P]ATP series was probed with 2A7-A1 (anti-SERCA2a antibody) and the $^{32}P_i$ series was probed with 2D12 (anti-PLB antibody) followed by alkaline phosphatase.

The cross-linking-induced mobility shift is clearly visible in the Western blot detecting the Ca^{2+}-ATPase protein (**Fig. 18A**, SERCA2a panel 1). The ~100% cross-linked sample ran as a single, slightly higher molecular weight band (PLB/SER). The ~50% cross-linked sample ran as a doublet with an upper band containing PLB/SER, and a slightly lower band containing PLB-free SERCA2a. In the ~0% cross-linked sample, the Ca^{2+} pump ran as a single lower band (PLB-free SERCA2a). Consistent with this interpretation, in the 2D12 Western blot showing only SERCA2a cross-linked to PLB (**Fig. 18A**, PLB/SER panel 2), only the upper band of the SERCA2a doublet reacted with the anti-PLB antibody. These results confirm that PLB/SER and PLB-free SERCA2a run with slightly different mobility on acrylamide gels, forming two distinct bands. When the previously obtained autoradiographs showing formation of *E*1~P and *E*2-P (**Fig. 18A**, *E*1~P panel 3, and *E*2-P panel 4) were superimposed over the SERCA2a doublet, only the lower band containing PLB-free SERCA2a had been phosphorylated by either [γ-^{32}P]ATP or $^{32}P_i$. Therefore, whereas PLB-free SERCA2a readily underwent the kinetic half-reactions to form both *E*1~P and *E*2-P, PLB/SER remained entirely unphosphorylatable under all conditions.

These results confirm the hypothesis that SERCA2a with PLB bound is entirely catalytically inactive.

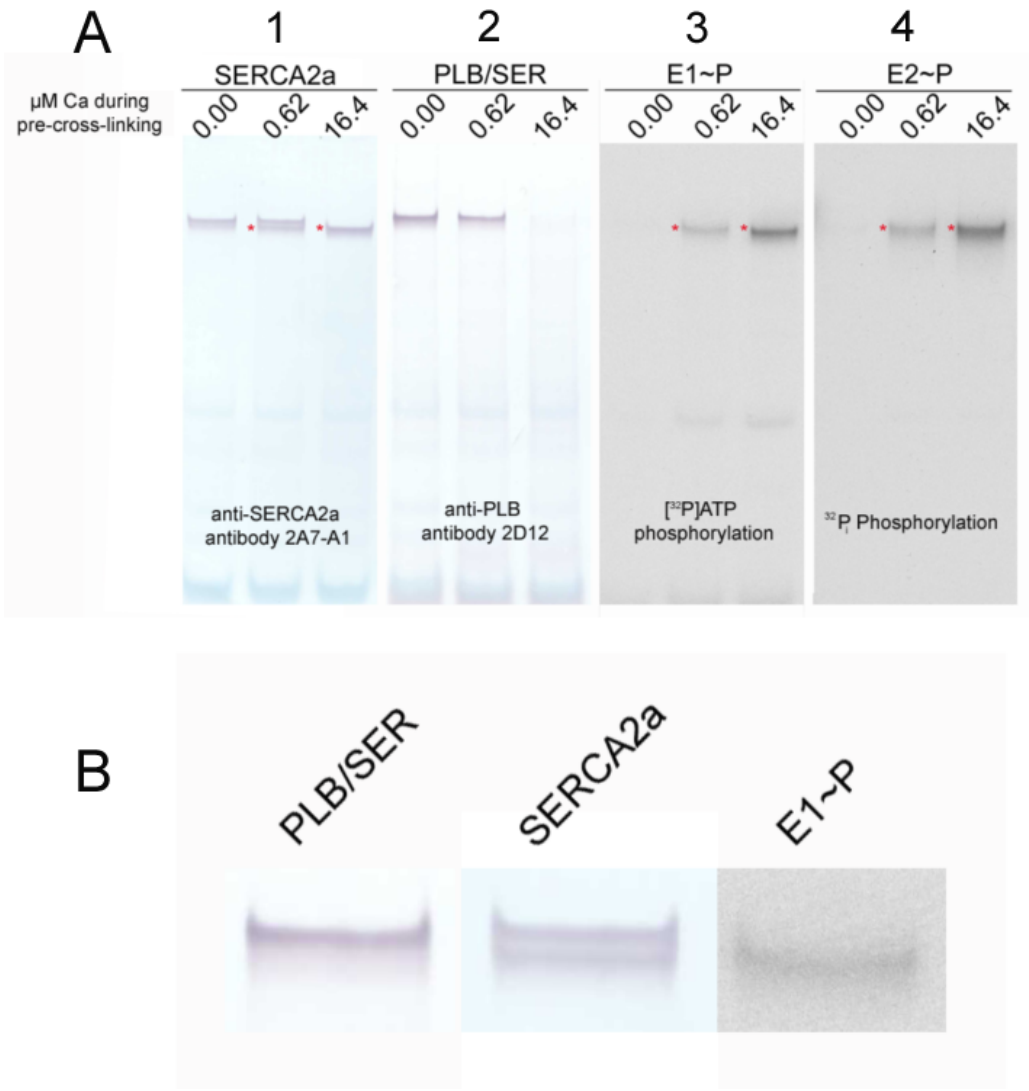

Figure 18. Phosphorylation of Pre-Cross-Linked Membranes and LDS-PAGE Resolution of PLB-free SERCA2a from PLB/SER N30C-PLB was pre-cross-linked to SERCA2a with KMUS at 0, 0.62, and 16.4 µM Ca^{2+} concentration and pelleted to remove all Ca^{2+} and excess cross-linker. Pre-cross-linked membranes were subjected to LDS-PAGE and Western blotting with the anti-SERCA2a (2A7-A1) and anti-PLB (2D12) antibodies, followed by alkaline phosphatase for protein visualization. Prior to LDS-PAGE, some of the pre-cross-linked membranes were phosphorylated under conditions favoring maximal phosphorylation by [γ-^{32}P]ATP or $^{32}P_i$, and autoradiographs showing the radioactive signals of E1~P and E2-P formation were obtained. A, panel 1 shows the total SERCA2a content in membrane samples pre-cross-linked at the Ca^{2+} concentration shown. Panel 2 shows only SERCA2a cross-linked to PLB (PLB/SER). Panel 3 shows the radioactive signal of E1~P formation form [γ-^{32}P]ATP. Panel 4 shows the radioactive signal of E2-P formation by $^{32}P_i$. Superimposition of panel 3 over panel 1 shows that only the lower band of the SERCA2a doublet was phosphorylated by [γ-^{32}P]ATP to form E1~P. Superimposition of panel 4 over panel 2 shows that only PLB-free SERCA2a was phosphorylated by $^{32}P_i$ to form E2-P. B, Close-up showing PLB/SER, total SERCA2a (SERCA2a), and maximal phosphorylation by [γ-^{32}P]ATP (E1~P) of the membrane sample pre-cross-linked at 0.62 µM Ca^{2+} concentration.

B. HYPOTHESIS 2: PLB DECREASES THE Ca^{2+} AFFINITY OF SERCA2a BY COMPETING WITH Ca^{2+} FOR BINDING TO THE ENZYME

1. CO-EXPRESSION OF SERCA2a WITH N30C-PLB, PLB3 AND PLB4

Using the Baculovirus expression system, SERCA2a was expressed alone in Sf21 insect cells, or co-expressed with N30C-PLB, PLB3, and PLB4. Protein expression levels in the membrane samples were determined by Western blotting with the anti-SERCA2a (2A7-A1) and anti-PLB (2D12) monoclonal antibodies. **Fig. 19** shows that similar levels of SERCA2a and PLB (± 20%) were co-expressed in the different membrane preparations. It should be noted that under the conditions used for SDS-PAGE (7% SDS), all three of the PLB mutants were entirely monomeric.

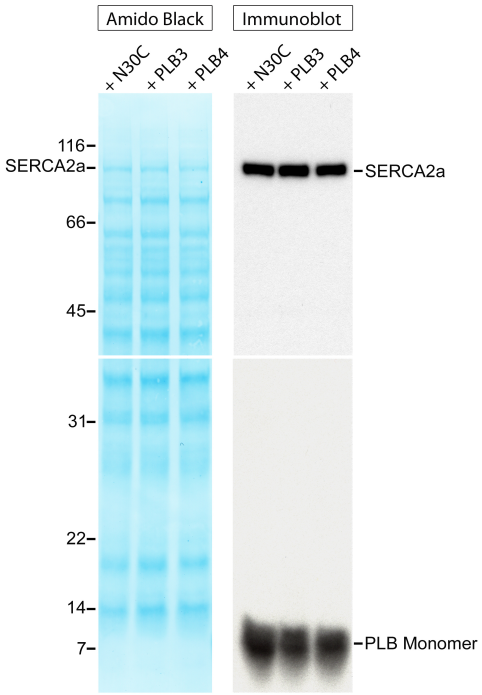

Figure 19. Amido Black Staining and Immunoblot of SERCA2a Co-Expressed with N30C-PLB, PLB3, and PLB4. SERCA2a and N30C-PLB, PLB3, or PLB4 were co-expressed in Sf21 insect cells. Membrane samples (11 µg) were then subjected to SDS-PAGE, transferred to nitrocellulose, and the nitrocellulose sheet stained with Amido Black (left panel). The nitrocellulose sheet was then cut in half, and the upper portion was probed with the anti-SERCA2a antibody, 2A7-A1, and the lower half was probed with the anti-PLB antibody, 2D12, followed by ^{125}I-protein A (right panel). Control experiments showed that the 2D12 antibody bound with equal strength to all three PLB mutants (data not shown). From **Akin, B.L.**, Chen, Z., and Jones, L.R (2010) *J.Biol.Chem*. **285**, 28540-28552.

2. Ca^{2+} ACTIVATION OF Ca^{2+}-ATPASE ACTIVITY AND Ca^{2+} INHIBITION OF PLB CROSS-LINKING TO SERCA2a

Ca^{2+}-stimulation of Ca^{2+}-ATPase activity of SERCA2a expressed alone and SERCA2a co-expressed with N30C-PLB, PLB3, and PLB4 was measured (**Fig. 20**). Based upon Western blots, Ca^{2+}-ATPase activities were corrected for variability in expression levels between preparations. SERCA2a expressed alone exhibited typical ATP hydrolysis, with half-maximal activation of Ca^{2+}-ATPase activity occurring at 0.16 μM Ca^{2+} (K_{Ca} = 0.16 μM), and maximal enzyme activity reached at the saturating Ca^{2+} concentration of 1-2 μM (**Fig. 4A** and **Table 1**). At Ca^{2+} concentrations greater than 2 μM, substantial back inhibition of the enzyme by Ca^{2+} was observed (58, 59). Co-expression of SERCA2a with N30C-PLB increased the K_{Ca} value for enzyme activation approximately 2-fold, from 0.16 μM to 0.33 μM, with little or no effect on the V_{max} of the enzyme measured at 1-2 μM Ca^{2+} (**Fig. 20A** and **Table 1**). The effect of N30C-PLB on enzyme activity observed here is identical to the effect of wild-type PLB reported previously (27). In contrast to N30C-PLB, PLB3 and PLB4 had large effects on both the K_{Ca} of enzyme activation and on V_{max}.

TABLE 1
K_{Ca} values (μM) for Ca^{2+}-ATPase activation and $E1$~P formation, and K_i values (μM) for Ca^{2+} inhibition of PLB cross-linking SERCA2a was expressed alone or co-expressed with N30C-PLB (N30C), PLB3 or PLB4 in insect cell microsomes. Ca^{2+}-ATPase activities and cross-linking were determined under identical conditions in the presence and absence of the anti-PLB antibody, 2D12, as described in the text. The $*K_{Ca}$ values shown in *parentheses* were calculated based upon the maximal activity determined for SERCA2a expressed alone (see Results). Results are means ± S.E. of 4-6 determinations.

Protein Expressed	K_{Ca} values			K_i values	
	Ca^{2+}-ATPase activity		$E1$~P	Cross-linking	
	- 2D12	+ 2D12		- 2D12	+ 2D12
SERCA2a	0.16 ± 0.01	0.16 ± 0.02	0.11 ± 0.02	ND	ND
+ N30C	0.33 ± 0.02 (*0.35 ± 0.02)	0.19 ± 0.00	0.36 ± 0.04	0.35 ± 0.03	ND
+ PLB3	0.53 ± 0.05 (*0.88 ± 0.03)	0.26 ± 0.02	1.16 ± 0.19	0.88 ± 0.02	0.27 ± 0.01
+ PLB4	0.70 ± 0.04 (*1.49 ± 0.02)	0.36 ± 0.01	2.05 ± 0.25	1.80 ± 0.17	0.45 ± 0.08

The K_{Ca} values were increased 3.3-fold (0.53 μM Ca^{2+}) and 4.4-fold (0.70 μM Ca^{2+}) by PLB3 and PLB4, respectively, when calculated based on the highest Ca^{2+}-ATPase activity achieved by SERCA2a co-expressed with these two mutants, which occurred at 2 μM Ca^{2+}. It should be noted that at 2 μM Ca^{2+} concentration, the V_{max} of the enzyme was inhibited by approximately 30% by both PLB3 and PLB4, relative to the same amount of SERCA2a expressed alone or with N30C-PLB (**Fig. 20A**). Nevertheless, complete reversal of Ca^{2+}-ATPase inhibition by PLB3 and PLB4 did occur at much higher Ca^{2+} concentrations (in the range of 100 - 200 μM), Ca^{2+} concentrations at which significant back inhibition of the enzyme occurred. Thus, in Ca^{2+}-ATPase assays, SERCA2a co-expressed with PLB3 or PLB4 can never achieve its maximal turnover rate, even though very high Ca^{2+} concentrations do completely reverse Ca^{2+}-ATPase inhibition by the supershifters. To correct for back inhibition of the enzyme by Ca^{2+}, we also calculated the K_{Ca} values for SERCA2a co-expressed with N30C-PLB, PLB3, and PLB4 using the V_{max} value for SERCA2a expressed alone (**Fig. 20A**, grey lines intersecting the abscissa) ($*K_{Ca}$ values). When calculated by this method, the $*K_{Ca}$ values for SERCA2a co-expressed with N30C-PLB, PLB3, and PLB4 were 0.35 μM, 0.88 μM, and 1.49 μM, respectively (**Table 1**, parentheses). These corrected $*K_{Ca}$ values indicate that 2.2-fold, 5.5-fold, and 9.3-fold higher Ca^{2+} concentrations are required to half-maximally activate SERCA2a co-expressed with N30C-PLB, PLB3, and PLB4, respectively.

Next, the relative binding affinities of the PLB mutants for SERCA2a were estimated by measuring Ca^{2+} inhibition of PLB cross-linking to the enzyme. All three PLB mutants cross-linked only to the cardiac Ca^{2+} pump expressed in insect cell membranes, and all cross-linking results reported here depict the PLB monomer bound to SERCA2a (**21**) (see EXPERIMENTAL PROCEDURES). In the absence of Ca^{2+}, strong cross-linking of all three PLB mutants to Lys^{328} of SERCA2a was observed, and cross-linking was completely eliminated by increasing Ca^{2+} concentration (**Fig. 20B**). The K_i values for Ca^{2+} inhibition of N30C-PLB, PLB3, and PLB4 cross-linking to SERCA2a were 0.35, 0.88, and 1.8 μM Ca^{2+}, respectively (**Table 1**). These K_i values for Ca^{2+} inhibition of cross-linking agree closely with the $*K_{Ca}$ values determined for half-maximal activation of Ca^{2+}-ATPase activity. This

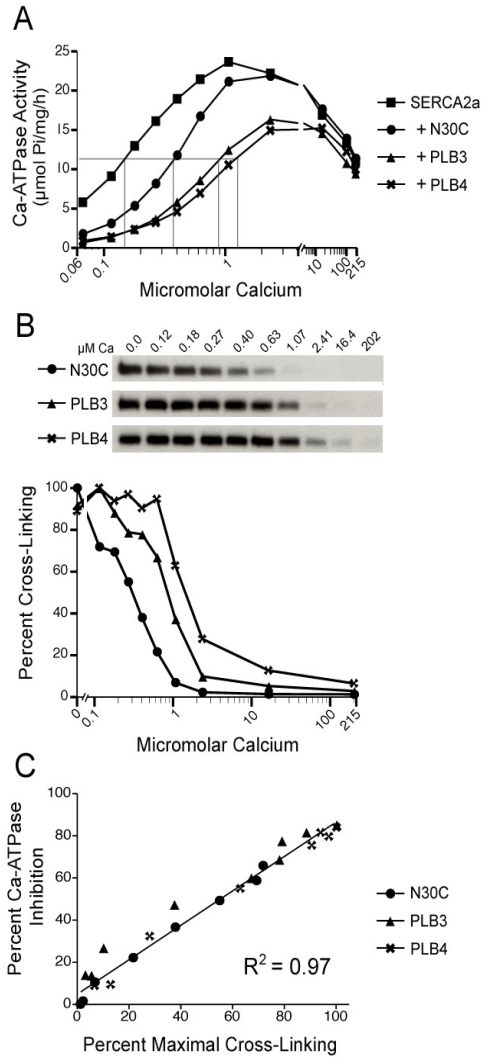

Figure 20. Ca^{2+} activation of Ca^{2+}-ATPase Activity and Ca^{2+} Inhibition of Cross-linking SERCA2a was expressed alone or co-expressed with N30C-PLB, PLB3, or PLB4 in Sf21 cells and SERCA2a and PLB expression levels were determined by Western blotting. Panel A depicts Ca^{2+}-ATPase activities measured as described under "EXPERIMENTAL PROCEDURES". Enzyme activities were normalized to expression levels of SERCA2a expressed alone. The grey line intersecting the ordinate indicates the 50% V_{max} value determined for SERCA2a expressed alone. Panel B shows cross-linking of the PLB mutants to SERCA2a determined under identical conditions as the Ca^{2+}-ATPase assay. Aliquots were taken from the Ca^{2+}-ATPase assay and cross-linked for 15 sec with 1mM KMUS at 37°C. Samples were then subjected to SDS-PAGE and immunoblotting with the anti-PLB antibody, 2D12. Protein bands in the upper panel show SERCA2a cross-linked with the PLB monomer. PLB cross-linking is quantified in the graph below. The graph in Panel C was derived from the data in panels A and B. Percent maximal PLB cross-linking to SERCA2a (determined in the absence of Ca^{2+}) was calculated at each Ca^{2+} concentration for each PLB mutant, and then plotted against the percent inhibition of Ca^{2+}-ATPase activity by PLB obtained at the same Ca^{2+} concentration. The percent inhibition of Ca^{2+}-ATPase activity by PLB at each Ca^{2+} concentration was calculated by dividing the Ca^{2+}-ATPase activity of membranes expressing SERCA2a plus PLB by the Ca^{2+}-ATPase activity of membranes expressing SERCA2a alone, and multiplying by 100. From **Akin, B.L.**, Chen, Z., and Jones, L.R (2010) *J.Biol.Chem*. **285**, 28540-28552.

demonstrates a strong correlation between PLB binding to *E*2, and decreased Ca^{2+} affinity of SERCA2a determined by the Ca^{2+}-ATPase assay. This conclusion is strengthened by plotting the percent maximal PLB cross-linking to SERCA2a (determined at each Ca^{2+} concentration covering the range from 0.12 μM to 200 μM), against the percent inhibition of Ca^{2+}-ATPase activity determined at the same Ca^{2+} concentrations (**Fig. 20C**). For all three PLB mutants, regardless of inhibitory strength, there was strong correlation (R^2 = 0.97) between extent of PLB cross-linking to SERCA2a and degree of enzyme inhibition. These data strongly suggest that SERCA2a with bound PLB is catalytically inactive, and point to competitive binding of PLB and Ca^{2+} as the mechanism of enzyme inhibition.

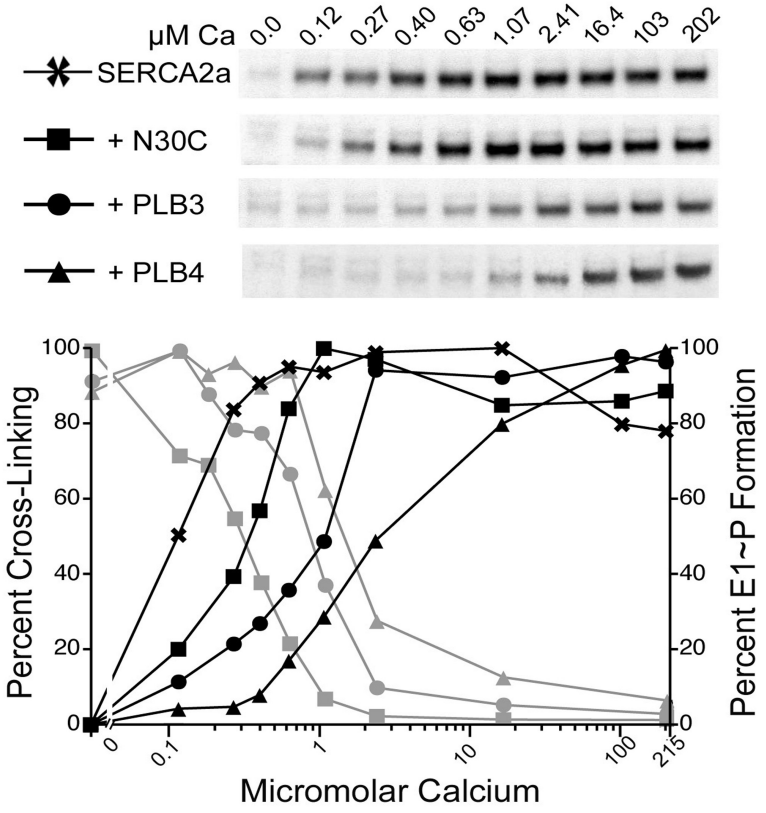

Figure 21. PLB Effect on Formation of the Phosphorylated Enzyme Intermediate Ca^{2+} stimulation of phosphoenzyme formation by [γ-^{32}P]ATP was determined for SERCA2a expressed alone, and co-expressed with each PLB mutant. The upper panel is the autoradiograph depicting the radioactive phosphoenzyme, and results are plotted below (dark lines). For comparison, Ca^{2+} effects on N30C-PLB (squares), PLB3 (circles), and PLB4 (triangles) cross-linking to SERC2a are also displayed (grey lines), taken from Fig. 20B. From **Akin, B.L.**, Chen, Z., and Jones, L.R (2010) *J.Biol.Chem*. **285**, 28540-28552.

3. Ca^{2+} STIMULATION OF *E*1~P FORMATION CORRELATED WITH Ca^{2+} INHIBITION OF PLB CROSS-LINKING TO SERCA2a

Consistent with the Ca^{2+}-ATPase results, when Ca^{2+} stimulation of phosphoenzyme formation from ATP was monitored similar shifts in K_{Ca} by the different PLB mutants were observed (**Fig. 21**). The K_{Ca} for SERCA2a expressed alone was 0.11 μM, whereas when co-expressed with N30C-PLB, PLB3, and PLB4, the K_{Ca} values were 0.36 μM, 1.16 μM, and 2.05 μM (**Table 1**), respectively. These K_{Ca} values are nearly identical to the K_i values determined for Ca^{2+} inhibition of PLB cross-linking (grey lines). These results are particularly significant due to the fact that back inhibition of the Ca^{2+} pump is not a factor when phosphoenzyme formation from [γ-^{32}P]ATP is monitored, therefore, no correction for loss of enzyme turnover at high Ca^{2+} concentration is required when K_{Ca} values are estimated by this method.

4. THE EFFECT OF 2D12 ON Ca^{2+}-ATPASE ACTIVITY AND PLB CROSS-LINKING

The anti-PLB monoclonal antibody, 2D12, recognizes residues 7-13 of PLB and reverses PLB inhibition of the Ca^{2+}-pump by physically disrupting PLB binding to SERCA2a (6). 2D12 reverses enzyme inhibition by wild-type PLB (38) and N30C-PLB virtually completely (6), but only partially reverses the effects of several supershifting PLB mutants on Ca^{2+}-ATPase activity (58). This suggests that the PLB supershifters may bind more tightly to the Ca^{2+} pump than wild-type PLB or N30C-PLB, but this has not been demonstrated directly. Therefore, in order to confirm tighter binding of the PLB supershifters, and to show that the Ca^{2+} affinity of the enzyme is restored commensurate with dissociation of PLB from SERCA2a, we measured the effect of 2D12 on N30C-PLB, PLB3, and PLB4 cross-linking to SERCA2a simultaneously with Ca^{2+}-ATPase activity.

Ca^{2+}-ATPase activity of SERCA2a co-expressed with N30C-PLB, PLB3, and PLB4 was measured in the presence of 8 μg of 2D12 (4.44 μM), a concentration sufficient to completely saturate PLB (**Fig. 22**, **A-C**). As shown previously (6), the

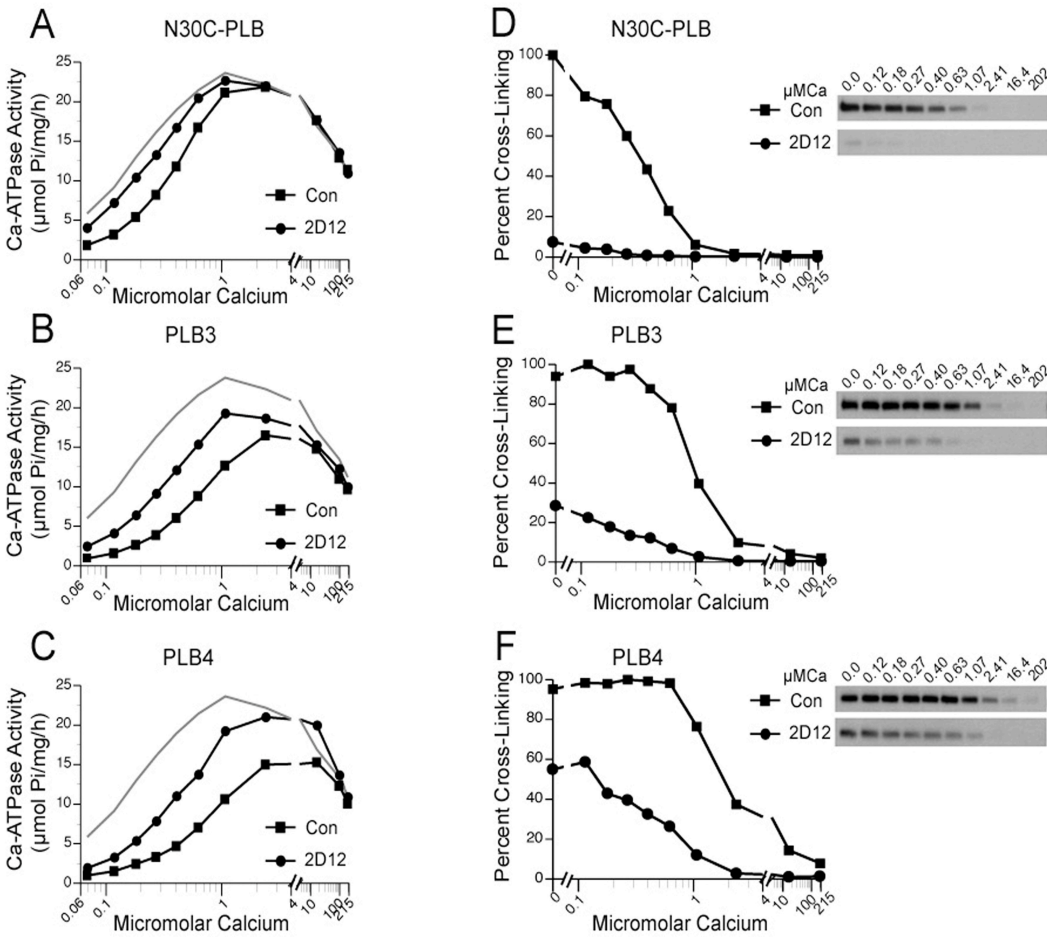

Figure 22. Effect of 2D12 on Ca^{2+}-ATPase activity (A-C) and PLB cross-linking to SERCA2a (D-F) Ca^{2+}-ATPase activities were determined in the presence (2D12) and absence (Con) of 2D12 as described under "EXPERIMENTAL PROCEDURES" for membranes co-expressing SERCA2a and each PLB mutant. Grey lines show results obtained for membranes expressing SERCA2a alone. Cross-linking of PLB to SERCA2a was determined under identical conditions as the Ca^{2+}-ATPase assay. From **Akin, B.L.**, Chen, Z., and Jones, L.R (2010) *J.Biol.Chem*. **285**, 28540-28552.
.

2D12 antibody restored the Ca^{2+} affinity of SERCA2a co-expressed with N30C-PLB nearly completely, decreasing the K_{Ca} from 0.33 to 0.19 µM Ca^{2+}, compared to 0.16 µM Ca^{2+} for SERCA2a expressed alone (**Table 1**). On the other hand, 2D12 only partially restored the Ca^{2+} affinity of the enzyme co-expressed with the superinhibitory mutants PLB3 and PLB4, shifting the K_{Ca} values from 0.53 to 0.26 µM for PLB3, and from 0.70 to 0.36 µM for PLB4. Also, whereas 2D12 had little or no effect on the V_{max} of the enzyme co-expressed with N30C-PLB, 2D12 increased the V_{max} of the enzyme co-expressed with PLB3 and PLB4 significantly. In the

presence of the antibody at 1-2 μM Ca^{2+}, Ca^{2+} pumps co-expressed with PLB3 and PLB4 achieved 80 - 95% of the maximal activity of Ca^{2+} pumps expressed alone.

The effects of 2D12 on PLB cross-linking during the same assay are shown in **Fig. 22**, **D-F**. Consistent with previous results, 2D12 inhibited cross-linking of N30C-PLB to the Ca^{2+} pump nearly completely in the absence of Ca^{2+} and at all Ca^{2+} concentrations tested (6). This explains why Ca^{2+} pump inhibition by N30C-PLB is 30% or less at each Ca^{2+} concentration tested when Ca^{2+}-ATPase activity was measured in the presence of 2D12. On the other hand, PLB3 and PLB4 cross-linking to SERCA2a in the absence of Ca^{2+} was substantially reduced by addition of 2D12, but not eliminated altogether (25% and 53% maximal cross-linking persisted, respectively). Even in the presence of the antibody, Ca^{2+} concentrations of 1 μM or higher were required to completely dissociate PLB3 and PLB4 from the Ca^{2+} pump (**E** and **F**). These cross-linking results agree well with the results of the Ca^{2+}-ATPase assays, which showed that the enzyme was significantly inhibited by PLB3 and PLB4 even in the presence of 2D12. In experiments not shown, the binding affinity of PLB for 2D12 was determined to be 0.1 μM. Therefore, we conclude that the binding affinities of PLB3 and PLB4 for SERCA2a must be very high, at least within the range at which PLB binds 2D12.

5. THE EFFECT OF Ca^{2+} ON PLB CROSS-LINKING TO D351A

In order to test directly for competition between PLB and Ca^{2+} for binding to SERCA2a, we took advantage of the Ca^{2+}-pump mutant, D351A. During catalysis, Asp^{351} is phosphorylated by ATP to form the high-energy acylphosphoprotein intermediate, $E1{\sim}P{\cdot}Ca_2$ (**Fig. 4**). Replacement of aspartic acid at this position renders the enzyme catalytically inactive (53, 54). Although inactive at the site of ATP hydrolysis, D351A retains the ability to bind Ca^{2+} and maintains the thermodynamic equilibrium between *E*1 and *E*2 (53, 55, 56). Therefore, if PLB acts by stabilizing *E*2 and shifting the $E1{\cdot}Ca_2 \leftrightarrow E2{\cdot}$PLB equilibrium away from *E*1, then this effect should be fully reproducible with D351A. The advantage of using D351A for these experiments is that enzyme turnover is prevented; hence the system is at equilibrium

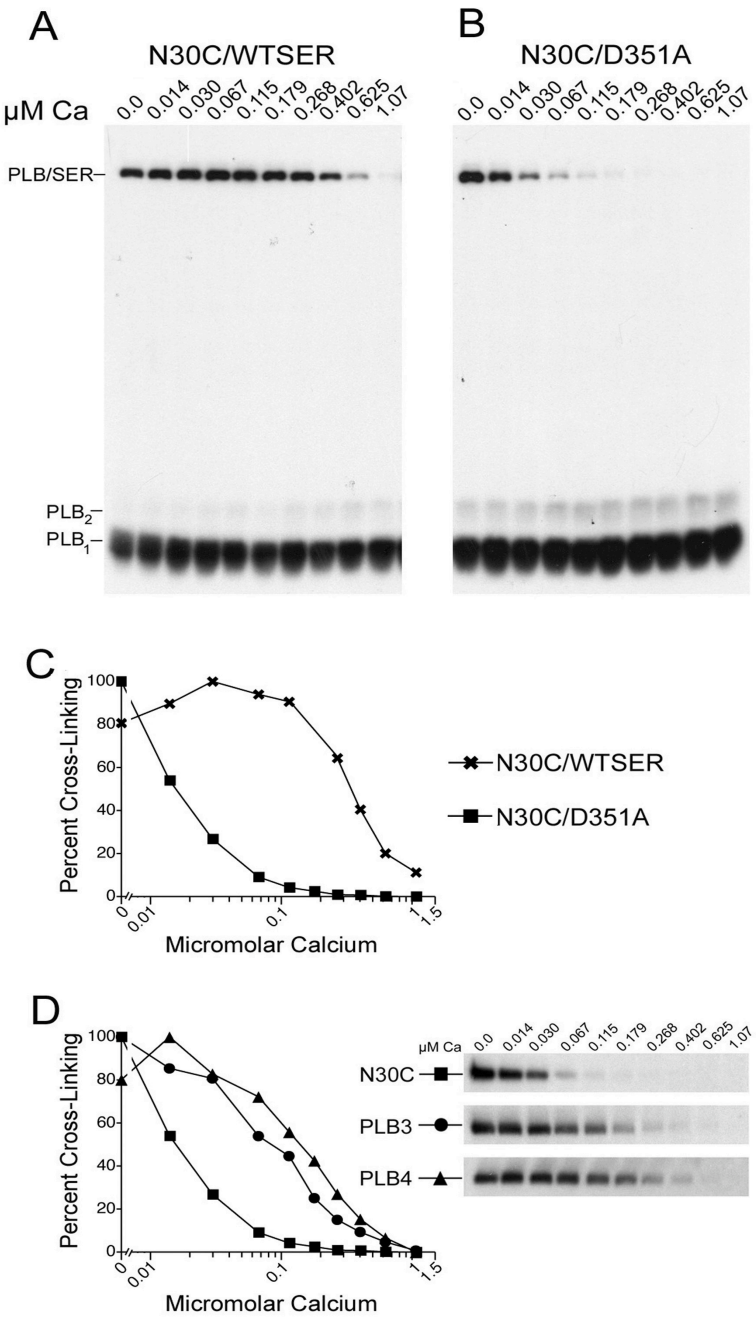

Figure 23. Ca^{2+} effect on PLB cross-linking to D351A Ca^{2+} inhibition of N30C-PLB cross-linking to wild-type SERCA2a (A) and D351A (B) was determined under Ca^{2+}-ATPase assay conditions, as described under "EXPERIMENTAL PROCEDURES." PLB/SER designates the PLB monomer cross-linked to the Ca^{2+} pump at 110 kDa, and free PLB monomers (PLB_1) and dimers (PLB_2) are visible below at 6 kDa and 12 kDa, respectively. The full autoradiographs are shown, demonstrating the highly specific cross-linking reaction; PLB cross-linked exclusively to expressed wild-type SERCA2a or D351A in Sf21 membranes. C, Graph of Ca^{2+} inhibition of N30C-PLB cross-linking to wild-type SERCA2a and D351A. D, Ca^{2+} inhibition of N30C-PLB, PLB3, and PLB4 cross-linking to D351A. K_i values for Ca^{2+} inhibition of cross-linking to D351A are listed in RESULTS. From **Akin, B.L.**, Chen, Z., and Jones, L.R (2010) *J.Biol.Chem*. **285**, 28540-28552.

with respect to Ca^{2+} binding (**Fig. 4**). Consistent with previous results with SERCA1a, we first confirmed that the D351A mutant made from SERCA2a exhibited no Ca^{2+}-ATPase activity, and was not phosphorylatable by [γ-^{32}P]ATP to form *E*1~P (54), nor by P_i to form *E*2-P (53) (data not shown).

Next, the affinity of D351A for Ca^{2+} was compared to that of wild-type SERCA2a by measuring Ca^{2+} inhibition of N30C-PLB cross-linking. In the absence of Ca^{2+}, D351A and wild-type SERCA2a bound comparable amounts of N30C-PLB (**Fig. 23, A** and **B**). However, a strikingly lower Ca^{2+} concentration was sufficient to disrupt N30C-PLB cross-linking to D351A (K_i = 18 nM) compared to wild-type SERCA2a (K_i = 280 nM) (**Fig. 23C**). In fact, the Ca^{2+} affinity of D351A determined by this method (18 nM) is approximately 9-fold higher than the Ca^{2+} affinity of wild-type SERCA2a estimated by Ca^{2+}-ATPase assay (0.16 μM in **Table 1**). Assuming that N30C-PLB decreases the Ca^{2+} affinity of D351A by approximately 2-fold (as it does for wild-type SERCA2a), the Ca^{2+} affinity of D351A expressed alone is likely even higher than this, in the range of 10 nM. This remarkably high Ca^{2+} affinity for D351A was first reported by MacIntosh *et al.* (55), but subsequently not confirmed (56) (see DISCUSSION). **Fig. 23A** also points out the highly specific nature of the PLB to SERCA2a cross-linking reaction, with PLB cross-linking exclusively to the Ca^{2+} pump protein expressed in Sf21 membranes.

Ca^{2+}-inhibition of N30C-PLB, PLB3, and PLB4 cross-linking to D351A was then measured (**Fig. 23D**). As predicted from results with wild-type SERCA2a, progressively higher concentrations of Ca^{2+} were also required to dissociate N30C-PLB (K_i = 18 ± 3 nM), PLB3 (K_i = 131 ± 25 nM) and PLB4 (K_i = 234 ± 23 nM) from D351A (means ± S.E from 4 determinations). **Fig. 23D** demonstrates unambiguously that N30C-PLB and the supershifting PLB mutants, PLB3 and PLB4, inhibit Ca^{2+} binding to D351A. This result is consistent with the hypothesis that PLB competes with Ca^{2+} for binding to SERCA2a.

C. HYPOTHESIS 3: PLB BINDS EXCLUSIVELY TO THE *E*2·ATP CONFORMATION OF THE Ca^{2+} PUMP

1. THE EFFECT OF TG AND NUCLEOTIDES ON PLB CROSS-LINKING TO WILD-TYPE SERCA2a

To investigate the specific conformation of the Ca^{2+} pump that binds PLB, and confirm the relative binding affinities of the PLB mutants for SERCA2a, the effects of TG and nucleotides on PLB cross-linking to SERCA2a were measured in the absence of Ca^{2+}. It was shown previously that N30C-PLB binds preferentially to the *E*2 state of SERCA2a stabilized by bound nucleotide (21), and that TG antagonizes formation of this state.

TABLE 2
K_{TG} values (μM) for TG inhibition of PLB cross-linking to the Ca^{2+}-ATPase
TG inhibition of PLB cross-linking to wild-type SERCA2a (SERCA2a) and D351A was determined in the presence (+ATP) and absence (No Nuc) of 3 mM ATP. K_i values were the TG concentration at which PLB cross-linking was 50% inhibited as read directly from the data plots. Results are the means ± S.E. of 4-5 determinations.

Protein expressed	K_{TG} values	
	No Nuc	+ ATP
SERCA2a		
+ N30C	0.07 ± 0.02	0.23 ± 0.05
+ PLB3	0.07 ± 0.01	4.87 ± 0.53
+ PLB4	0.10 ± 0.01	7.78 ± 1.0
D351A		
+ N30C	0.07 ± 0.005	0.17 ± 0.04
+ PLB3	0.08 ± 0.02	13.3 ± 5.2
+ PLB4	0.11 ± 0.02	24.3 ± 1.9

When measured in the absence of ATP, TG potently inhibited the cross-linking of all three PLB mutants to SERCA2a (**Fig. 24, A** and **B**). The K_i values for TG inhibition of N30C-PLB, PLB3, and PLB4 cross-linking to SERCA2a were low and similar (0.07 μM, 0.07 μM and 0.10 μM, respectively) (**Table 2**), and within range of Ca^{2+} pumps present within the reaction tubes (~ 0.3 μM). Thus, TG bound virtually stoichiometrically to the Ca^{2+} pump (34, 35), whether co-expressed with N30C-PLB, PLB3, or PLB4. However, addition of 3 mM ATP to the assay tubes dramatically increased the concentration of TG required to inhibit PLB3 and PLB4 cross-linking to

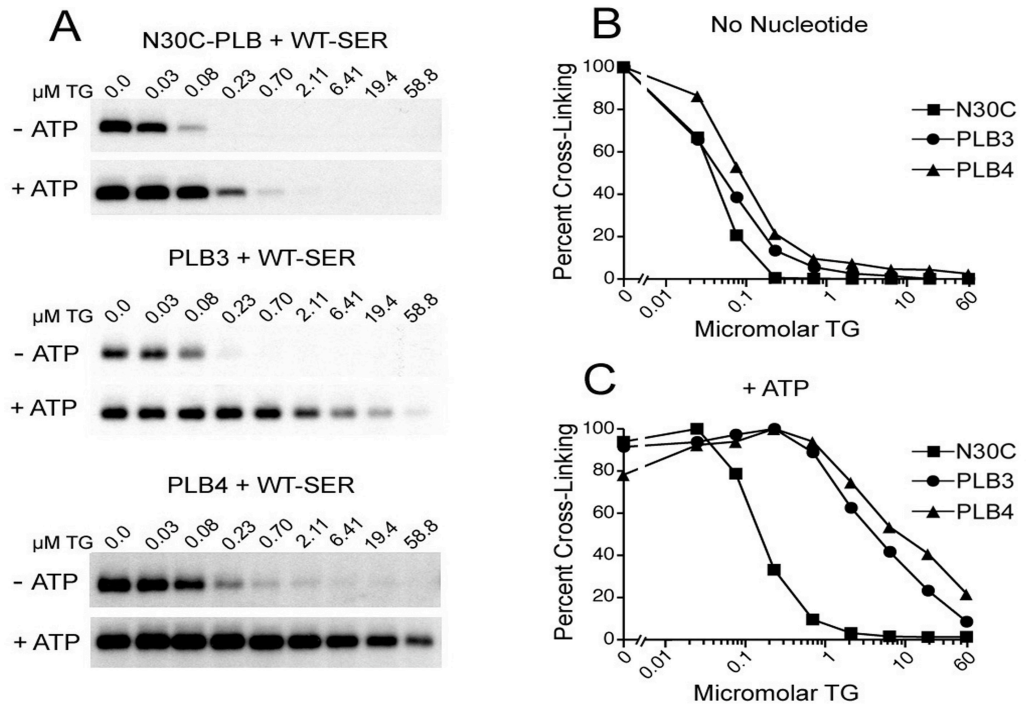

Figure 24. TG effect on PLB cross-linking A**,** autoradiographs showing concentration dependence of TG inhibition N30C-PLB, PLB3, and PLB4 cross-linking to SERCA2a, measured in the absence (-ATP) and presence (+ATP) of 3 mM ATP. B and C, graphs of TG inhibition of cross-linking, determined in the absence and presence of 3 mM ATP, respectively. From **Akin, B.L.**, Chen, Z., and Jones, L.R (2010) *J.Biol.Chem*. **285**, 28540-28552.

SERCA2a. The K_i values (**Fig. 24, A** and **C**) increased from 0.07 μM to 4.9 μM for PLB3, and from 0.10 μM to 7.8 μM for PLB4, whereas for N30C-PLB, addition of ATP only increased K_i value from 0.07 μM to 0.23 μM (**Table 2**). That is a remarkable 70-fold (PLB3) and 78-fold (PLB4) decrease in TG binding affinity induced by ATP when supershifting PLB mutants are present. It should be pointed out that the concentration of PLB present in the reaction tubes was approximately 1.0 μM, which is considerably lower than the concentration of TG required to significantly inhibit cross-linking of PLB3 and PLB4 to the Ca^{2+}-ATPase in the presence of ATP (**Fig. 24C**). Thus the affinity of the two PLB supershifters for *E*2·ATP must be even greater than the affinity of TG for *E*2·ATP, which is within the nanomolar range or lower (34, 35). The same results with PLB3 or PLB4 were obtained whether membranes were pre-incubated with TG for 5 min or 60 min prior

to initiation of the cross-linking reactions with KMUS, indicating that the supershifters prevent formation of a dead-end complex by TG (34) under these conditions.

Like ATP, ADP also dramatically increased the K_i value for TG inhibition of PLB cross-linking to the Ca^{2+}-ATPase, whereas AMP had no significant effect (**Fig. 25A** demonstrated with PLB4). These results confirm previous findings that both ATP and ADP, but not AMP, stabilize the *E*2 state that favors PLB binding (21). We then measured the binding affinity of SERCA2a for ATP determined at different

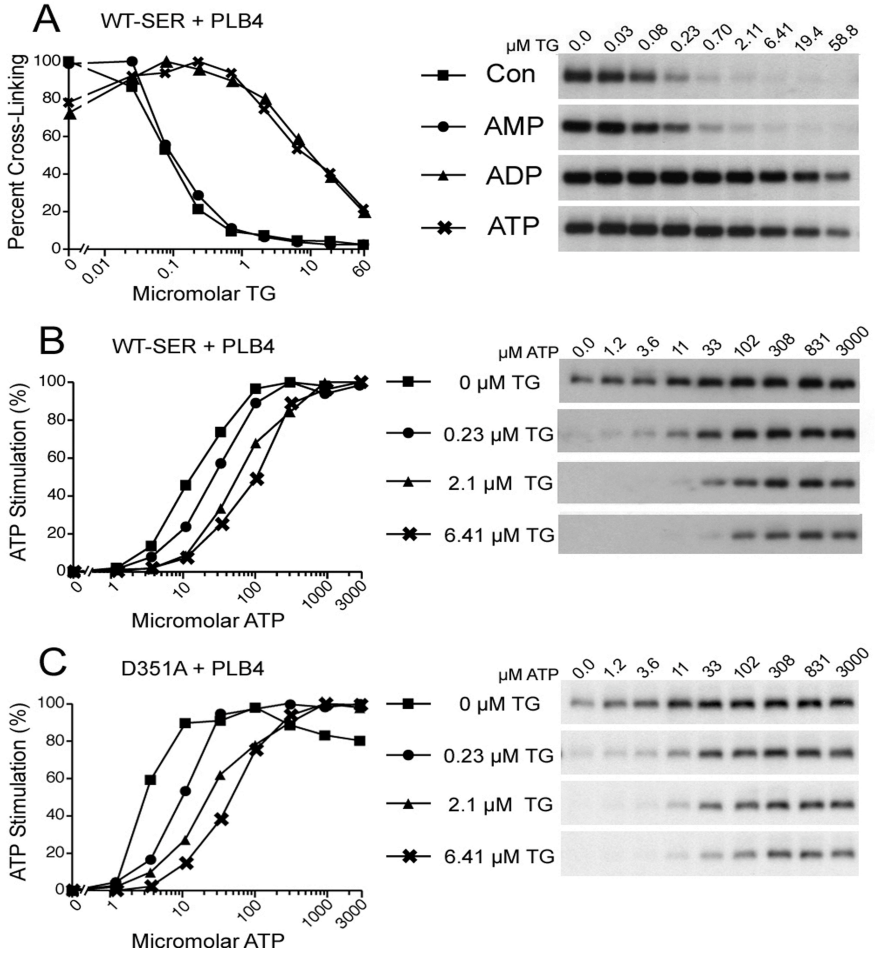

Figure 25. Nucleotide Effect on PLB4 Cross-Linking to Wild-Type SERCA2a and D351A A, effect of 3 mM AMP, ADP, ATP, and no added nucleotide (Con) on PLB4 cross-linking to wild-type SERCA2a. TG concentrations were varied as indicated. B, ATP stimulation of PLB4 cross-linking to wild-type SERCA2a, determined at different TG concentrations. ATP concentrations were varied as indicated. C, ATP stimulation of PLB4 cross-linking to D351A, determined at different TG concentrations. From **Akin, B.L.**, Chen, Z., and Jones, L.R (2010) *J.Biol.Chem*. **285**, 28540-28552.

concentrations of TG (**Fig. 25B**). Successively higher concentrations of ATP were required to stimulate PLB4 cross-linking to the Ca^{2+}-ATPase when the concentration of TG was increased. In the absence of TG, the affinity of SERCA2a for ATP was 9 μM; in the presence of 6.4 μM TG, the affinity of the enzyme for ATP was decreased 10-fold, to approximately 100 μM (**Table 3**). These K_{ATP} values for SERCA2a measured in the absence of Ca^{2+} agree well with those in previous reports, and confirm for SERCA2a, that TG significantly reduces the affinity of the enzyme for ATP at the modulatory nucleotide-binding site (60-62). Collectively, these results demonstrate that PLB binds to a single conformation of SERCA2a, *E*2 with bound nucleotide, and this state is distinct from the *E*2 conformation binding TG (see DISCUSSION), all of which is consistent with the hypothesis that PLB binds exclusively to the *E*2·ATP conformation of the Ca^{2+} pump.

2. THE EFFECTS OF TG AND NUCLEOTIDES ON PLB CROSS-LINKING TO D351A-SERCA2a

Similar nucleotide effects on PLB binding to D351A were noted. The K_i values for TG inhibition of cross-linking of all three PLB mutants to D351A were low and similar when assessed in the absence of ATP, but dramatically increased for PLB3 and PLB4 when ATP was included (**Table 2**). TG also substantially decreased the ATP binding affinity of D351 (**Fig. 25C** and **Table 3**). Interestingly, the affinity of D351A for ATP was only about 2-fold greater than the affinity of wild-type

TABLE 3
K_{ATP} values (μM) for ATP stimulation of PLB4 cross-linking to the Ca^{2+}-ATPase, determined at different TG concentrations K_{ATP} values are the ATP concentration at which cross-linking was half-maximal as determined directly from the plot. Results are the means ± S.E. of 3-5 determinations.

TG (μM)	K_{ATP} values	
	SERCA2a	D351A
0	9.0 ± 1.5	4.0 ± 0.9
0.23	34.0 ± 7.8	15.3 ± 2.7
2.11	65.0 ± 10.4	24.0 ± 1.5
6.41	103 ± 12.0	46.0 ± 4.0

SERCA2a for ATP (**Table 3**), which is substantially lower than the ATP binding affinity of D351A made from SERCA1a (55, 56) (see DISCUSSION).

3. THE EFFECTS OF VANADATE ON PLB CROSS-LINKING TO SERCA2a

According to results above with TG, the binding affinities of N30C-PLB and the supershifters for the *E*2 state of SERCA2a are much higher than previously predicted (51). Therefore, to confirm these surprising results, we used a second lower affinity Ca^{2+} pump inhibitor, vanadate, to estimate the binding affinities of the PLB mutants for SERCA2a. Vanadate inhibits the Ca^{2+}-ATPase with micromolar affinity, and like TG is proposed to bind preferentially to the nucleotide-free, *E*2 conformation

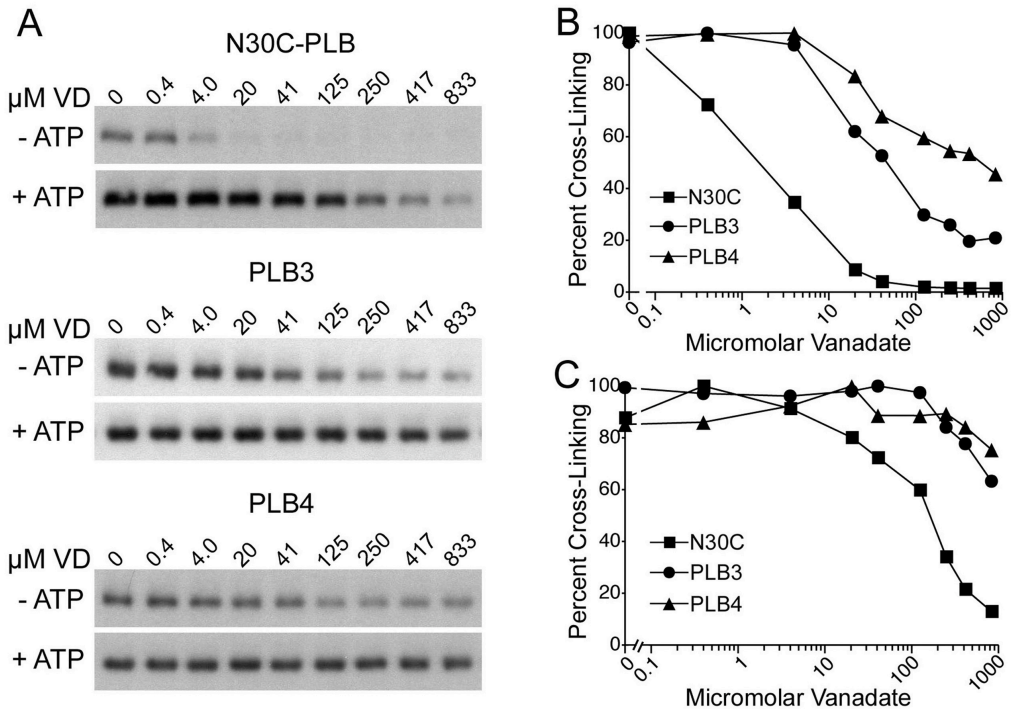

Figure 26. Vanadate Effect on PLB Cross-Linking to SERCA2a A**,** autoradiographs showing concentration dependence of vanadate inhibition N30C-PLB, PLB3, and PLB4 cross-linking to SERCA2a, measured in the absence (-ATP) and presence (+ATP) of 36 μM ATP. B and C, graphs of vanadate inhibition of cross-linking, determined in the absence and presence of 36 μM ATP, respectively. From **Akin, B.L.**, Chen, Z., and Jones, L.R (2010) *J.Biol.Chem*. **285**, 28540-28552.

of the Ca^{2+} pump (63). **Fig. 26** shows that in the absence of Ca^{2+} and ATP, vanadate inhibited cross-linking of all three PLB mutants to SERCA2a. However, significantly higher concentrations of vanadate were required to inhibit PLB3 (K_i = 46 μM) and PLB4 (K_i = 380 μM) cross-linking to SERCA2a, relative to N30C-PLB (K_i = 1.6 μM, **Fig. 26B**). Moreover, maximal cross-linking of PLB3 and PLB4 to SERCA2a could only be inhibited by 80% and 60% at 1 mM vanadate, the highest concentration tested. When 36 μM ATP was included in the buffer, the K_i for vanadate inhibition of N30C-PLB cross-linking to SERCA2a was increased 125-fold, from 1.6 μM (no nucleotide) to 200 μM vanadate (36 μM ATP), and cross-linking of PLB3 and PLB4 to SERCA2a became nearly completely vanadate resistant (**Fig. 26C**). At 3 mM ATP, vanadate failed to inhibit cross-linking of any PLB mutant to the Ca^{2+}-ATPase (data not shown). Thus, results with vanadate also show that PLB binds with surprisingly high affinity to the *E*2 state of SERCA2a when nucleotide is present.

CHAPTER 4—DISCUSSION

The purpose of this dissertation research was to investigate the molecular mechanism of PLB regulation of Ca^{2+}-ATPase activity. Three hypotheses were tested, each one specifically designed to address a fundamental point in the mechanism of PLB action. Using chemical cross-linking in conjunction with PLB mutants of increasing inhibitory function, new insights were gained on the catalytic activity of PLB-bound SERCA2a, the effect of PLB on the Ca^{2+} affinity and V_{max} of the enzyme, and the specific conformation of SERCA2a required for PLB binding.

A. HYPOTHESIS 1: SERCA2a WITH PLB BOUND IS CATALYTICALLY INACTIVE

PLB inhibits Ca^{2+}-ATPase activity of SERCA2a by decreasing apparent Ca^{2+} affinity of the enzyme, and PLB effects on Ca^{2+} affinity are reversed by phosphorylation of PLB by PKA or CaMKII, and by micromolar Ca^{2+} concentration (2, 3). However, whether disinhibition of the Ca^{2+} pump requires complete dissociation of PLB from the SERCA2a has remained unclear. In a study in which fluorescence resonance energy transfer was used to monitor protein-protein interactions between PLB and the Ca^{2+}-ATPase, Mueller *et al.* concluded that the affinity of PLB for the Ca^{2+} pump is so high that under physiological conditions PLB essentially never dissociates (36). The authors suggested Ca^{2+}-induced structural changes in SERCA cause significant conformational rearrangements in PLB, but PLB remains tightly bound nonetheless (36). Similarly, using frequency-domain fluorescence spectroscopy to monitor interactions between PLB and the Ca^{2+} pump, Li *et al.* concluded that dissociation of PLB is not requisite for Ca^{2+} pump activation (37).

In contrast to the findings of Mueller *et al.* (36) and Li *et al.* (37), here it was shown definitively that SERCA2a with PLB irreversibly bound (PLB/SER) is catalytically inactive (**Figs. 15-17**). Whereas PLB-free SERCA2a readily underwent the kinetic half-reactions to form both *E*1~P and *E*2-P, SERCA2a with PLB bound was completely devoid of catalytic activity and entirely unphosphorylatable under all

conditions (**Figs. 16** and **17**). From these results we conclude that when PLB is bound, SERCA2a is immobilized in the Ca^{2+}-free *E*2 state, and in order for the catalytic cycle to resume, PLB must first completely dissociate from the enzyme. Therefore, by mass action PLB reduces the fraction of Ca^{2+}-pumps available to bind and transport Ca^{2+}, which would be manifested as a decrease in the apparent Ca^{2+} affinity of the enzyme, the hallmark of PLB regulation of SERCA2a (2, 3).

B. HYPOTHESIS 2: PLB DECREASES THE Ca^{2+} AFFINITY OF SERCA2a BY COMPETING WITH Ca^{2+} FOR BINDING TO THE ENZYME

1. PLB SUPERSHIFTERES REVEAL COMPETITIVE BINDING OF PLB AND Ca^{2+} TO SERCA2a

It is generally accepted that PLB decreases the apparent Ca^{2+} affinity of the Ca^{2+}-ATPase, while having little or no effect on the V_{max} of the enzyme measured at saturating Ca^{2+} concentration (2, 3). However, whether PLB increases the K_{Ca} of Ca^{2+}-ATPase activation by decreasing the actual Ca^{2+} binding affinity of the enzyme (21, 23, 44, 64), or by affecting one or more catalytic steps in the reaction cycle (36-41) has remained unclear. Here this question was addressed directly, using cross-linkable PLB mutants of increasing inhibitory potency (PLB4 > PLB3 > N30C-PLB). We showed that successively higher concentrations of Ca^{2+} were required to both activate the enzyme co-expressed with N30C-PLB, PLB3, and PLB4 and to dissociate N30C-PLB, PLB3, and PLB4 from the Ca^{2+} pump (**Figs. 20** and **21**). Moreover, there was a direct correlation between the degree of PLB binding to SERCA2a and the extent of PLB inhibition of Ca^{2+}-ATPase activity at all Ca^{2+} concentrations tested with all three PLB mutants (**Fig. 20C**). These results strongly suggest that PLB competes with Ca^{2+} for binding to the Ca^{2+}-ATPase, and that SERCA2a with PLB bound is catalytically inactive.

2. CONFIRMING COMPETITIVE BINDING OF PLB AND Ca^{2+} TO SERCA2a USING CATALYTICALLY INACTIVE D351A

The Ca^{2+} pump mutant D351A cannot hydrolyze ATP, but retains strong Ca^{2+} binding and maintains the Ca^{2+}-dependent equilibrium between *E*1 and *E*2. Like the wild-type enzyme, progressively higher concentrations of Ca^{2+} were required to dissociate the increasingly potent PLB mutants from D351A. Thus at each Ca^{2+} concentration tested, progressively more *E*2·PLB was formed by the increasingly inhibitory PLB mutants, meaning that less *E*1 was available for Ca^{2+} binding (**Fig. 23D**). Therefore, by stabilizing the enzyme in a Ca^{2+} free state, PLB decreases Ca^{2+} binding to the pump and alters the kinetics of enzyme activation by Ca^{2+}.

The results shown here with the PLB supershifters and D351A unambiguously confirm that PLB decreases Ca^{2+} binding to SERCA2a, and provide very strong evidence for mutually exclusive binding of PLB and Ca^{2+} to the Ca^{2+} pump. In contrast to these results, several other groups have recently suggested that PLB binding to SERCA2a is unperturbed by Ca^{2+} binding (36, 37). These authors contend that localized structural changes in PLB, rather than complete dissociation of PLB from SERCA2a, account for the Ca^{2+}-induced inhibition of PLB cross-linking observed by our group (36, 37). However, PLB has been cross-linked to SERCA2a at numerous points of interaction located within both domains of PLB and two different regions of the Ca^{2+}-pump (6, 21-23), and in each case, PLB cross-linking was completely inhibited by micromolar Ca^{2+} concentration. Most importantly, in the work presented here we showed that higher concentrations of Ca^{2+} were required to inhibit cross-linking of the increasingly inhibitory PLB mutants to both D351A and wild-type SERCA2a (**Figs. 20** and **23**). Nevertheless, we accept the unlikely possibility that PLB does bind to the Ca^{2+} bound enzyme, but that PLB interactions with the enzyme in *E*1 have not been detected by our cross-linking technique. However, we can conclude with certainty that if PLB does bind to the Ca^{2+}-bound enzyme, then the PLB binding site in *E*1 is distinct from the inhibitory PLB binding site in *E*2 described by our work, and one in which PLB does not effect Ca^{2+} pump activity.

3. THE EFFECTS OF PLB ON THE V_{max} OF SERCA2a

According to our model PLB competes with Ca^{2+} for binding to SERCA2a, therefore at saturating Ca^{2+} concentration PLB should be completely dissociated from the Ca^{2+} pump and have no effect on maximal enzyme activity. Here we showed that PLB molecules of normal inhibitory strength (N30C-PLB) do not significantly affect the V_{max} of the Ca^{2+}-ATPase (**Fig. 20**). This result is contrary to conclusions of several recent studies in which PLB was reported to either decrease (44) or increase (42, 43, 45) the V_{max} of the Ca^{2+}-ATPase. Using our viral constructs and the 2D12 antibody, Waggoner *et al*. (44) recently noted a modest reduction (~20%) in the V_{max} of SERCA2a expressed alone compared to SERCA2a co-expressed with wild-type PLB. This is in disagreement with an earlier study in which no effect on V_{max} was noted (64). We believe that the modest reduction in V_{max} observed by Waggoner *et al*. (44) is more apparent than real. **Fig. 20A** points out that when Ca^{2+}-ATPase activities are carefully corrected for Ca^{2+} pump expression levels, there is little or no inhibition of the enzyme at saturating Ca^{2+} concentrations when SERCA2a is co-expressed with PLB mutants of normal inhibitory potency (N30C-PLB). Moreover, this relief of Ca^{2+}-ATPase inhibition at saturating Ca^{2+} concentration is entirely consistent with the complete dissociation of N30C-PLB from SERCA2a observed at 1-2 μM Ca^{2+} by chemical cross-linking (**Fig. 20B**). The studies in which wild-type PLB and some other PLB mutants were reported to actually increase the V_{max} of the Ca^{2+}-ATPase were all conducted with the purified rabbit skeletal muscle enzyme co-reconstituted with purified PLB from detergent solution (42, 43, 45). In this case, it is possible that enzyme protection by PLB during the reconstitution process may have artifactually affected the results, as was recently suggested (45). Regardless, in multiple studies using cellular expression systems, no increase in V_{max} by PLB has been noted (2, 3).

In contrast to N30C-PLB, the superinhibitory PLB mutants PLB3 and PLB4 did significantly reduce maximal enzyme activity measured at saturating Ca^{2+} concentration (**Fig. 20A**). At Ca^{2+} concentrations greater than 1-2 μM, the Ca^{2+} pump loses significant activity due to back inhibition of the enzyme by Ca^{2+} (58, 59). Ca^{2+} concentrations in excess of 100 μM are required to dissociate PLB3 and PLB4 from SERCA2a, therefore the Ca^{2+} pump co-expressed with PLB3 and PLB4 can never

achieve as high of a V_{max} as the enzyme expressed alone or co-expressed with N30C-PLB. The effects of N30C-PLB and the PLB supershifters on maximal enzyme activity observed here are entirely consistent with the model of mutually exclusive binding of PLB and Ca^{2+} as the mechanism of PLB regulation of SERCA2a.

4. THE PHYSIOLOGICAL EFFECTS OF PLB

The results shown here illustrate how wild-type PLB is perfectly poised to regulate cardiac contractile kinetics in intact myocardium, and may help to explain the detrimental effects of superinhibitory PLB on cardiac function observed in transgenic mouse models (29-31). Ca^{2+} concentrations within the cardiomyocyte range from nanomolar to 1-2 μM (1), and the affinity of wild-type PLB for SERCA2a allows it to associate and dissociate from the enzyme over the same Ca^{2+} concentration range at which contractile force develops. At low cytosolic Ca^{2+} concentrations at which myofilament contractile force is low, the affinity of PLB for the Ca^{2+}-pump is high and enzyme inhibition by PLB is substantial, but still reversible by phosphorylation by protein kinase A (2, 3) or by the 2D12 antibody (5). At high Ca^{2+} concentrations yielding peak contractile force, PLB is completely dissociated from the Ca^{2+} pump and the enzyme is maximally active. However, for supershifting PLB mutants the situation is different. By virtue of their very high binding affinities for SERCA2a, the supershifters remain significantly bound to the Ca^{2+} pump and continue to inhibit the enzyme at Ca^{2+} concentrations that are normally saturating. At Ca^{2+} concentrations high enough to dissociate these potent PLB molecules from the Ca^{2+} pump (10-200 μM Ca^{2+}) (**Fig. 20**), significant back inhibition of the enzyme occurs. Thus, maximal Ca^{2+}-ATPase activity can never be realized when SERCA2a is co-expressed with potent PLB supershifters, even after phosphorylation of PLB by protein kinase A or after addition of the 2D12 antibody, both of which reduce the affinity of PLB for the Ca^{2+} pump. Therefore, these results provide a mechanism to explain why transgenic mice overexpressing the most potent PLB supershifters develop cardiac hypertrophy, heart failure, and premature death (29-31).

5. STRUCTURAL CONSIDERATIONS: LONG DISTANCE COMMUNICATION BETWEEN THE Ca^{2+} BINDING SITES AND THE CATALYTIC SITE

Using PLB as a reporter molecule, we were able to estimate the Ca^{2+} and nucleotide binding affinities of D351A relative to wild-type SERCA2a, and make comparisons with previous determinations made for the skeletal muscle enzyme (SERCA1a). In an earlier study, MacIntosh *et al.* (55) used TNP-8N_3-ATP photolabeling to measure the Ca^{2+} and ATP binding affinities of D351A (rabbit skeletal isoform) expressed in COS membranes. The authors found that relative to wild-type Ca^{2+}-ATPase, D351A had an extraordinarily high affinity for both Ca^{2+} (> 10-fold increase) and ATP (20 - 100 fold increase) (55). They postulated that Ala substitution at Asp^{351} significantly increases the ATP affinity of the Ca^{2+}-ATPase by relieving electrostatic repulsion between the γ-phosphate of ATP and Asp^{351} of the wild-type enzyme. Moreover, they proposed that mutationally induced conformational changes at the site of ATP binding within the cytoplasmic head group were transmitted to the Ca^{2+} binding sites located at the membrane, substantially increasing the Ca^{2+} affinity of the enzyme. The very high ATP affinity of D351A, but not the high Ca^{2+} affinity, was confirmed in a subsequent study by Marchand *et al.* (56), also with SERCA1a. In this later report, ATP- and Ca^{2+}-binding affinities were determined for the purified enzyme in detergent solution.

Here, using PLB cross-linking to estimate Ca^{2+} affinity, we also noted an extremely high Ca^{2+} affinity for D351A, this time using the cardiac muscle isoform (SERCA2a). Our results indicate that D351A has a Ca^{2+} affinity at least 10 times higher than wild-type SERCA2a (**Fig. 7A**). This result is consistent with the earlier findings of MacIntosh *et al*. (55), but inconsistent with the results of Marchand *et al*. (56). It is well known that non-ionic detergents like $C_{12}E_8$ and dodecy-maltoside substantially decrease the Ca^{2+}-binding affinity of SERCA pumps (65, 66), which may explain the failure of Marchand *et al.* to detect an increase in Ca^{2+} affinity for D351A (56).

Regarding ATP affinity, we determined a K_d value of 9 μM for the wild-type enzyme, which is well within the range reported by other investigators for ATP binding at the low-affinity modulatory binding site of *E*2 measured in the absence of Ca^{2+} (60-62). For D351A, we noted a modest 2.3-fold increase in ATP affinity relative to wild-type SERCA2a (K_d = 4.0 μM), in contrast to the two studies above which reported a much higher nucleotide binding affinity for D351A measured under similar conditions (55, 56). However, our results appear to be consistent with the recently determined crystal structure of the E2(TG)-AMPPCP complex, representing *E*2 with ATP bound at the modulatory site (20). According to this structure, ATP fits more loosely into the modulatory site (ATP binding site in *E2*) relative to the catalytic site. When ATP is bound to *E2*, the γ-phosphate is 9Å away from the phosphorylation site, making the electrostatic repulsion between the γ-phosphate and the negatively charged Asp^{351} much less pronounced than what occurs when ATP is bound to *E*1 (20). Thus ATP affinity at the modulatory site may be less affected by the D351A mutation because the γ-phosphate of ATP does not interact closely with Asp^{351} when ATP is bound here. Nevertheless, our results with D351A demonstrate that there is long-range communication between the catalytic site and the Ca^{2+} binding sites, and removal of the negative charge at Asp^{351} strikingly enhances the Ca^{2+} binding affinity at the two Ca^{2+} binding sites in the membrane.

C. HYPOTHESIS 3: PLB BINDS EXCLUSIVELY TO THE *E*2·ATP CONFORMATION OF THE Ca^{2+} PUMP

Where in the catalytic cycle of SERCA2a does PLB act to slow or inhibit enzyme turnover? Mueller *et al.* (36) and Li *et al.* (37) have proposed that PLB acts at multiple kinetic steps in the Ca^{2+}-pump's reaction cycle. Alternately, others have proposed that PLB acts at a single step, but there is disagreement with respect to which step. Tada *et al.* (39), Antipenko *et al.* (40) have suggested that PLB slows the rate of phosphoenzyme decomposition (*E*2-P to *E*2·P_i transition, see **Fig. 4**). Cantilina *et al.* (38) and Afara *et al.* (41) proposed that PLB blocks the conformational change that accompanies binding of the first Ca^{2+} ion, facilitating

binding of the second. In contrast, we contend that PLB blocks the transition from *E*2 to *E*1, by stabilizing a single SERCA2a conformational state, *E*2·ATP. An earlier kinetic study by our group (64) showed that PLB had no effect on either the rate the *E*1·Ca to *E*1'·Ca transition as proposed by Cantilina *et al.* (38) and Afara *et al.* (41), nor the rate of *E*2-P to *E*2·P_i transition, as proposed by others (39, 40). Here, it was shown directly that PLB decreases Ca^{2+} binding to *E*1 by stabilizing the enzyme in the Ca^{2+}-free *E*2 state, thereby decreasing the equilibrium constant for Ca^{2+} binding. Moreover, using the effectors thapsigargin, vanadate, 2D12, and nucleotides (AMP, ADP, and ATP) we showed that PLB cross-linking was augmented substantially by ADP and ATP (*E*2·ATP) (**Fig. 25**), but inhibited by thapsigargin (*E*2·TG) (**Fig. 24**), vanadate (**Fig. 26**) and by binding of the 2D12 antibody to PLB (**Fig. 21**). These results support the hypothesis that PLB binds to the *E2*·ATP conformation of SERCA2a and blocks the transition to *E*1.

1. PLB BINDS TO DEPROTONATED *E*2·ATP

Early studies of the Ca^{2+}-ATPase showed that in the absence of Ca^{2+}, the intrinsic tryptophan fluorescence of SERCA was substantially increased by ATP and ADP, but was unaffected by AMP (60). This nucleotide-induced increase in fluorescence intensity was completely inhibited by TG, which was subsequently shown to reduce the affinity of the Ca^{2+}-ATPase for ATP through uncompetitive inhibition (61, 62). Similarly, PLB cross-linking to SERCA2a occurs in the absence of Ca^{2+}, is enhanced by ATP and ADP, but inhibited by TG (6, 21). Based upon these similarities, it was suggested that the physiological state detected by changes in fluorescence induced by nucleotide binding to *E*2 (60-62), is the unique *E*2·ATP state that binds PLB (21).

In a recent study by Jensen *et al.* (20), it was suggested that TG stabilizes the fully protonated H_nE2 state of the Ca^{2+} pump, and that ATP binding at the modulatory site stimulates deprotonation of *E*2, initiating the transition to *E*1. Here, using ATP stimulation of PLB cross-linking to measure ATP binding at different TG concentrations, we confirmed the ATP affinities of *E*2 and *E*2·TG reported previously

(60-62). Moreover, we showed that ATP dramatically increases the resistance of the *E*2·PLB complex to TG, shifting the K_i values for TG inhibition of cross-linking by 100-200 fold for the supershifters PLB3 and PLB4 (**Table 2**). Thus, the PLB supershifters and ATP interact synergistically at *E*2, stabilizing an *E*2·ATP·PLB ternary complex that is remarkably resistant to TG. These results suggest that the *E*2·ATP state detected by ATP-induced changes in Trp fluorescence (60-62) and by chemical cross-linking of PLB (6, 21), may be the deprotonated *E*2·ATP state with ATP bound at the modulatory site. Moreover, TG may inhibit formation of this specific conformation, not by blocking ATP binding, but by hindering ATP stimulated deprotonation of the enzyme. Consistent with this interpretation, PLB does not bind to the P_i (**Fig. 12**) or vanadate (**Fig. 26**) bound forms of the enzyme, both of which interact with protonated H_nE2 state like TG (67). Also as observed with TG, ATP strongly enhances PLB cross-linking to SERCA2a in the presence of P_i (**Fig. 12**) and vanadate (**Fig. 26**), being able to compete for P_i (32) or vanadate binding (63, 68) to the Ca^{2+}-ATPase.

2. THE AFFINITY OF PLB FOR SERCA2a

Given TG's reputation as an extremely potent, irreversible inhibitor of the Ca^{2+}-ATPase (34, 35), we were surprised to discover that TG did not disrupt the ternary complex between the PLB supershifters and *E*2·ATP, even when membranes were pre-incubated for up to 1 hour with greater than stoichiometric concentrations of TG. Moreover, under these conditions favoring *E*2·ATP, PLB3 and PLB4 bind even more tightly to SERCA2a than does TG, the highest affinity SERCA inhibitor identified to date (34, 35). Crystallographic studies have revealed that TG binds to *E*2 in a cavity formed between transmembrane helices M3, M5, and M7, near the cytoplasmic membrane surface (18). This is on the opposite face of *E*2 from the PLB binding site, which is predicted to extend along the groove formed between transmembrane helices M2, M4, and M9, based on cross-linking results (21, 22, 51). Our results suggest that binding of PLB at its site must drastically distort the TG binding pocket. Nonetheless, under enzyme turnover conditions, TG is the more

powerful SERCA inhibitor. In the presence of Ca^{2+}, catalytic activity is completely inhibited by TG through formation of a dead-end complex (34), whereas Ca^{2+}-ATPase inhibition by the PLB supershifters remains reversible, albeit at very high Ca^{2+} concentrations (**Fig. 20**). It should be pointed out that TG binding to $E1 \cdot Ca^{2+}$ as well as to $E2$ has been noted in many studies (20, 34, 69-71), and that the ability of TG to bind to different conformational states of SERCA may contribute to its apparently irreversible effect on Ca^{2+}-ATPase activity.

These results with TG indicate that the binding affinity of the PLB supershifters (PLB3 and PLB4) for $E2 \cdot ATP$ measured in the absence of Ca^{2+} is in the nanomolar range or lower. The affinities of the PLB mutants for SERCA2a were also estimated using the lower affinity Ca^{2+}-pump inhibitor vanadate, and the anti-PLB antibody, 2D12. Vanadate inhibits the Ca^{2+}-ATPase with micromolar affinity, and our cross-linking results indicated that N30C-PLB has an affinity for $E2 \cdot ATP$ in the range of vanadate, whereas the affinities of PLB3 and PLB4 for SERCA2a are much greater. In addition, using 2D12 to estimate the binding affinities of the PLB mutants for SERCA2a in the absence of Ca^{2+}, we found that the affinity of PLB for the 2D12 antibody (0.1 μM) was similar to the affinity of N30C-PLB for Ca^{2+}-ATPase, but less than the affinity of the PLB supershifters for SERCA2a. Therefore, using effectors that act both on the Ca^{2+}-ATPase (TG and vanadate) and on PLB itself (2D12), we conclude that the affinity of PLB for the Ca^{2+}-pump is much greater than previously thought (51). In the absence of Ca^{2+} and in the presence of ATP, N30C-PLB has an affinity for SERCA2a in the micromolar range, whereas PLB3 and PLB4 bind with nanomolar affinity or higher.

D. CONCLUSION AND FURTURE DIRECTIONS

The overall conclusion of this work is that PLB inhibits Ca^{2+} binding to SERCA2a by stabilizing the enzyme in a Ca^{2+}-free $E2$ state. Clearly, PLB binding has long-range conformational effects on both the cytoplasmic domains and the transmembrane domain, and these effects are likely even more profound with the PLB supershifters. ATP binding to $E2$ accelerates the $E2$ to $E1 \cdot Ca_2$ transition by

stimulating H^+/Ca^{2+} cation exchange (20), while at the same time inducing structural changes that promote PLB binding. So, is the conformation of SERCA2a that binds to PLB really deprotonated *E*2·ATP, or Ca^{2+}-free *E*1 (62), or perhaps something in between (70)? Until the crystal structure of PLB-bound SERCA2a is determined we have no way of knowing. It was recently suggested that TG "rigidifies" the transmembrane domain of the Ca^{2+} pump, making it unresponsive to conformational changes occurring within the cytosolic domain (62). It is this ability of TG to fix the transmembrane helices that has enabled the Ca^{2+}-free, TG-bound enzyme to be crystallized, providing valuable structural information about the Ca^{2+}-ATPase in different *E*2 states (18). However, all of the *E*2 structures determined to date have been in the presence of irreversible inhibitors like TG or cyclopiazonic acid (72), and it is unclear how closely these inhibitor-bound structures resemble other, perhaps more physiological states of the enzyme (62). It is therefore our long-term goal to crystallize the Ca^{2+} pump complexed with PLB in order to provide a structure of *E*2 stabilized by a reversible inhibitor that is physiologically active in the heart. Here, we have shown that in the absence of Ca^{2+}, the binding affinities of the supershifters are several fold higher than even TG, making the goal of crystallizing the Ca^{2+}-free enzyme stabilized by PLB3 or PLB4 seem plausible.

REFERENCES

1. Bers, D.M. 2000. Calcium fluxes involved in control of cardiac myocytes contraction. *Circ. Research.* 87:275-281.

2. Simmerman, H.K.B., and Jones, L.R. 1998. Phospholamban: Protein structure, mechanism of action, and role in cardiac function. *Physiol. Rev.* 78:921-927.

3. MacLennan, D.H., and Kranias, E.G. 2003. Phospholamban: a crucial regulator of cardiac contractility. *Nat Rev Mol Cell Biol.* 4:566-577.

4. Luo, W., Grupp, I.L., Harrer, J., Ponniah, S., Grupp, G., Durffy, J.J., Doetschman, T., and Kranias, E.G. 1994. Targeted ablation of the phospholamban gene is associated with markedly enhanced myocardial contractility and loss of beta-agonist stimulation. *Circ. Research.* 75:401-409.

5. Sham, J.S., Jones, L.R., and Morad, M. 1991. Phospholamban mediates the beta-adrenergic-enhanced Ca^{2+} uptake in mammalian ventricular myocytes. *Am. J. Physiol.* 261:H1344-H1349.

6. Chen, Z., Akin, B.L., and Jones, L.R. 2007. Mechanism of reversal of phospholamban inhibition of the cardiac Ca^{2+}-ATPase by protein kinase A and by anti-phospholamban monoclonal Antibody 2D12. *J. Biol. Chem.* 282:20968-20976.

7. Seidman, J.G., and Seidman, C. 2001. The genetic basis for cardiomyopathy: from mutation identification to mechanistic paradigms. *Cell.* 104:557-567.

8. Haghighi, K. Gregory, K., and Kranias, E.G. 2004. Sacroplasmic reticulum Ca-ATPase–phospholamban interactions and dilated cardiomyopathy. *Biochem. Biophys. Res. Comm.* 322:1214-1222.

9. Haghighi, K., Kolokathis, F., Pater, L., Lynch, R.A., Asahi, M., Gramolini, A.O., Fan, G.C., Tsiapras, D., Hahn, H.S., Adamopoulos, S., Liggett, S.B., Dorn, G.W., MacLennan, D.H., Kremastinos, D.T., and Kranias, E.G. 2003. Human phospholamban null results in lethal dilated cardiomyopathy revealing a critical difference between mouse and human. *J. Clin. Invest.* 111:869-876.

10. Schmitt, J.P., Kamisago, M., Asahi, M., Li, G.H., Ahmad, F., Mende, U., Kranias, E.G., MacLennan, D.H., Seidman, J.G., and Seidman, C.E. 2003. Dilated cardiomyopathy and heart failure caused by a mutation in phospholamban. *Science.* 299:1410-1413.

11. Haghighi, K., Kolokathis, F., Gramolini, A.O., Waggoner, J.R., Pater, L., Lynch, R.A., Fan, G.C., Tsiapras, D., Parekh, R.R., Dorn, G.W., MacLennan, D.H., Kremastinos, D.T., and Kranias, E.G. 2006. A mutation in the human phospholamban gene, deleting arginine 14, results in lethal, hereditary cardiomyopathy. *PNAS.* 103:1388-1393.

12. Hoshijima, M. 2005. Gene therapy targeted at calcium handling as an approach to the treatment of heart failure. *Pharmacol Ther.* 105:211-228.

13. Tomaselli, G.F., and Marban, E. 1999. Electrophysiological remodeling in hypertrophy and heart failure. *Cardiovascular Res.* 42:270-283.

14. Hasenfuss, G., and Pieske, B. 2002. Calcium cycling in congestive heart failure. *J. Mol. Cell Cardiol.* 34:951-969.

15. Movsesian, M.A., Karimi, M., Green, K., and Jones, L.R. 1994. Ca^{2+}-transporting ATPase, phospholamban, and calsequestrin levels in nonfailing and failing human myocardium. *Circulation.* 90:653-657.

16. Bublits, M., Poulsen, H., Morth, J.P., and Nissen, P. 2010. In and out of the cation pumps: P-Type ATPase structure revisited. *Current Opinion Structural Biology* 20:1-10.

17. Lee, A.G. 2002. Ca^{2+}-ATPase structure in the E1 and E2 conformations: mechanisms, helix-helix and helix-lipid interactions. *Biochimica et Biophusica Acta.* 1565:246-266.

18. Toyoshima, C. 2008. Structural aspects of ion pumping by Ca^{2+}-ATPase of sarcoplasmic reticulum *Arch. Biochem. Biophys.* 476:3-11.

19. Green N.M., and MacLennan, D.H. 2002. Calcium calisthenics. *Nature.* 418:598-599.

20. Jensen, A.M., Sørensen, T.L., Olesen, C., Møller, J.V., and Nissen P. 2006. *EMBO J.* 25:2305-2314.

21. Jones, L.R., Cornea, R.L., and Chen, Z. 2002. Close proximity between residue 30 of phospholamban and cysteine 318 of the cardiac Ca^{2+}-pump revealed by intermolecular thiol cross-linking. *J. Biol. Chem.* 277:28319-28329.

22. Chen, Z., Akin, B.L., Stokes, D.L., and Jones, L.R. 2006. Cross-linking of C-terminal residues of phospholamban to the Ca^{2+} pump of cardiac sarcoplasmic reticulum to probe spatial and functional interactions within the transmembrane domain. *J. Biol. Chem.* 281:14163-14172.

23. Chen, Z., Akin, B.L., and Jones, L.R. 2010. Ca^{2+} binding to site I of the cardiac Ca^{2+} pump is sufficient to dissociate phospholamban. *J. Biol. Chem.* 285:3253-3260.

24. Akin, B.L., Chen, Z., and Jones, L.R. 2010. Superinhibitory phospholamban mutants compete with Ca^{2+} for binding to SERCA2a by stabilizing a unique nucleotide-dependent conformational state. *J. Biol. Chem.* 285:28540-28552.

25. Simmerman, H.K., Kobayashi, Y.M., Autry, J.M., and Jones, L.R. 1996. A leucine zipper stabilizes the pentameric membrane domain of phospholamban and forms a coiled-coil pore structure. *J. Biol. Chem.* 271:5941-5946.

26. Kimura, Y., Kurzydlowski, M., Tada, M., and MacLennan, D.H. 1997. Phospholamban regulates the Ca^{2+}-ATPase through intramembrane interactions. *J. Biol. Chem.* 272:15061-16064.

27. Autry, J.M., and Jones, L.R. 1997. Functional co-expression of the canine cardiac Ca^{2+} pump and phospholamban in spodoptera frugiperdia (Sf21) cells reveals new insights on ATPase regulation *J. Biol. Chem.* 272:15872-15880.

28. Kimura, Y., Asahi, M., Kurzydlowski, K., Tada, M., and MacLennan, D.H. 1998. Phospholamban domain Ib mutations influence functional interactions with the Ca^{2+}-ATPase isoform of cardiac sarcoplasmic reticulum. *J. Biol. Chem.* 273:14238-14241.

29. Zvaritch, E., Backx, P.H., Jirik, F., Kimura, Y., Leon, S., Schmidt, A.G., Hoit, B.D., Lester, J.W., Kranias, E.G., and MacLennan, D.H. 2000. The transgenic expression of highly inhibitory monomeric forms of phospholamban in mouse heart impairs cardiac contractility. *J. Biol. Chem.* 275:14985-14991.

30. Zhai, J., Schmidt, A.G., Hoit, B.D., Kimura, Y., MacLennan, D.H., and Kranias, E.G. 2000. Cardiac-specific overexpression of a superinhibitory pentameric phospholamban mutant enhances inhibition of cardiac function *in vivo*. *J. Biol. Chem.*275:10538-10544.

31. Haghighi, K., Schmidt, A.G., Hoit, B.D., Brittsan, A.G., Yatani, A., Lester, J.W., Zhai, J., Kimura, Y., Dorn, G.W., MacLennan, D.H., and Kranias, E.G. 2001. Superinhibition of sarcoplasmic reticulum function by phospholamban induces cardiac contractile failure. *J. Biol. Chem.* 276:24145-24152

32. Masuda, H., and de Meis, L. 1973. Phosphorlyation of the sarcoplasmic reticulum membrane by orthophosphate inhibition by calcium ions. *Biochemistry*. 12:4581-4585.

33. McIntosh, D.B., and Boyer, P.D. 1983. Adenosine 5'triphosphate modulation of catalytic intermediates of calcium ion activated adenosinetriphosphate of sarcoplasmic reticulum subsequent to enzyme phosphorylation. *Biochemistry.* 22:2867-2875.

34. Sagara, Y., Fernandez-Belda, F., de Meis, L., and Inesi, G. 1992. Transmembrane segment M3 is essential to thapsigargin sensitivity of the sarcoplasmic reticulum Ca^{2+}-ATPase. *J. Bio. Chem.* 267:12606-12613.

35. Lytton, J., Westlin, M., and Hanley, M.R. 1991. Thapsigargin inhibits the sarcoplasmic or endoplasmic reticulum Ca-ATPase family of calcium pumps. *J. Biol. Chem.* 266:17067-17071.

36. Mueller, B., Karim, C.B., Negrashov, I.V., Kutchai, H., and Thomas, D.D. 2004. Direct detection of phospholamban and sarcoplasmic reticulum Ca-ATPase interaction in membranes using florescence resonance energy transfer. *Biochemistry.* 43:8754-8765.

37. Li, J., Bigelow, D.J., and Squier, T.C. 2004. Conformational changes within the cytoplasmic portion of phospholamban upon release of Ca-ATPase inhibition. *Biochemistry.* 43:3870-3879.

38. Cantilina, T., Sagara, Y., Inesi, G., and Jones, L.R. 1993. Comparative studies of cardiac and skeletal sarcoplasmic reticulum ATPases. Effect of a phospholamban antibody on enzyme activation by Ca^{2+}. *J. Biol. Chem.* 23:17018-17025.

39. Tada, M., Ohmori, F., Yamada, M., and Abe, H. 1979. Mechanism of the stimulation of Ca^{2+}-dependent ATPase of cardiac sarcoplasmic reticulum by adenosine 3':5'-monophosphate-dependent protein kinase. Role of the 22,000-dalton protein. *J. Biol. Chem.* 254:319-326.

40. Antipenko, A.Y., Spielman, A.I., and Kirchberger, M.A. 1997. Comparison of the effects of phospholamban and jasmone on the calcium pump of cardiac sarcoplasmic reticulum. Evidence for modulation by phospholamban of both Ca^{2+} affinity and V_{max} (Ca) of calcium transport. *J. Biol. Chem.* 272:2852-2860.

41. Afara, M.R., Trieber, C.A., Ceholski, D.K., and Young, H.S. 2008. Peptide inhibitors use two related mechanisms to alter the apparent calcium affinity of the sarcoplasmic reticulum calcium pump. *Biochemistry*. 47:9522-9530.

42. Reddy, L.G., Cornea, R.L., Winters, D.L., McKenna, E., and Thomas, D.D. 2003. Defining the molecular components of calcium transport regulation in a reconstituted membrane system. *Biochemistry.* 42:4585-4592.

43. Trieber, C.A., Douglas, J.L., Afara, M., and Young, H.S. 2005. The effects of mutation on the regulatory properties of phospholamban in co-reconstituted membranes. *Biochemistry.* 44:3289-3297.

44. Waggoner, J.R., Huffman, J., Froehlich, J.P., and Mahaney, J.E. 2007. Phospholamban inhibits Ca-ATPase conformational changes involving the E2 intermediate. *Biochemistry.* 46:1999-2009.

45. Trieber, C.A., Afara, M., and Young, H.S. 2009. Effects of phospholamban transmembrane mutants on the calcium affinity, maximal activity, and cooperativity of the sarcoplasmic reticulum calcium pump. *Biochemistry.* 48:9287-9296.

46. Cornea, R.L., Jones, L.R., Autry, J.M., and Thomas, D.D. 1997. Mutation and phosphorylation change the oligomeric structure of phospholamban in lipid bilayers. *Biochemistry.* 36:2960-2967.

47. Reddy, L.G., Jones, L.R., and Thomas, D.D. 1999. Depolymerization of phospholamban in the presence of calcium pump: a fluorescence energy transfer study. *Biochemistry.* 38:3954-3962.

48. Hou, S., and Robia, S.L. 2010. Relative affinity of calcium pump isoforms for phospholamban quantified by fluorescence resonance energy transfer. *J. Molec. Biol.* 402:210-216.

49. Robia, S.L., Campbell, K.S., Kelly, E.M., Hou, Z., Winters, D.L., and Thomas, D.D. 2007. Förster transfer recovery reveals that phospholamban exchanges slowly from pentamers but rapidly from the SERCA regulatory complex. *Circ. Research.* 101:1123-1129 .

50. Kelly, E.M., Bossuyt, J., Bers, D.M., and Robia, S.L. 2008. Phospholamban oligomerization, quaternary structure, and sarco(endo)plasmic reticulum calcium ATPase binding measured by fluorescence resonance energy transfer in living cells. *J. Biol. Chem.* 283:12202-12211.

51. Toyoshima, C., Asahi, M., Sugita, Y., Khanna, R., Tsuda, T., and MacLennan, D.H. 2003. Modeling of the inhibitory interaction of phospholamban with the Ca^{2+} ATPase. *PNAS.* 100:467-472.

52. Inesi, G. Kurzmack, M., Conan, C., and Lewis, D.E. 1980. Cooperative calcium binding and ATPase activation in sarcoplasmic reticulum vesicles. *J. Biol. Chem.* 255:3025-3031.

53. Zhang, Z., Lewis, D., Strock, C., Inesi, G., Nakasako, M., Nomura, H., and Toyoshima, C. 2000. Detailed characterization of the cooperative mechanism of Ca(2+) binding and catalytic activation in the Ca(2+) transport (SERCA) ATPase. *Biochemistry.* 39:8758-8767.

54. Maruyama, K., and Maclennan, D.H. 1988. Mutation of aspartic acid-351, lysine- 352, and lysine-515 alters the Ca^{2+} transport activity of the Ca^{2+}-ATPase expressed in COS-1 cells. *PNAS.* 85:3314-3318.

55. McIntosh, D.B., Woolley, D.G., MacLennan, D.H., Vilsen, B., and Andersen, J.P. 1999. Interaction of nucleotides with Asp(351) and the conserved phosphorylation loop of sarcoplasmic reticulum Ca(2+)-ATPase. *J. Biol. Chem.* 274:25227-25236.

56. Marchand, A., Winther, A.M., Holm, P.J., Olesen, C., Montigny, C., Arnou, B., Champeil, P., Clausen, J.D., Vilsen, B., Andersen, J.P., Nissen, P., Jaxel, C., Møller, J.V., and le Maire, M. 2008. Crystal structure of D351A and P312A mutant forms of the mammalian sarcoplasmic reticulum Ca(2+) -ATPase reveals key events in phosphorylation and Ca(2+) release. *J. Biol. Chem.* 83:14867-14882.

57. Jones, L.R., Besch, H.R., Jr., and Watanabe, A.M. 1978. Regulation of the calcium pump of cardiac sarcoplasmic reticulum. Interactive roles of potassium and ATP on the phosphoprotein intermediate of the (K^+,Ca^{2+})-ATPase. *J. Biol. Chem.* 253:1643-1653.

58. Cornea, R.L., Autry, J.M., Chen, Z., and Jones, L.R. 2000. Reexamination of the role of the leucine/isoleucine zipper residues of phospholamban in inhibition of the Ca^{2+} pump of cardiac sarcoplasmic reticulum. *J. Biol. Chem.* 275:41487-41494.

59. Jones, L.R. 1979. Mg^{2+} and ATP effects on K^+ activation of the Ca^{2+}-transport ATPase of cardiac sarcoplasmic reticulum. *Biochim. Biophys. Acta.* 557:230-242.

60. Lacapere, J.J., Bennett, N., Dupont, Y., and Guillain, F. 1990. pH and magnesium dependence of ATP binding to sarcoplasmic reticulum ATPase. Evidence that the catalytic ATP-binding site consists of two domains. *J. Biol. Chem.* 265:348-353.

61. DeJesus, F., Girardet, J.C., and Dupont, Y. 1993. Characterisation of ATP binding inhibition to the sarcoplasmic reticulum Ca(2+)-ATPase by thapsigargin. *FEBS.* 332:229-232.

62. Montigny, C., Picard, M., Lenoir, G., Gauron, C., Toyoshima, C., and Champeil, P. 2007. Inhibitors bound to Ca(2+)-free sarcoplasmic reticulum Ca(2+)-ATPase lock its transmembrane region but not necessarily its cytosolic region, revealing the flexibility of the loops connecting transmembrane and cytosolic domains. *J. Biol. Chem.* 46:15162-15174.

63. Pick, U. 1982. The interaction of vanadate ions with the Ca-ATPase from sarcoplasmic reticulum. *J. Biol. Chem.* 257:6111-6119.

64. Mahaney, J.E., Autry, J.M., and Jones, L.R. 2000. Kinetics studies of the cardiac Ca-ATPase expressed in Sf21 cells: new insights on Ca-ATPase regulation by phospholamban. *Biophys. J.* 78:1306-1323.

65. Watanabe, T., Lewis, D., Nakamoto, R., Kurzmack, M., Fonticelli, C. and Inesi, G. 1981. Modulation of calcium binding in sarcoplasmic reticulum adenosinetriphosphatase. *Biochemistry.* 20:6617-6625.

66. Montigny, C., Arnou, B., Marchal, E., and Champeil, C. 2008. Use of glycerol-containing media to study the intrinsic fluorescence properties of detergent-solubilized native or expressed SERCA1a. *Biochemistry.* 46:12159-12174.

67. Inesi, G., Lewis, D., and Murphy, A. 1984. Interdependence of H^+, Ca^{2+}, and Pi (or vanadate) sites in sarcoplasmic reticulum ATPase. *J. Biol. Chem.* 259:996-1003.

68. Anderson, J.P., and Møller, J.V. 1985. The role of Mg^{2+} and Ca^{2+} in the simultaneous binding of vanadate and ATP at the phosphorylation site of sarcoplasmic reticulum Ca^{2+}-ATPase. *Biochim. Biophys. Acta.* 815:9-15.

69. Fortea, M.I., Soler, F., and Fernandez-Belda, F. 2001. Unravelling the interaction of thapsigargin with the conformational states of Ca(2+)-ATPase from skeletal sarcoplasmic reticulum. *J. Biol. Chem.* 276:37266-37272.

70. Inesi, G., Lewis, D., Toyoshima, C., Hirata, A., and de Meis, L. 2008. Conformational fluctuations of the Ca^{2+}-ATPase in the native membrane environment. Effects of pH, temperature, catalytic substrates, and thapsigargin. *J. Biol. Chem.* 283:1189-1196.

71. Wictome, M., Henderson, I., Lee, A.G., and East, J.M. 1992. Mechanism of inhibition of the calcium pump of sarcoplasmic reticulum by thapsigargin. *Biochem. J.* 283:525-529.

72. Moncoq, K., Trieber, C.A., and Young, H.S. 2007. The molecular basis for cyclopiazonic acid inhibition of the sarcoplasmic reticulum calcium pump. *J. Biol. Chem.* 282:9748-9757.

CURRICULUM VITAE

Brandy Lee Akin

CURRENT POSITION

Postdoctoral Research Fellow
Krannert Institute of Cardiology
Indiana University School of Medicine

EDUCATION

Bachelor of Science, 2003
Purdue University
Major: Biological Sciences
Minor: Chemistry

Doctor of Philosophy, 2010
Indiana University
Major: Biochemistry and Molecular Biology
Minor: Life Sciences
Dissertation: "Investigating the Molecular Mechanism of Phospholamban Regulation of the Cardiac Ca^{2+} Pump of Sarcoplasmic Reticulum"

HONORS AND AWARDS

Jack Davis Award for Best Seminar by a Graduate Student 2005-2006, Department of Biochemistry and Molecular Biology, Indiana University School of Medicine

PROFESSIONAL SOCIETIES

Biophysical Society

LABORATORY EXPERIENCE

2001-2002 Volunteer Student Researcher for Dr. William Cooper, Department of Biology, Indiana University-Purdue University, Fort Wayne.

2003-2004 Research Technician for Dr. Larry Jones, Krannert Institute of Cardiology, Indiana University School of Medicine

POSTERS AND PRESENTATIONS

1. "Impaired Junctin Binding by D307H Calsequestrin, a missense cardiac CSQ mutant causing ventricular tachycardia in humans" 2004. Poster presentation at Gordon Research Conference on Cardiac Regulatory Mechanisms, Colby-Sawyer College, New London, NH.

2. "Only SERCA2a unfettered by phospholamban is catalytically active" 2007. Platform presentation at Biophysical Society Meeting, Baltimore, MD.

3. "Superinhibitory phospholamban mutants compete with Ca^{2+} for binding to SERCA2a" 2008. Poster presentation at Gordon Research Conference on Cardiac Regulatory Mechanisms, Colby-Sawyer College, New London, NH.

4. "Cross-linkable, gain of function phospholamban mutant reveals the molecular mechanism of SERCA2a inhibition" 2009. Platform presentation at Biophysical Society Meeting, Boston, MA.

PUBLICATIONS

1. Cooper, W.E., Perez-Mellado, V., Vitt, L.J., and **Budzynski, B.L.** 2002. Behavioral responses to plant toxins by two omnivorous lizard species. *Physiol. Behav.* 76:297-303.

2. Cooper, W.E., Perez-Mellado, V., Vitt, L.J., and **Budzynski, B.L.** 2003. Cologne as a pungency control in tests of chemical discrimination: effects of concentration, brand, and simultaneous and sequential presentation. *Ethology* 21:101-106.

3. Chen, Z., **Akin, B.L.**, Stokes, D.L., and Jones, L.R. 2006. Cross-linking of C-terminal residues of phospholamban to the Ca^{2+} pump of cardiac sarcoplasmic reticulum to probe spatial and functional interactions within the transmembrane domain. *J. Biol. Chem*. 281:14163-14172.

4. Knollmann, B.C., Chopra, N., Hlaing, T., **Akin, B.**, Yang, T., Ettensohn, K., Knollmann, B. E.C., Horton, K.D., Weissman, N.J., Holinstat, I., Zhang, W., Roden, D.M., Jones, L.R., Franzini-Armstrong, C., and Pfeifer K. 2006. *Casq2* deletion causes sarcoplasmic reticulum volume increase, premature Ca^{2+} release, and catecholaminergic polymorphic ventricular tachycardia. *J. Clin. Invest.* 116:2510-2520.

5. Chen, Z., **Akin, B.L.**, and Jones, L.R. 2007. Mechanism of reversal of phospholamban inhibition of the cardiac Ca^{2+}-ATPase by protein kinase A and by anti-phospholamban monoclonal antibody, 2D12. *J. Biol. Chem*. 282:20968-20976.

6. Chopra, N., Kannankeril, P.J., Yang, T., Hlaing, T., Holinstat, I., Ettensohn, K., Pfeifer, K., **Akin, B.**, Jones, L.R., Franzini-Armstrong, C., and Knollmann, B.C. 2007. Modest reductions of cardiac calsequestrin increase sarcoplasmic reticulum Ca^{2+}-leak independent of luminal Ca^{2+} and trigger ventricular arrhythmias in mice. *Circ. Research.* 101:617-626.

7. Chopra, N., Yang, T., Asghari, P., Moore, E.D., Huke, S., **Akin, B.**, Cattolica, R.A., Perez, C.F., Hlaing, T., Knollmann-Ritschel, B.E., Jones, L.R., Pessah, I.N., Allen, P.D., Franzini-Armstrong, C., and Knollmann, B.C. 2009. Ablation of triadin causes loss of cardiac Ca^{2+} release units, impaired excitation-contraction coupling, and cardiac arrhythmias. *Proc. Natl. Acad. Sci.* 106:7636-7641.

8. Chen, Z., **Akin, B.L.**, and Jones, L.R. 2010. Ca^{2+} binding to site I of the cardiac Ca^{2+} pump is sufficient to dissociate phospholamban. *J. Biol. Chem.* 285:3253-3260.

9. **Akin, B.L.**, Chen, Z., and Jones, L.R. 2010. Superinhibitory phospholamban mutants compete with Ca^{2+} for binding to SERCA2a by stabilizing a unique nucleotide-dependent conformational state. *J. Biol. Chem.* 285:28540-28552.

ABSTRACTS

1. **Akin, B.L.**, Chen, Z., and Jones, L.R. 2007. Only SERCA2a unfettered by PLB is catalytically active. *Biophys. J.* 8a.

2. Chen, Z., **Akin, B.L.**, and Jones, L.R. 2007. Decreased binding of protein kinase A phosphorylated phospholamban (P-PLB) to the cardiac Ca^{2+} pump (SERCA2a) revealed by use of cross-linking reagents. *Biophys. J.* 8a.

3. Nagesh, C., **Akin, B.L.**, Jones, L.R., Coffa, S., Shen, X., Perez, C.F., Allen, P.D., and Knollmann, B.C. 2007. Triadin null mice have reduced junctional SR proteins and dysfunctional SR Ca^{2+} release. *Biophys. J.* 134a.

4. Chopra, N., Kannankeril, P.J., Hlaing., T., Coffa, S., **Akin, B.**, Yang, T., Zhang, W., Pfeifer, K., Jones, L.R., and Knollmann, B.C. 2007. Modest reductions in cardiac calsequestrin render mice susceptible to ventricular arrhythmias. *Biophys. J.* 352a.

5. **Akin, B.L.**, Chen, Z., and Jones, L.R. 2009. Cross-Linkable, gain-of-function phospholamban (PLB) mutant reveals the molecular mechanism of SERCA2a inhibition. *Biophys. J.* 142a-143a.

6. Chen, Z., **Akin, B.L.**, and Jones, L.R. 2009. Ca^{2+} binding to site I of the cardiac Ca^{2+} pump (SERCA2a) is sufficient to dissociate phospholamban (PLB). *Biophys. J.* 210a-211a.

7. **Akin, B.L.**, and Jones, L.R. 2010. Highly specific, conformationally-dependent cross-linking of Lys^{27} of phospholamban to SERCA2a in SR vesicles from humans. *Biophys. J.* (in press).